TRABECULAR BONE VARIATION IN MID AND UPPER CRANIOFACIAL REGIONS OF FOUR ANTHROPOIDS

LESLIE C. PRYOR SMITH

Presented to the Faculty of the Graduate School of

The University of Texas at Arlington in Partial Fulfillment

of the Requirements

for the Degree of

MASTER OF ARTS IN ANTHROPOLOGY

THE UNIVERSITY OF TEXAS AT ARLINGTON

May 2011

ACKNOWLEDGEMENTS

I would like to thank my committee chair and advisor Dr. Shelley Smith for her commitment to the betterment of my thesis project and manuscript. I am grateful for all the support and encouragement she has given me during my time at UT Arlington. I would also like to thank my committee member, Dr. Naomi Cleghorn, at UT Arlington for her comments and suggestions to help improve this work.

This thesis could not have been possible without the help of Dr. Paul Dechow at Baylor College of Dentistry. I have benefited tremendously from his impressive wealth of knowledge and experience, not just in primate anatomy and biomechanics, but in the broader range of biomedical sciences. I want to thank Dr. Lynne Opperman, professor at Baylor College of Dentistry, for her time, advice and encouragement throughout this project. I also thank Allen Mortimer and Mitra Bolouri for their work in the initial stages of this project.

It would be ungracious not to mention the love and support I have received from my friends and family since I began this project. In particular, I would like to thank my father, Gerald, my mother, Claire, and my brother, Jerry for nurturing my curiosity and truth seeking nature. Last but not least, I thank my best friend and husband, Colby. He has shown me unrelenting patience, encouragement, and support throughout my time in graduate school. I am grateful to him for keeping me laughing even during the most stressful of times.

I dedicate this thesis to my mother, Claire, for teaching me the importance of diligence.

April 8, 2011

ABSTRACT

TRABECULAR BONE VARIATION IN MID AND UPPER CRANIOFACIAL REGIONS OF FOUR ANTHROPOIDS

Leslie Claire Pryor Smith, M.A.

The University of Texas at Arlington, 2011

Supervising Professor: Shelley L. Smith

Some posit that robust supraorbital tori seen in fossil hominin species are an adaptation to hard object feeding, while others believe that supraorbital morphology is overdesigned for mastication in robust species. Strain gage analysis of primate craniofacial regions finds that strain is much lower in the supraorbital region relative to the zygomatic region, however, the mechanisms behind bone adaptation to loads is not fully understood. While variations in cortical bone material properties in a few primate species have been determined, no one has explored the variation in cranial trabecular bone. This study used microcomputed tomography to assess the variation in trabecular bone structure in the supraorbital and zygomatic regions of 10 humans, 4 baboons, 1 chimpanzee, and 1 gorilla.

Significant differences in the degree of anisotropy, an indication of trabecular bone strength relative to orthogonal axes, were region specific, but significant differences in bone volume fraction, positively correlated with density, were species specific. Furthermore, differences in the degree of anisotropy by region were consistent with differences in cortical

bone surface strain determined by other researchers using strain gage analysis. Trabecular bone structural variables also differed in distribution by species and region.

The results of this study suggest that trabeculae adapt their primary orientation in response to relative strain endured during mastication, but that other variables related to density and strength may have a genetic component. Moreover, the results of this study support the hypothesis that robust craniofacial features may be genetic or epigenetic adaptations to fallback feeding strategies. There is a tremendous amount of variation in trabecular bone morphometric variables among species and between regions, suggesting that trabecular bone orientation and structure plays an essential role in craniofacial bone adaptation.

TABLE OF CONTENTS

LIST OF ILLUSTRATIONS

LIST OF TABLES

CHAPTER 1

INTRODUCTION

1.1 The Adaptive Significance of the Supraorbtial Region in Primates

In the field of primate functional morphology, there has been much debate over the variation found in the mid and upper facial regions of living and extinct primates (Hylander and Picq, 1989; Picq and Hylander, 1989; Hylander et al., 1991; Ross et al., 2011). In particular, around two million years ago, the hominin fossil record shows large variation in the supraorbital and zygomatic regions of contemporaneous species of early *Homo* and robust australopithecines. It is believed that a dramatic environmental change occurred during this time, which affected the type and availability of food in hominin regions (reviewed by Klein, 2009).

Because bone form is responsive to stress[1], some have suggested that robust zygomatic and supraorbital regions, belonging to robust australopithecines, are the result of greater stresses in these regions caused by larger muscles of mastication, required for the chewing of hard food objects (Endo, 1966; Teaford and Ungar, 2000; Strait et al., 2009). More specifically, it is hypothesized that greater stresses regularly endured by these regions selected for robust features and induced adaptive remodeling to peak strain[2] magnitudes, resulting in greater bone mass and microstructural alignment. In place of robust muscles and cranial features, early *Homo* may have had differing strategies to process hard foods and exploit other food niches.

However, there is not enough evidence to support these hypotheses (Susman, 1991; Wood and Collard, 1999; Aiello and Andrews, 2000). If it can be shown that the supraorbital and

[1] Stress is a measure of force per unit of area.
[2] Strain is deformation of an object induced by stress; it is defined as the change in length divided by the total length.

zygomatic regions in more robust primate species are adapted to withstand greater stress imposed by the muscles used during mastication, we can deduce that the robust supraorbital region observed in robust australopithecines is more likely an adaptation to hard object feeding.

The hypothesized relationship between robust craniofacial regions and mastication carries over into other primate species. There are many monkey species with pronounced supraorbital regions, and extant apes, such as gorillas and chimps, are robust in zygomatic and supraorbital regions, relative to their closest living cousins, *Homo sapiens*. In an attempt to understand the relationship between bone adaptive remodeling and masticatory stress in the craniofacial region of primates, researchers conduct strain gage experiments. These experiments are performed on both live animals and anatomical tissues; strain gages are attached to the surfaces of bone, the bone is systematically loaded, and strains are recorded. These studies are able to determine the values of strain experienced, for example, in the supraorbital and zygomatic regions of a monkey when it bites a nut or chews on a piece of fruit. According to Rubin and Lanyon (1985), most vertebrate bone remodels to maintain the same range of peak strain. In other words, most vertebrate bone will remodel (bone deposition or resorption) so that the stresses imposed during repetitive activities will result in a particular range of strain. Therefore, if the robust morphology in supraorbital and zygomatic regions is caused by mastication, observable peak strains in both regions should be similar during simulated mastication. However, strain gage studies by Endo (1966), Hylander and colleagues (1987; 1989; 1991; 1997), and Ross and colleagues (2011), among others, find that the supraorbital region in various extant primates undergoes significantly less strain during mastication than the zygomatic arch and the zygoma. These studies suggest that the robust supraorbital region observed in many extinct and extant primate species is overbuilt, and for this reason its structure is primarily not an adaption to mastication forces. Several alternative hypotheses have been proposed such as those by Tappen (1973) and Lieberman (1998), who

respectively suggest that the robust supraorbital region of hominins could have evolved as added protection against blows to the face or is a structural consequence of sphenoid position.

While other hypotheses about the evolution of the robust australopithecine supraorbital region maintain plausibility, observed differences in strain during mastication in the supraorbital and zygomatic regions cannot rule out hypotheses that supraorbital morphology is responsive to masticatory stress. By comparing the cortical bone properties in the human supraorbital region of normal and edentulous human individuals, Dechow et al. (2010) showed that the material properties in this region *are* significantly affected by a change in mastication. Furthermore, Turner (1999) developed a new theory, "the principle of cellular accommodation," that proposes that different regions of bone possess different strain thresholds for remodeling. Therefore, the supraorbital region may have a lower strain threshold and demonstrate a greater bone remodeling response than the zygomatic region. It has been suggested that the zygomatic region has a greater strain threshold in order to withstand more frequent loading of a greater magnitude (Kupczik et al., 2009).

Fortunately, strain gage experimentation is not the only method designed to test the effect stress has on bone form. Because bone responds to stress on a macrostructural *and* microstructural level, bone biomechanists can instead look at the microstructural, or material, properties of bone, such as density, to determine its mechanical properties: those which describe its behavior under load. Experiments designed to determine the material and mechanical properties of primate craniofacial cortical bone have added to our understanding of primate craniofacial bone mechanics, while inspiring further inquiry regarding the evolution of robust and gracile facial features. For instance, we know that there are significant differences in properties by region and between species, but we do not fully understand the roles of bone's various components, such as cortical and trabecular, in its overall behavior and to what extent these roles vary by region and between primate species (Dechow et al., 1993; Peterson and

Dechow, 2002, 2003a; Schwartz-Dabney and Dechow, 2003; Peterson et al., 2006; Wang and Dechow, 2006; Wang et al., 2006b).

Like cortical bone, the material properties of trabecular bone are also important factors in the mechanical behavior of bone during function (Lanyon, 1974; Hayes and Snyder, 1981; Biewener et al., 1996; Cowin, 2001; Pearson and Lieberman, 2004; Pontzer et al., 2006; Ruff et al., 2006). Yet, specific and individual variations in the structure of the trabecular regions in the face and the related functional implications have been overlooked. Quantifications of variations in the material properties and mechanical behavior of trabecular bone, in the supraorbital and zygomatic regions of the primate craniofacial skeleton, are essential to our understanding of the relationship between the regional responses of bone to varying stress gradients and the role of biomechanical adaptation in the supraorbital region.

The material and mechanical properties of trabecular bone in postcranial regions have been studied in a number of investigations (Singh, 1978; Ryan and Ketcham, 2002; Ryan and Krovitz, 2006). The material properties of trabecular bone include structural descriptions, such as the average separation between and thickness of individual trabeculae, the average spacial orientation of trabeculae, and the bone volume fraction[3] of the entire trabecular region. All of these properties vary by region and affect the mechanical behavior of trabecular bone. Micro-computed tomography is a useful method for determining these properties, as it uses three dimensional models to calculate material properties (Feldkamp et al., 1989).

In this project, microcomputed tomography is used to quantify the variation in trabecular bone density, bone volume fraction, number, thickness, separation, structure model index, connectivity density, and anisotropy in the supraorbital and zygomatic region among anthropoid species *Homo*, *Pan*, *Gorilla*, and *Papio*.

[3] Bone volume fraction is a ratio of the volume of bone to the total volume occupied by the bone in space.

1.2 Hypotheses

I hypothesize that degree of anisotropy and bone volume fraction of trabecular bone in the supraorbital region is significantly lower relative to that found for the zygomatic regions. If measures of the degree of anisotropy and bone volume fraction in supraorbital trabecular regions are not significantly lower relative to zygomatic regions, it is possible that adaptive strain thresholding may differ by region.

Additionally, if robust supraorbital regions are primarily adapted to endure repetitive masticatory stress of greater magnitude, the trabecular bone in these regions may play a greater role in the overall response of the region to mastication. If degree of anisotropy and bone volume fraction are significantly higher in the supraorbital regions of more robust species relative to humans, this could indicate that the reduction of the supraorbital region in humans evolved to cope with a change in dietary strategy, as has been previously hypothesized. Alternatively, it is possible that that human trabecular bone in the supraorbital region will have strength indicating properties to compensate for the reduction in cortical bone bulk. Measures of the relative proportion of trabecular bone to cortical bone by region are needed to either weaken or support alternative possibilities.

1.3 Conclusion

The adaptive significance of robust supraorbital and zygomatic regions present in fossil hominins and extant apes is not fully understood. While it is theorized that variations in supraorbital and zygomatic robusticity are adaptations to feeding strategies, bone strain data from these regions suggest that the supraorbital region is overbuilt for mastication in extant ape and monkey species (Endo, 1966; Picq and Hylander, 1989). However, it is possible that the supraorbital region has a lower adaptive threshold for strain than other regions in the craniofacial skeleton. If so, the material and mechanical properties in the supraorbital region should indicate an adaptive response to masticatory stresses similar in magnitude and degree to those seen in the zygomatic region. Quantifying the material and mechanical properties of

trabecular bone in supraorbital and zygomatic regions of humans, chimps, gorillas, and baboons will answer questions regarding the evolutionary significance of such regions from a biomechanical perspective that strain gage studies cannot.

Furthermore, the data from this experiment will be useful to finite element modeling. In primate craniofacial functional morphology, finite element modeling is used to predict the overall deformation of the craniofacial complex in response to masticatory loading. It has been used to test a number of hypotheses regarding the adaptive significance of the functional morphology of the entire craniofacial region in primates (Richmond et al., 2005; Strait et al., 2005; Kupczik et al., 2007; Kupczik et al., 2009; Strait et al., 2009; Strait et al., 2010; Ross et al., in press). Incorporating accurate regionally specific bone material properties in models of the craniofacial complex improves the validity of FEM, yet previous FEM studies have lacked mechanical property data for trabecular bone in the entire craniofacial region (Dechow and Hylander 2000; Richmond et al. 2005; Strait et al. 2005). The results from this study can be incorporated into future finite element models to obtain more accurate predictions of the craniofacial deformation response to mastication in primates.

CHAPTER 2

BACKGROUND

2.1 Introduction

Vertebrate bone is a structurally complex composite of living cells and mineral compounds, and its formation is responsive to its mechanical environment (Koch, 1917; Currey, 2002). Trabecular bone research has primarily focused on identifying the relationship between the material properties and mechanical behavior of trabecular structure, how this relationship changes in different anatomical locations and between vertebrate species, the rules that govern this relationship, and the roles of genetics, environment and epigentics.

Trabecular bone biomechanics has been of interest to bone biologists for almost two centuries, and improved methodologies of the late 20th century, such as microcomputed tomography and finite element analysis, have allowed more accurate descriptions of trabecular structure and function (Feldkamp et al., 1989; Kuhn et al., 1990; Goulet et al., 1994; Laib et al., 2000). These studies have focused on the vertebral column and anatomical locations associated with locomotion, such as the femur and calcaneus (Goldstein, 1987; Biewener et al., 1996; Ryan and Ketcham, 2002; Ryan and Krovitz, 2006). Even though the functional significance of craniofacial variation in primates is a topic of contention, there are no studies that investigate the structure and behavior of trabecular bone within such regions.

The primate craniofacial region is of great interest to evolutionary scientists and functional anatomists because of the variability observed in fossil and extant primate species. To explore possible reasons for this variation, functional morphologists, such as Bari Endo (1966) and William Hylander and colleagues (1987; 1989; 1991; 1997) have focused on the strain variations in the supraorbital and zygomatic regions of the primate face, and Dechow and colleagues have explored variations in the microstructural properties of primate craniofacial

cortical bone (Dechow et al., 1992; Dechow et al., 1993; Peterson and Dechow, 1998, 2002, 2003a; Peterson et al., 2006; Wang and Dechow, 2006; Wang et al., 2006b; Dechow et al., 2010). Furthermore, finite element modeling has become a useful tool to researchers, to test hypotheses about how craniofacial regions of bone behave collectively (Richmond et al., 2005). The following paragraphs review relevant findings from trabecular bone research and explain how determining the material and mechanical properties of trabecular bone in the craniofacial region of primates can help answer questions regarding primate evolution.

2.2 The Mechanical Properties of Trabecular Bone

2.2.1 Introduction

The mammalian skeletal system is a structurally complex organ that provides support for the body of an organism, as well as resilience and flexibility that aid in an organism's interaction with its environment. Bone maintains an ideal balance of both rigidity and flexibility due to its molecular composition and the organization of collagen and calcium phosphate. Currey (2002) argues that understanding the mechanical function of bone is critical to an understanding of both the micro and macrostructural variation of bone tissue. This relationship, while not fully understood, is useful to many types of researchers, in particular functional morphologists. A basic description of the hierarchical structure of bone and relevant aspects of bone biomechanics, reviewed by Currey (2002), Martin et al. (1998) and Evans (1973), will be provided before a description of the historical and present day contributions to our knowledge of trabecular bone mechanics is discussed.

2.2.2 Bone: a Dynamic, Multi-level Structure

On the molecular level, bone consists of a mixture of collagen, calcium phosphate, water, polysaccharides, proteins, cells, and blood vessels. Collagen is composed of fibrous proteins; a variety of different types of collagen is found in all animals. It forms a variety of connective tissues and it undergoes mineralization in vertebrate animals to form the skeletal system. In bone formation, type 1 collagen consists of fibrils arranged both randomly, as in

woven bone, or in sheets, as in lamellar bone. Fibrils are composed of microfibrils, or structures made from the stacking of triple helices of tropocollagen proteins linked by hydrogen bonds. The length of the polypeptides that make up tropocollagen, along with its particular molecular composition of amino acids (which prevent rotation) and nitrogen (which prevents hydrogen bonding) allow it to maintain its flexibility as a molecule. After formation, the collagen may eventually undergo mineralization, in which minuscule crystal structures formed of calcium phosphate embed within it. The bonding mechanism and organization of the mineral component and collagen fibers of bone is not fully understood; however, cellular activity is likely responsible (reviewed by Martin et al., 1998; reviewed by Currey, 2002).

There are four main types of living cells found in bone and these, directly or indirectly, are responsible for the building up and breaking down of bone. Bone lining cells are derived from osteoprogenitor cells and are found in the cortex and outer layer of the bone, which make up the periosteum and endostoeum, respectively. They are multifunctional, allowing the passage of ions from the body to the bone and giving rise to osteoblasts. Osteoblasts build osteoid (the collagenous matrix) and are suspected to also build the mineral component. Bone lining cells also communicate with cells embedded within bone, called osteocytes, through a network of cell processes embedded in canal-like structures called canaliculi. The fourth type of cell involved in bone remodeling, derived from a macrophage-like cell, is the osteoclast, which will cling to a ruffled surface and break up and filter bone through its multinucleated cell body. Osteoclasts form resorption cavities, the process of which begins Haversian remodeling, discussed below (reviewed by Martin et al., 1998; reviewed by Currey, 2002).

The microstructural organization of bone varies among vertebrate species, by age, and by location. Three basic types of primary bone are found in mammals: woven, parallel-fibered bone, and lamellar bone. Woven bone forms quickly and is disorganized. In humans, it makes up the skeleton of infants and children. It is also used in the bone fracture healing process. Lamellar bone, on the other hand, forms slowly and is more organized. Parallel-fibered bone,

as its name suggest, is more organized than lamellar bone; bone is laid down in parallel sheets. This type of bone characterizes the outer layer of a bone shaft, for example. In bone remodeling, Haversian, or secondary, bone is formed from lamellar bone when osteoblasts and osteoclasts work together to build osteons, highly organized structures that consist of a large canal, called the Haversian canal, and concentric layering of lamellae. Haversian canals encase vascular networks within cortical bone, enclosing nerves and vessels and allowing for circulation of nutrients (reviewed by Martin et al., 1998; reviewed by Currey, 2002).

Beyond the organization of the microstructural component of bone, such as the lamellae and canaliculi, bone structure can differ on the macrostructural level as well. This variability, which is often continuous, divides bone into two types: cortical and trabecular. Cortical bone, as described by Currey (2002) is almost solid with a small amount of space devoted to vessels, resorption cavities, canaliculi, and osteocytes. Cortical bone is the major mineralized component of the vertebrate skeleton, making up the cortex of the bone surrounding the marrow filled cavity. Trabecular bone is characterized by larger, visable openings, and is found branching off of cortical bone into the marrow filled cavity. Like cortical bone, trabecular bone in young mammals is made up of woven bone, but in older mammals can be made of primary lamellar bone, or carved out of secondary bone. In trabecular bone, lamellae run perpendicular or oblique to its struts, creating jagged surfaces. The jagged surface appearance is not visable to the unaided eye. Trabecular bone structure is often described as consisting of two main structural components: plates and rods. Rods are formed by cylindrical struts of around 0.1 mm in diameter and 1.0 mm in length that typically form right angles in connection to other struts (Singh, 1978; Currey, 2002). However, this description is oversimplified and does not explain the range of variation that can be seen in the trabecular structure of even one individual.

2.2.3 Introduction to Bone Biomechanics

Mammalian bone (cortical and trabecular) is a dynamic tissue. Its formation and remodeling is highly coordinated with environmental stimuli: epigenetic, hormonal, and mechanical, which occur during development and adulthood (Currey 2002, Martin et al. 1988).

There are several types of forces that bones are routinely subjected to during development and daily activities: compression, tension, torsion, and shear. Compression occurs when forces apply pressure in a direction that reduces the volume of the object. Conversely, an object under tension is pulled from opposite ends. Torsion occurs when an object is twisted around an axis, and a shear force is one in which parallel forces are imposed on the object in opposite directions.

When a structure is subjected to some force, with a defined magnitude, direction, and location, it is said to undergo stress. In biomechanics, stress is defined as force per unit area, or

$$\sigma = \text{Force/Area}$$

and results in strain, or a measure of deformation.

$$\varepsilon = \text{change in length/ length}$$

$$\text{shear } \varepsilon = \text{change in angle}$$

Both values are important in understanding the behavior of a material.

Poisson's Ratio and Elastic Modulus

One useful mechanical description is based on the relationship between two measures of strain. When a material undergoes tension in the longitudinal directional, it lengthens in the longitudinal direction and in the case of most materials, shrinks in the perpendicular direction, or the transverse direction. The ratio between longitudinal and transverse strain is described as Poisson's ratio (reviewed by Evans, 1973; reviewed by Martin et al., 1998).

The stress and strain relationship produces what is called a stress strain curve, as illustrated in Figure 2.1.

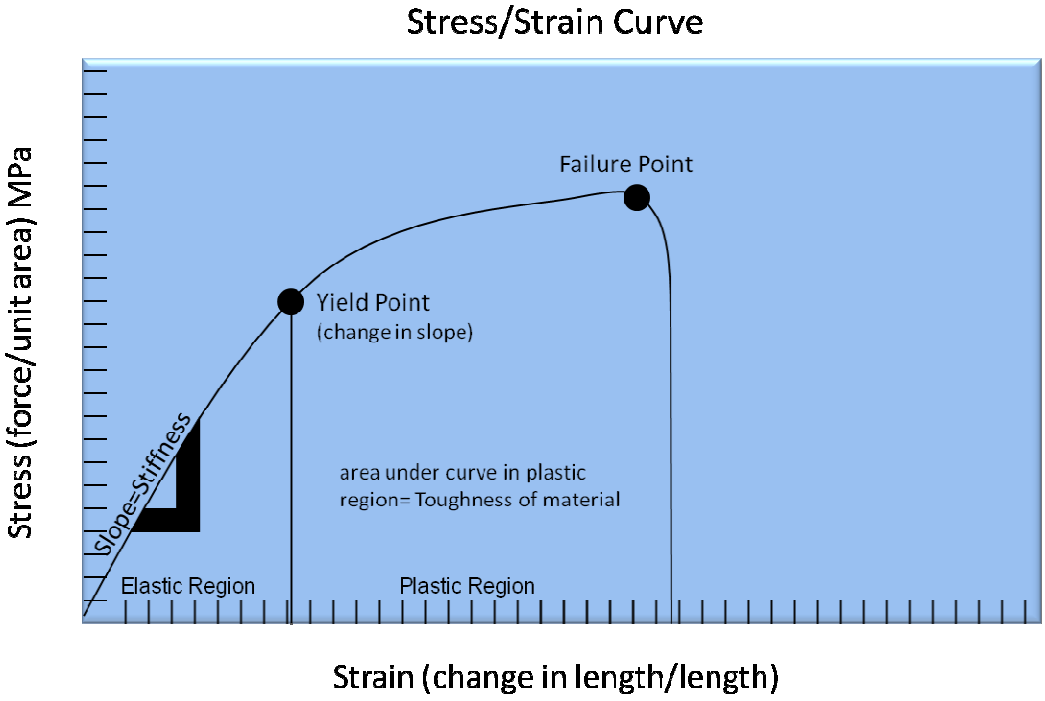

Figure 2.1 Stress/Strain Curve

The plastic region of the curve describes the behavior of the material under stress where permanent deformation occurs. The area under the plastic region of the curve provides a measure of the toughness of the material and is represented in units of work energy per unit volume. The ratio of stress to strain determines a material's stiffness. Under tension and compression, this value is called the elastic modulus, and under shear loading it is called the shear modulus. It is defined as the slope of a line tangent to the straightest part of the stress strain curve and it varies by material and direction. Shear and elastic modulus are usually measured in megapascals (MPa) in elastic solids (reviewed by Evans, 1973; reviewed by Martin et al., 1998).

If a material has the same elastic modulus in all directions, it is described as isotropic. However, most biological materials are not isotropic, but rather are anisotropic. Anisotropy can have several meanings depending on context. To declare that a material is anisotropic can

simply mean that there is a difference in elastic modulus in more than one direction. To measure an object's degree of anisotropy is to compare the elastic modulus, or similar directional vector in one direction of the material, to the elastic modulus in a direction orthogonal to it. There are two types of anisotropy in bone: transverse isotropy and orthotropy. Bone is most often transversely isotropic at a tissue level of organization, in that elastic moduli or directional prominence is equal or similar in two orthogonal directions and significantly different in the third direction. An orthotropic material differs in elastic modulus in all three directions. Stiffness can be influenced by structural variations on the microstructural (i.e., lamellae orientation in cortical bone) and macrostructural (i.e., trabeculae orientation in trabecular bone) level.

Ultrasonic testing on cortical bone samples gives values of elastic modulus based on the velocity of the ultrasound traveling through the material. The microstructure of cortical bone may be organized such that the bone is stiffer in one direction than another, in which case the ultrasound will travel faster in that direction. When using ultrasonic testing on cortical bone, elastic anisotropy is often described by a ratio of the elastic modulus in the direction of maximum stiffness to that in direction of least stiffness: E1/E2. In the case of larger structures, such as cancellous or trabecular bone, elastic modulus is not only affected by the microstructural component of bone organization but also by the gross level of bone organization: the composite direction of the trabecular struts. When assessing the anisotropy of trabecular bone, as well as other elastic properties, it is considered as a continuous material; this is because considering the elastic behavior of individual trabeculae is computationally difficult and it is the combination of many trabeculae that determine the elastic behavior (Harrigan et al., 1988). Due to the hierarchical organization of bone, describing its elastic properties can be challenging. However, great progress has been made in bone material research technology and methodology in the last 50 years, progress that began with early observations regarding the structural importance of bone.

2.3 Historical Outline and Technique Development

2.3.1 Pre 20th Century: Discovering the Relationship between Bone Form and Function

A historical outline of cancellous bone research by Koch (1917) disclosed that Galileo conducted important research on beam mechanics. In 1693, Galileo was the first individual to note the mechanical significance of bone form. Several attempts were made in the mid 1700s to describe the pattern of trabecular bone in the femoral neck and head, but it was not until the 1800s that investigators began to explore the relationship of cancellous bone architecture of the femoral head to its structure and function. In 1838, Ward attempted to identify a relationship between the cancellous structure of the femoral neck and its gross form, suggesting that trabeculae are organized in a manner that supports the extended neck. He believed that there were tensile stresses in the neck and compressive stresses in the head of the femur. In 1857, Wyman expanded on Ward's (1838) description of stresses in the femoral head and neck by studying the organization of trabeculae in a two dimensional cross section (Wyman, 1857; reviewed by Koch, 1917). He elaborated on a third type of trabecular structure that served to connect tensile struts (which extended from the lateral part of the shaft, curving to meet the middle of the articular surface of the head) with compressive struts (which run in straight lines from the medial shaft to the articular surface of the head). In 1858, Humphry noted that the struts form 90 degree angles with the articular surface of the head of the femur and each other (Humphry, 1858; reviewed by Koch, 1917).

In the mid 19th century there were primarily two individuals whose work on the cancellous bone of the femur would establish the direction of thought and discovery that followed: Carl Culmann and Hermann von Meyer (reviewed by Koch, 1917; reviewed by Cowin, 2001). Culmann, a German mathematician and engineer, became interested in trabecular bone structure in 1867, when he attended a meeting in which von Meyer proposed the importance of trabecular structure in a number of human bone specimens. Culmann theorized that certain structures could be characterized by lines of maximum internal stress. He compared von

Meyer's drawing of the trabecular structure of the human femur to a structure similar to it in shape, the Fairbairn crane. He found that the lines of stress calculated for the crane closely resembled the pattern of trabecular bone in the femur. These models inspired Julius Wolff's (1892) influential publication*, The Law of Bone Remodeling*. Wolff's (1892) model proposes that the struts of cancellous bone rigidly correspond to stress trajectories, forming right angles to one another, producing a direct and mathematical relationship between stress and trabecular structure. Although it is often given credit for being novel and revolutionary, some argue that the work of Julius Wolff is simply a summary of previous contributions to the field of bone biomechanics. Additionally, Cowin (2001; p 30-1) believes that many of Wolff's conclusions are based on a "false premise:" the assumption that stress trajectories in a solid, homogenous material resemble those in trabecular architecture. Wolff (1892) also proposed a relationship between trabecular form and the condition of bone in its static state (loaded only by normal body weight). Not only was his concept of static bone loading an unnatural depiction of environmental stress, but the reference of his hypothesis as a "law" misrepresents its validity and has propagated a misunderstanding of Wolff's contribution that continues in present times. The rigid relationship of trabecular bone form to function that Wolff (1892) hypothesized was repeatedly criticized by researchers in Wolff's time as well at present (reviewed by Koch, 1917; Cowin, 2001; Ruff et al., 2006).

2.3.2 Trabecular Bone Research in the Last 50 Years

Throughout the last 50 years, the relationship of trabecular bone form to function has been continually investigated and validated by many researchers (Lanyon, 1974; Hayes and Snyder, 1981; Biewener et al., 1996; Cowin, 2001; Pearson and Lieberman, 2004; Pontzer et al., 2006; Ruff et al., 2006). With the initiation of strain gage experiments in the late 1960s and early 1970s, researchers were able to compare trabecular and cortical bone morphology to observable strain patterns induced by real life activities, providing evidence for the basic theories of Culmann, Von Meyer, and Wolff (Lanyon and Smith, 1969; Lanyon, 1973; Lanyon,

1974). Using rosette strain gages, Lanyon (Lanyon, 1973; Lanyon, 1974) found that trabecular bone orientations in the calcanei of sheep were significantly correlated with principle tensile and compressive strain orientations. Hayes and Snyder (1981) showed that trabecular orientation corresponds greatly to the directions of principle stress in the human patella. Many studies in the 20th century also revealed important principles guiding bone biomechanics, regarding the relationship of trabecular architecture to mechanical function, unknown to Wolff (1892) and the scientists of his time. By looking at principle strain magnitudes and orientations during the development of the potoroos (a marsupial) calcaneus, Biewener et al. (1996) found that changes in trabecular orientation in response to stress occur during development and are unaffected by the removal of stress post development. Pontzer et al. (2006) conducted a study on the sensitivity of trabecular alignment in response to changes in load in the knee of juvenile guinea fowl, finding that trabecular bone formation is reactive to peak compressive forces. Rafferty (1998) determined that cortical and trabecular bone distribution in the femoral neck of *Pan*, *Homo*, *Pongo*, and a series of New World monkey species is a function of both body size and locomotor mode.

Also in the last 50 years, improved methodologies allowed researchers to more accurately describe trabecular bone structure and also to quantify material and mechanical properties. Singh (1978) classified trabecular bone into seven types based on examination of trabecular samples from different regions in the human body using a binocular loupe and a stereoscopic microscope at a magnification of x20. He determined that when plate-like structures replace the struts, the trabecular bone becomes more oriented. Therefore the degree of anisotropy is directly proportional to the relative number of plates within the trabecular network. See Table 1 for Singh's (1978) detailed description of variation in trabecular structure. A series of descriptive studies of trabecular structure from the 1970's, using a scanning electron microscope, found a broad range of variation in multiple trabecular descriptors (connectivity,

anisotropy, etc) that vary by anatomical location (Whitehouse et al., 1971; Whitehouse, 1974; Whitehouse and Dyson, 1974a; Keaveny and Hayes, 1993).

Feldkamp and colleagues (1989) were the first to use microcomputed tomography to analyze trabecular bone structure and claim that "the method has the potential for overcoming many of the limitations of current approaches to the study of bone architecture at the microscopic level" (Feldkamp et al., 1989: 3; Ruegsegger, 2001). Today, the main method of trabecular structural analysis is by microCT, in which high resolution x-ray tomographic scans are reconstructed and mathematical methods are used to determine structural properties, such as average trabecular thickness, separation, material[4] and apparent[5] densities, degree of anisotropy[6], and primary angle of orientation. Computed tomography is an ideal method for trabecular bone analysis because it is non-destructive and allows for visualization and testing of trabecular bone as a three-dimensional structure (Goulet et al., 1994; Ulrich et al., 1999; Laib et al., 2000). Micro-CT density measurements of 3-dimensional samples have been compared to those from 2-dimensional samples. Specifically, Kuhn et al. (1990) evaluated the accuracy of microCT to analyze bone volume fraction[7] (BVF) and trabecular plate density. They found that measurements from the micro-CT were very accurate based on the same measurements taken from histological sections. Methods for determining anisotropy, trabecular thickness, and separation, etc. are more accurate for 3-dimensional structures than for 2-dimensional, or surface based structures (Odgaard, 1997). Elastic properties can also be obtained from computed tomography scans through finite element analysis. Other methods used for obtaining the material and mechanical properties of trabecular bone include elastic/inelastic buckling,

[4] Material density is the density of bone material only, measured in mg of hydroxyapetite per cubic centimeter.
[5] Apparent density is the overall density of both bone and space within the bone; it is also measured in mg of hydroxyapetite per cubic centimeter.
[6] The degree to which trabecular struts are oriented in one direction; DA>1 means that struts are more oriented in at least one direction.
[7] Bone volume fraction is the ratio of bone volume to the total volume.

uniaxial tensile testing, bending tests, ultrasonic techniques, and micro and nanoindentation methods (reviewed by Guo, 2001).

Table 2.1 Description of Trabecular Bone by Singh (1978)

Type	Subtype	Plates and Rod	Thickness and Length	Orientation	Location
I		Fine straight or curved rods; delicate meshwork	0.08-0.14 mm diameter; 1 mm long	No prominent orientation	Found in many areas of the body, mainly in deeper portions of the ends of long bones and can extend into the shaft
II		Consists of both plates and rods			
	IIa	Similar delicate meshwork as type 1, but contains plates; varies in ratio of plates to rods	Plates are 0.1 to 0.2 mm thick and 1 mm long	Variable based on plate to rod ratio	Found in the ends of long bones, the body of the pubis, and in the glenoid fossa of the scapula
	IIb	Similar to IIa, but plates are more extensive and irregularly shaped, connected by smaller plates and rods, showing many fenestrations	Plates can be several inches long	Shows well marked orientation	Found in the calcaneus
	IIc	Plates are parallel, separated by rods, similar to those described as type 1 at a distance of .4-.8 mm	Plates are 0.16-0.3 mm thick and several millimeters in length	Shows strong orientation, as plates can retain their parallel pattern for up to a centimeter of space	Found close to articular surfaces, namely the lower end of the femur
III		Made up almost completely of plates that undergo lateral anastomoses			

Table 2.1-continued

	IIIa	Meshwork made up primarily of plates	Plates are 0.1-0.2 mm thick and 1 mm long	Strong or weak orientation	
	IIIb	Network of parallel plates with no rods present; plates anastomose to form tubular spaces	Plates are 0.12-0.24 mm thick; tubular spaces are 0.7-2.0 mm thick	Tubes are aligned with orientation of stress	Found in the ends of the tibia, neighboring articular surfaces; found in bodies of lower vertebrae
	IIIc	Thick plates separated by small spaces; a honeycomb like appearance is created due the enlargement of spaces moving away from the articular surface	Plates are 0.2-0.4 mm; spaces are 0.4-0.6 mm across		Found in dense trabecular regions at articular surfaces, i.e. the head of the femur, the patella, and the upper cervical vertebrae

Methods of Microcomputed Tomography

There are three methods primarily used to determine degree of anisotropy in a trabecular structure that can be applied to a 3-dimensional CT or u-CT scan. These are star volume distribution (SVD), star length distribution (SLD) and mean intercept length (MIL). The Scanco Medical uCT 35 uses the MIL method to determine the eigenvectors and anisotropy of trabecular bone structure. This method was first described by Whitehouse (1974) in reference to two pictures of trabecular bone cross sections taken with a scanning electron microscope. Whitehouse (1974) uses the Quantimet Analyzing Computer to measure the average length of trabecular bone and marrow interfaces by projecting a series of parallel lines in orthogonal planes. These averages are expressed as a function of direction and magnitude in the form of

eigenvalues. When eigenvalues are plotted as angles on a polar diagram, an ellipse is drawn. The ratio of the length from the origin to the longest edge to the length from the origin to the shortest edge is the ratio that expresses degree of anisotropy. Harrigan and Mann (1984) expanded Whitehouse's (1974) technique to include three dimensions, in which the plotting of mean lengths creates an ellipsoid (refer to Figure 2.2). Thus, by plotting the mean intercept lengths on a polar diagram, three values that describe such an ellipsoid also represent magnitude and orientation of direction in orthogonal planes of a three dimensional structure. A ratio of the greatest vector to the least provides a single unit description of a degree of anisotropy.

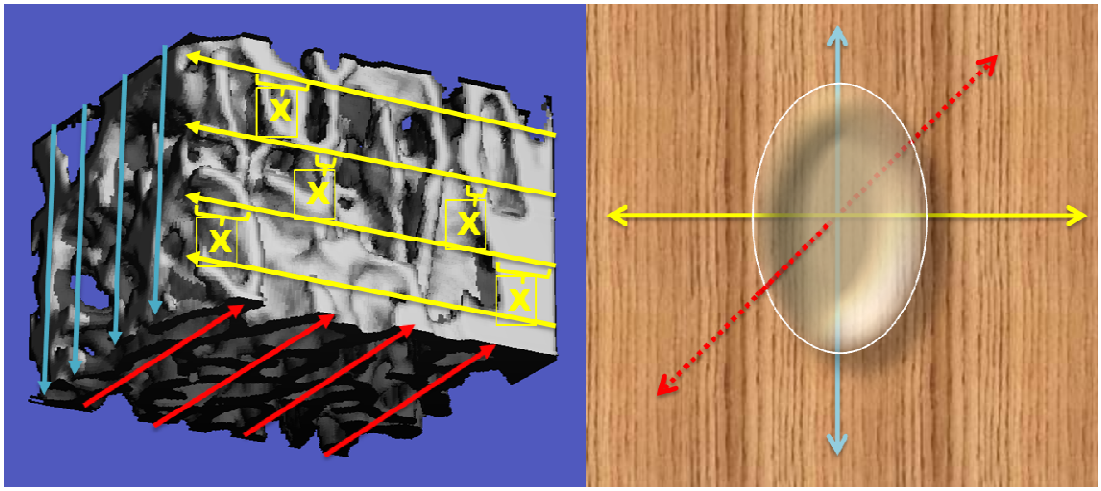

Figure 2.2 MIL Method and Anisotropy Ellipsoid; the mean of x in each plane when plotted on polar diagram always forms an ellipsoid

The star volume distribution method (SVD) was created by Cruz-Orive et al. (1992) as a simple method to characterize anisotropy of steel, but can be carried over to other materials, such as trabecular bone. With this method, a conical beam radiates from a random point, x, within the material and terminates along the termination of bone. The volume of the beam is a function of the direction in which in radiates, and these volumes, based on the placing of

multiple points, x, are averaged and multiplied by 4π, to obtain the star volume distribution. This method is similar to the SLD, shown in Figure 2.3, described by Odgaard (1997), except that instead of a cone, a line radiates from point x.

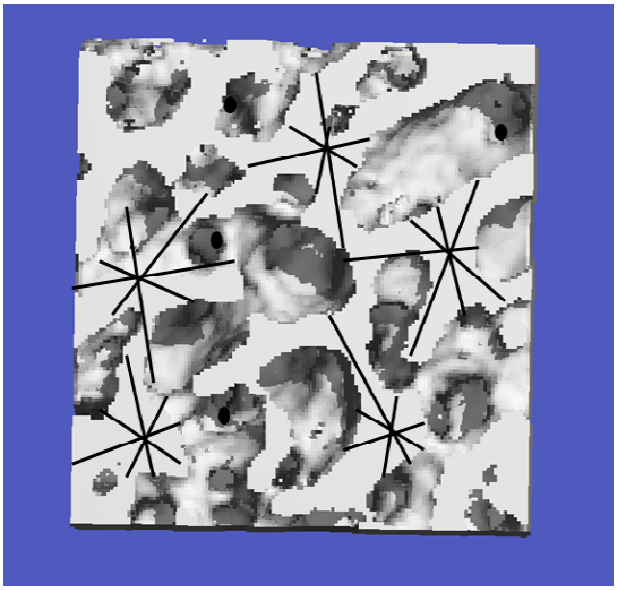

Figure 2.3 Star Length Distribution Method; lines radiate from randomly placed points within a volume; these vectors are used to estimate anisotropy, average thickness and separation, etc.

There is some debate over the best method for calculating anisotropy. Ketcham (2005) compared the MIL, SVD, and SLD methods and also looked at the effects of shape of the volume of interest and the number of orientations and points that are sampled. He suggested that MIL measurements are affected by spatial distribution or the shape of the volume of interest and that the most ideal results are obtained from spherical volumes of interest. However, Laib et al. (2000) claim that the MIL method programming for the Scanco Medical uCT is not affected by the edges of the volume of interest, making a volume of interest that encompasses the entire trabecular region a more accurate measure of its anisotropy (as a spherical volume of interest inevitably neglects large regions of trabeculae within the bone cavity). Ryan and Ketcham (Ryan and Ketcham, 2002) also argue that trabecular orientation distribution does not always

conform to the ellipsoid shape proposed by Whitehouse (1974) and Harrigan and Mann (1984) . Using rose diagrams calculated from the SLD method, they show that while elliptical in nature, these distributions may be quite irregular, and the predicted maximum eigenvector may not be the actual maximum eigenvector. In conclusion, multiple methods exist for determining the degree of anisotropy in a three dimensional structure, and there is unresolved debate as to which of these methods provides the best determination of DA.

Mean intercept length can also be used to calculate trabecular separation, thickness and number; however, it is suggested by the Scanco Medical uCT user guide that the values obtained by MIL for those particular parameters are affected by the shape of the sample. Therefore, the Scanco Medical uCT 35 also provides these values determined by the distance transformation method. This method, created by Hildebrand and Rüegsegger (1997), works by placing spheres in every area of the sample, occupying both space and bone (Figure 2.4). The diameter of each sphere is contained in either volume. The diameters of each sphere in either space are averaged, controlling for the shape and volume of the sample. These values are expressed as a value per millimeter or cubic millimeter. For example, a sample with a trabecular number of 0.8 would be expressed as an average of 0.8 trabeculae in every one cubic millimeter. A trabecular separation of 2.1 mm would mean that the average distance of separation between trabeculae in the sample is 2.1 mm.

.

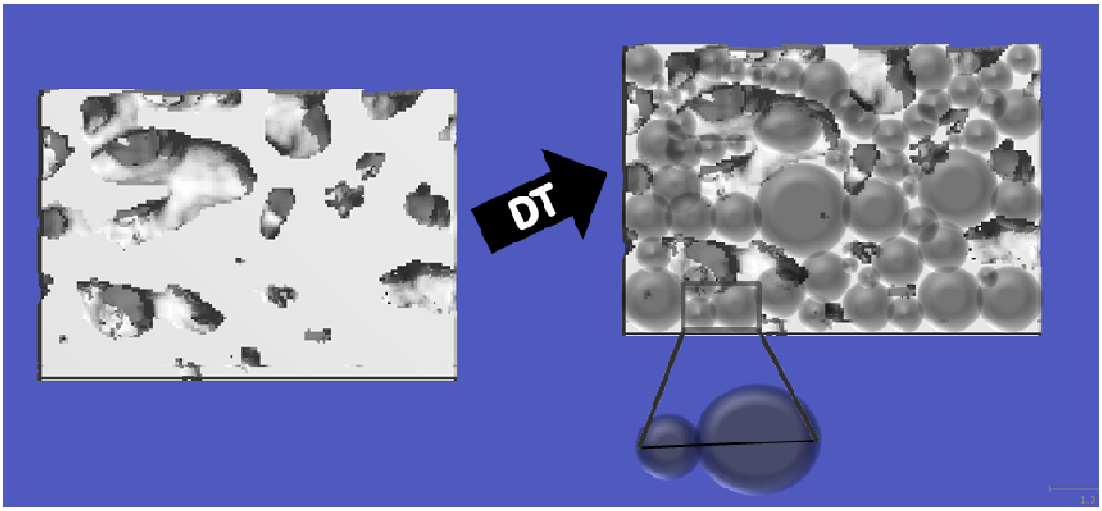

Figure 2.4 Distance Transformation Method; the sphere diameters are averaged to obtain trabecular thickness and separation

Micro-CT software can also be used to test the mechanical properties of trabecular bone structure through finite element analysis. Building a finite element model of trabecular bone from a micro-CT scan is ideal as the density and architectural properties of the scanned trabecular bone can be included directly as part of the model. A higher resolution provides a more accurate analysis of the structural characteristics of bone, such as density, connectivity, thickness, number, and anisotropy and therefore a more accurate finite element (FE) model (Harrigan and Mann, 1984; Feldkamp et al., 1989).

Most finite element (FE) studies of skeletal structures that include trabecular bone model it as a continuum, because if the trabecular bone were modeled with structural detail, it would increase the complexity of the model beyond that which can be easily solved with most available computers. Yet this assumption has been criticized by Harrigan et al. (1988). Trabecular bone modeled as a continuum, or cellular solid, results in the averaging of its material properties throughout the structure. This averaging is problematic at cortical and trabecular bone interfaces and where there are large stress gradients (Harrigan et al., 1988). Bourne and van der Meulen (2004) show that FE models that account for this variation, by using high resolution scans, are more accurate than FE models that assume trabecular structure and

density are homogeneous. Finite element modeling of micro-CT scans of trabecular bone has proceeded in a number of other studies (Van Rietbergen et al., 1995; van Rietbergen et al., 1998a; Van Rietbergen et al., 1998b; Van Rietbergen et al., 1999; Nomoto et al., 2006). It is clear that possible variation in trabecular structure cannot simply be ignored in studies of craniofacial skeletal function, yet this area has received virtually no investigation; there are no data on variation in material properties of trabecular bone at any level that are available for incorporation into FE models of primate craniofacial structures.

The Form and Function of Trabecular Bone

Along with the cortical component of bone, the trabecular component is important in predicting the overall mechanical behavior of a whole bone or skeletal region. Studies in the late 20th century focused on identifying the specific correlations between particular bone material properties, such as density or surface area to volume ratio, and bone mechanical properties. Interpreting the relationship between material and structural properties of bone and bone stiffness and strength is difficult; such relationships vary by anatomical region, by species and among individuals within a species. Several studies described in the paragraphs following illustrate the complex interactions of trabecular bone structure and function.

As in cortical bone, material density, or bone mineral density (BMD), and apparent density are reliable estimators of trabecular bone stiffness and strength (Carter and Hayes, 1977a; Rice et al., 1988; Ulrich et al., 1999). Turner (1989, 1992) used data from his study of bovine trabecular bone to conclude that 90% of the variance in yield strain and 70-78% of the variance seen in the elastic modulus can be explained by density and textural anisotropy. Goldstein et al. (1993) found that among one hundred human trabecular specimens from human postcranial metaphyseal regions, 80% of the variation in elastic modulus and strength could be explained by density and orientation. Trabecular bone elastic modulus in postcranial human and bovine bone ranges from 0.76 to 20 GPa (reviewed by Guo, 2001).

Many bone biomechanical studies have examined the relationship between the apparent density and the mechanical properties of trabecular bone (Keaveny and Hayes, 1993). Based on compression tests of human and bovine cortical and trabecular bone samples, Carter and Hayes (1977b) found a power relationship between not only apparent density and strength, but apparent density and modulus as well, in which strength is proportional to apparent density squared, and the modulus is proportional to apparent density cubed. Using data from other experiments, Rice et al. (1988) also found a squared relationship between modulus and apparent density. More recently, Morgan et al. (2003) showed that the relationship between elastic modulus and apparent density is site-dependent, in that elastic modulus prediction error can increase by as much as 60% if the issue of site-dependence is ignored.

As shown by Turner (1992) and Goldstein et al. (1993), the amount of anisotropy and the stiffness orientations are also important influences on the mechanical behavior of trabecular bone. The anisotropy of trabecular bone has a significant influence on overall bone strength, and differences in orientation affect the behavior of bone in certain stress conditions (Turner, 1992). Other structural indices are also important in determining the mechanical properties of trabecular bone. Ulrich et al. (1999) used microCT FE and bone morphometric analysis[8] to determine the relationship between the elastic properties of trabecular bone and various mechanical properties of 242 samples of trabecular bone from the femoral head, the calcaneus, the iliac crest and lumbar vertebrae of 70 human donors. They found that several structural characteristics, when combined with bone volume fraction (BVF)[9] improved the correlation, expressed as R^2, with stiffness and strength estimates. Specifically, R^2 values increased from 53% to 82% when degree of anisotropy (DA) was added to BVF values in predictions of elastic properties in the femoral head specimens. The further addition of trabecular separation (measured in mm) to BVF and DA values increased R^2 to 92%. However, these percentages

[8] Bone morphometric analysis produces material property data determined by distance transformation and MIL.
[9] Bone volume fraction is defined as the ratio of bone volume to the total volume.

varied by anatomical location, such that degree of anisotropy had the greatest predictive power in the femoral head and trabecular separation had the greatest predictive power in the calcaneus.

Studies of the material properties and mechanical behavior of trabecular bone in recent years have demonstrated that the two share a complex relationship which is site, individual, and species dependent. The variability seen in this relationship emphasizes the importance of looking at trabecular structure and function in all areas of the skeleton and among multiple species.

2.3.3 Conclusion

Researchers first began to describe trabecular bone patterns in the human femoral neck in the mid 1700s, and by the 1800's they began to explore the relationship of trabecular bone architecture to overall bone function (Koch, 1917). Twentieth century bone biomechanical research relied on improved methodologies to describe a range of trabecular bone material and mechanical properties (Whitehouse, 1974; Whitehouse and Dyson, 1974b; Singh, 1978). The most prevalent methodology used for determining the material properties of trabecular bone today is microcomputed tomography; this is because it is non-destructive and allows the testing of trabecular bone as a three-dimensional structure, as opposed to two-dimensional images which are limited to analysis in the x and y plane (Goulet et al. 1994; Laib et al. 2000, Ulrich et al. 1999). Microcomputed tomography can also be used to gather data on the elastic properties of trabecular structure through finite element analysis. Through micro-CT analysis, using computational methods such as MIL and distance transformation, material properties such as bone mineral density (BMD), apparent density, and anisotropy have been shown to reliably predict trabecular bone stiffness and strength (Carter and Hayes, 1977a; Rice et al., 1988; Turner et al., 1990; Turner, 1992; Ulrich et al., 1999). Recent studies of trabecular bone have demonstrated that its form and function share a complex relationship which is site, individual,

and species dependent. This variability reaffirms the importance of looking at trabecular structure and function in multiple areas of the skeleton and among multiple species.

2.4 The Mechanical Significance of Supraorbital and Zygomatic Regions in Anthropoids

2.4.1 Introduction

There has been extensive research on the zygomatic and supraorbital regions in primates from the biomechanical perspective, but this work has focused mainly on external form and not on internal structure. This perspective assumes that macro and micro bone structure results from adaptation to strain produced by muscle contraction and other forces applied to bone in an individual's life. Many have hypothesized that increased prominence and robusticity of the zygoma and browridge is the result of greater muscular activity due to the repetitive mastication of harder food items (Rak, 1983; Strait et al., 2009). Endo (1966), through experimentation on human cadavers, found that the browridge does experience strain during incisal biting. As the masticatory muscles on the side of the skull contract, there is a downward tensile force placed on the browridge and an upward compression created by the bite force. As this stress occurs repetitively throughout the lifetime of the individual, presumably the bone in the area will respond by modeling and remodeling in response to the functional demand. Rak (1983) hypothesized that the robust zygomaticoalveolar region found in australopithecine crania served as a pillar of support during the mastication of hard food objects, but that the lateral orbital wall in these animals served a similar purpose as in *Homo* and *Gorilla*, enduring tensile strain in response to the temporalis and masseter muscle usage. He also hypothesized that the more robust *Paranthropus bosei* have a more pronounced and protruding browridge because the masseter muscle origin site differs, relieving the lateral orbital wall of heavy tensile stresses. Because mastication occurs regularly throughout life, it is an ideal explanation for craniofacial cortical bone remodeling, if such models can be truly validated. Facial robusticity resulting from greater mastication forces is also an explanation within an evolutionary context, as the most robust supraorbital and zygomatic regions occur mostly among species with other robust cranial

features, such as *Paranthropus*. Members of the genus *Paranthropus*, or the robust australopithecine group, are theorized to be adapted to a harder, more bulky diet than contemporaneous hominid species (Rak, 1985; Teaford and Ungar, 2000).

2.4.2 *Endo and the Beam Model*

The most widely used model of strain for the supraorbital region is Endo's (1966) beam model. Endo (1966) modeled the face using a series of beams, including a beam representing the browridge. He established four primary sources of strain in the facial region: the masseter muscle, the temporalis muscle, the joint reaction force (which occurs at the temporal-mandibular joint), and bite force. Endo (1966) tested this model using 24 dry adult crania from Japan and one gorilla. Strain gages were applied to the middle and upper portions of the face of the specimens. Tension was applied to pieces of canvas glued to the skull in order to simulate muscle forces. Strain gage testing on the crania showed fairly consistent results compared to strain gage testing on a beam model. Endo (1966) made several observations related to the loaded browridge based on this model. First, when the front teeth were loaded, the lower third of the frontal bone experienced strain. Second, incisive and canine loading, and not molar loading, produced the largest strains in the supraorbital region. Third, loading of the anterior teeth produced the greatest strain in the medial and lateral portions of the supraorbital region. Endo's (1966) explanation was that the forehead, if positioned more vertically in relation to the bending stresses produced by vertical bite forces, would be more effective at resisting masticatory stress. On the other hand, more of a sloping forehead would require some type of buttressing, as seen in a more prominent browridge. Endo (1966) therefore concluded that the structure of the supraorbital region is due to the effect that bending stresses have in this area.

Given Endo's (1966) demonstration of the browridge as a beam, other studies attempted to model the biomechanical relationships in the face (Russell, 1983, 1985). Russell's (1985) study, for example, concluded that supraorbital development is proportional to the level of stress that accompanies habitual tooth loading. She found that there are significant average

increases in net bending stresses that correspond to a significant increase in the supraorbital development of young and middle aged females. However, Hylander and colleagues (Hylander and Picq, 1989; Picq and Hylander, 1989) argued against several of the assumptions upon which these studies were based.

After an analysis of Endo's (1966) study, Picq and Hylander (1989) came to three main conclusions concerning the interpretations of his data. The first issue they raised was with Endo's (1966) conclusion that the relative magnitude of strain in the supraorbital region is similar to that in other areas of the craniofacial skeleton. They pointed out that strain in the browridge is low relative to strain magnitudes in other regions of the face. Second, Picq and Hylander (1989) believed that the muscle simulation procedure used by Endo (1966) is problematic. They pointed out that while the strain in the supraorbital region is higher during loading of the anterior teeth, Endo's (1966) simulated muscle forces were regionally disproportionate, with greater muscle force occurring for anterior tooth loading than posterior tooth loading. Finally, Picq and Hylander (1989) note that while a beam may be a more accurate model for the ape browridge, it is not an accurate model for human supraorbital loading, as the supraorbital region in humans is positioned more vertically. Picq and Hylander (1989) pointed out that Endo (1966) did recognize this, but he still continued to support the use of the beam model for the mechanical study of the human supraorbital region.

As a result of these observations, Hylander et al. (1991) conducted a strain gage experiment to test the hypothesis that browridge development in primates is responsive to masticatory stress. In this *in vivo* experiment, the authors attached strain gages to the supraorbital region of 5 adult (3 female, 2 male) crab eating macaques, *Macaca fascicularis,* and one olive baboon, *Papio anubis,* all under anesthesia during surgery. Strain gages were attached to the dorsal interorbital region and the lateral surface of the zygomatic arch in one set of three experiments, and attached to the dorsal orbital region and the lateral surface of the zygomatic arch in one set of four experiments. The monkeys were then fed foods of a variety of

hardness, including monkey biscuits, carrots, almonds, and prunes. The strains produced by the mastication sequence of each food item were recorded and strain patterns were digitized. This analysis, which was designed to detect the bending of the skull in the frontal plane and the twisting of the skull around an anteroposterior axis, found that the browridge in primates is bent in the frontal plane, but that there is no evidence to support that the browridge experiences higher strains as a result of incision as opposed to mastication. Hylander et al. (1991) stated that browridge morphology is not a product of masticatory loads, because strain detected in the area is low relative to other areas of the face, including the zygoma and the zygomatic arch. Based on strain gage analysis of the zygomatic arch, Hylander and Johnson (1997) found that the strains observable in the zygomatic arch are highly variable by region, with the highest strains found in the anterior region, intermediate strains found in the middle of the arch (anterior to the zygomaticotemporal suture) and the lowest strains observed in the posterior region (posterior to the zygomaticotemporal suture).

2.4.3 Conclusion

Beam models and strain gage experiments have been highly useful in the field of biomechanics. They have shown that there is significantly less strain in the supraorbital region compared to the zygomatic region and the zygomatic arch, and they have shown that the supraorbital region in anthropoids experiences bending in the frontal plane during mastication. However, as Hylander and colleagues (1989; 1991) point out, a beam is not accurate enough to model the supraorbital region and beam and plate models leave many unanswered questions about the response of various primate craniofacial morphologies to different magnitudes of loading (Hylander and Johnson, 1997; Ross et al., 2011). In more recent years, the advancement of modeling techniques has allowed for more accurate modeling of the primate craniofacial region. Ross et al. (2011) combine strain data from previous studies with their own strain data from the supraorbital and zygomatic regions (including the arch) of *Macaca* crania to validate an *in silico* model created by a CT scan and to test several hypotheses regarding the

craniofacial morphology of several primate species. They hypothesize that "low strained bony sheets around the orbit" in the primate face are adapted to provide support for the brain, and eyeball, and musculature involved in mastication (Ross, 2001; Ross et al., 2011 ; p 9). The advanced form of modeling and analysis used by Ross et al. (2011) reconstructs the actual gross morphology of a cranium using a finite, yet large number of three dimensional simple elements; it is therefore able to produce a more realistic interpretation of the effects of bite and muscle force on the bone of the craniofacial skeleton.

2.5 Finite Element Analysis and Primate Evolution

2.5.1 Introduction

Finite element modeling and analysis (FEM and FEA, respectively) is an engineering tool that has recently become attractive to functional morphologists who explore the relationship between force and bone structure by observing deformation from loading in extant and extinct species (Richmond et al., 2005). In finite element studies, a geometric computer model of the structure of interest is created and then "meshed," a process that transforms the geometric structure into a finite number of simpler, smaller elements, or shapes, which are connected by nodes. The more complex and dense the mesh is, the more accurate the results will be. However, the computations are lengthier and more difficult to solve as the complexity of the mesh increases. Researchers cope with this relationship by making only particular regions of interest complex, other areas coarse, and in general reducing the size of the model to focus on the areas of primary interest.

Once the mesh is created, the model requires the input of the material properties of the structure such as Poisson's ratio, elastic modulus, and heat conductivity. The selection of material properties to incorporate is dependent on the type of material being modeled, whether or not it is isotropic, orthotropic, or transversely isotropic, and the physical conditions of the function being modeled (time, force and temperature factors, for example). Essential and non-essential boundary conditions are defined to simulate the stabilization of the object and the

forces being applied to the object, respectively. The elastic properties at each node and the force applied are used to determine the displacement of the nodes (or deformation of the model). The final step in FEA is validation, which is ideally carried out through in vivo and in vitro strain gage analysis.

Applications of FEA to functional morphology include modeling the response of individual bones to applied loads and comparing the response of morphologically varying skeletal designs (Richmond et al., 2005). FEA is particularly useful in that it provides a means for testing functional hypotheses regarding fossil primates, such as those surrounding the confounding variation seen in the cranial morphology of fossil hominids. Researchers interested in the cranial morphology of hominids have used FEA to explore the functional significance of variation in cranial structural features in extant and extinct primates, such as in the palate, zygoma, alveolus, cranial sutures, and masticatory muscles (Strait et al., 2005; Wang et al., 2006a; Strait et al., 2007; Kupczik et al., 2009; Strait et al., 2009).

2.5.2 Experimentation

Kupczik et al. (2009) conducted an *in vivo* strain gage experiment on juvenile individuals of *Macaca fascicularis*. Their goal was to test the relationship between the development of the browridges and masticatory stresses in the crab-eating macaque. They developed three CT based FE models of the macaque skull and applied masticatory forces estimated from the physiological cross-sections of the chewing muscles of the specimens. Each model was strained at varying bite points during FEA, and a strain energy density (SED)[10] map was created during postprocessing and superimposed upon the cranium. Similar to Picq and Hylander (1989), Kupczik et al. (2009) found that while strain is high in the zygomatic arch and the infraorbital areas, strain values recorded for the supraorbital region are comparatively low.

Ross and colleagues (in press) conducted in vivo strain gage analysis on the intraorbital surface of the supraorbital bone, the postorbital bar and septum, the anterior surface of the

[10] Strain energy density describes the concentrations, or magnitudes of strains in various skeletal regions.

postorbital bar, and the anterior root of the zygoma of *Macaca,* adding to data previously obtained from in vivo strain gage studies on the browridge, zygomatic arch, and medial orbital wall (Hylander et al., 1991). They used the combined data to validate a finite element model of a macaque and to test several hypotheses about deformation patterns in the craniofacial region of macaques based on the simpler models posited by Endo (1966), Rak (1983), and Hylander et al. (1991). After validation of the finite element model of the macaque cranium, they found that during mastication, the zygomatic arches undergo twisting and bending from masseter muscle force around an axis drawn from the anterior and posterior attachment of the muscle to the bone. Further, the twisting and bending of this region applied inferolaterally directed tension on the lateral region of the inner orbital wall, the infraorbital plate, and the anterior arch. This tension caused the curvature of the lateral orbital wall to bend outwards, or straighten, and this created compressive forces along the superior surface of the browridge and tensile forces on the inferior surface of the ridge. Tension in the superolateral and inferomedial regions and compression in the inferolateral and superomedial regions of the orbit was also observed. Ross et al. (in press) compare the deformation regime observed in their macaque model to Endo's (1966) data on stress and strain observed around the orbits in *Homo* and *Gorilla,* finding that all three species undergo a similar pattern of deformation in this region.

Using the macaque finite element model, Ross et al. (in press) demonstrated the high concentration of strain in the zygomatic arch and the anterior root of the zygomatic arch. The anterior root of the zygomatic arch sits medial to the masseter muscle and superior to the tooth row causing it to be subjected to high compressive and tensile forces. They claimed that the high tensile and compressive strains observed in the anterior root of the zygoma suggest that the region undergoes high shear strain. Because bone is weakest under shear strain, they argued that this region is a significant feeding adaption. In the in vivo model, Ross et al. (in press) found that chewing side did not have a significant effect on strain magnitude and orientation in the supraorbital and zygomatic regions, and they concluded that the primary

sources of strain in these areas originate from muscle forces. Unlike Endo (1966) they found that the portion of the supraorbital region that endures the greatest magnitude of strain during mastication is the postorbital bar.

2.6 The Mechanical Properties of Cortical Bone in Humans and Primates

As emphasized by Richmond et al. (2005), defining the material properties of the mesh elements is essential to producing an accurate FE model. However, this is one of the most challenging aspects of FE modeling, as bone is not isotropic, material properties vary from region to region, and different bones have macro and microstructural variance, such as in trabecular bone and within cortical plates.

The temperature, moisture, internal and external architecture, and the loading conditions (orientation and strain rate) of bone all influence its material properties. The material properties pertinent to this study include material density and bone volume fraction; degree of anisotropy, which quantifies differences in structural fabric orientation; elastic and shear modulus, or the ratio of unit stress and unit strain under tension/compression and shear respectively; and Poisson's ratio, which measures the ratio of the transverse strain to the axial strain (Evans, 1973; van Rietbergen et al., 1998a; Currey, 2002) . These values are interpreted in the context of strain rate and the orientation of strain. For instance, if less deformation occurs, and a lower elastic modulus is observed, in one direction as opposed to another, it can be suggested that the bone *may* be adapted to greater levels of strain endured in that direction throughout the life of the organism.

The mechanical properties of human and non-human primate craniofacial cortical bone have been studied extensively by researchers such as Dechow et al. (1993), Schwartz-Dabney and Dechow (2003), Peterson and Dechow (2002, 2003b), Peterson et al. (2006), and Wang et al. (2006b). Collective findings strengthen the hypothesis that the microstructure of bone is influenced by consistent epigenetic and environmental forces, including function, throughout the life of the organism. Importantly, they also reveal a significant amount of variation in mechanical

properties by region, among individuals and between species. These findings highlight the significance of understanding how the many components (micro and macro) influence the response of the whole structure. Studies of human cortical bone use wet and dry weight and thickness measurements to determine density. They use ultrasonic wave techniques to determine directions of maximum and minimum stiffness, and ultimately the elastic properties of specific craniofacial sites.

Dechow et al. (1993) found that the mechanical and material properties of cortical specimens obtained from the human supraorbital region and the buccal side of the mandible vary significantly by region (Dechow et al., 1992; Dechow et al., 1993). Mandibular bone was found to be stiffer than supraorbital bone, suggesting that the elastic properties of cortical bone may indicate variations in function by region.

Peterson and Dechow (2002) conducted such tests on the outer and inner tables of human parietal bone. They recorded higher densities in samples from the outer table of parietal bone, and found differences in the significant values of anisotropy between the outer and inner tables of parietal bone. These findings demonstrate how bone's many structural components may contribute disproportionately to its mechanical behavior as a whole. Cortical samples from the parietal were found to be transversely isotropic with DA similar in magnitude to that found in the diaphyses of long bones. Unlike cortical bone from compressively loaded long bones, such as the femur and tibia, the directions of maximum stiffness among these samples did not display any significant patterns in orientation. This suggests that cranial and long bone regions have similar microstructural properties, but that there are different and/or less consistent patterns of loading. Similarly, Peterson and Dechow (2003b) found 9 out of 36 sites sampled within the parietal, frontal, temporal, occipital, and zygomatic bones with statistically significant mean directions of maximum stiffness. Five of these were locations of muscle attachment, including one on the zygomatic arch, one between the temporal line and the sagittal suture of the temporal bone, and three on the parietal bone. The sample site on the zygomatic process of

the zygomatic bone had the largest directional value, and therefore the greatest anisotropy, and was also the only site with a significant mean direction of stiffness across individuals in the sample group. A possible explanation for the site's uniqueness provided by Peterson and Dechow (2003b) is that the masseter muscle attachment at this site is less complex than other muscle attachments, such as the temporalis or the nuchal muscles, and also has less surface area for attachment. The results of this study suggest that muscle attachments influence the elastic properties found in specific regions of cortical bone. Similar testing on the maxillary region of 15 adult dentate humans revealed regional variations in the principle axes of stiffness and cortical thickness (Peterson et al., 2006). The elastic properties determined for this region were on the whole more variable than those determined by Schwartz-Dabney and Dechow (2003) for the mandible.

Wang and Dechow (2006) found significant differences in elastic properties in the rhesus cranium compared to the same sites in human crania, and significant differences between sites with different functions. Wang et al. (2006b) showed that values of cortical density, thickness, shear and elastic moduli, and anisotropy vary by primate species and that the pattern observed in baboons is similar to the more closely related macaque and differs from the pattern observed in human crania.

Experimentation on the mechanical properties of cortical bone has shown that there is inter and intra-specific variation in craniofacial cortical bone microstructure. However, these studies do not tell us much about the importance of these variations and their overall effect on the craniofacial region among different species. A study by Strait et al. (2005) tested the effects of various mechanical properties on the analysis of a FEM of the cranium of *Macaca fascicularis*. They used four different sets of mechanical property data, including isotropic data from a human limb bone, isotropic data from a single cranial location of *Macaca mulatta*, isotropic data from multiple corresponding cranial locations of *M. mulatta*, and orthotropic data from corresponding cranial locations of *M. mulatta*. They validated the results of each analysis

with strain gage data. They determined that strain concentrations in all models were similar; however, they found that the fourth model produced the most accurate deformation pattern. This study suggests that the quantification of the mechanical properties of craniofacial trabecular bone in human and nonhuman primate taxa will improve the results of finite element modeling.

2.7 The Importance of Cellular Accommodation to Bone Remodeling

Studies of the mechanical properties of cortical bone in the human craniofacial complex by Dechow and colleagues suggest that low strain regions are possibly affected by function. Dechow et al. (1993) determined the mechanical properties of human cortical bone from various locations in the craniofacial region. Due to the results of Picq and Hylander (1989), which suggested that the supraorbital region received relatively little strain due to mastication, Dechow et al. (Picq and Hylander, 1989; 1993) hypothesized that the region would exhibit lower elastic moduli than other craniofacial regions. While the elastic modulus of the browridge was less than that of the mandible in this experiment, the authors still conclude that it appears that the browridge is adapted to resist some magnitude of loading. They found that the bone tissue in the supraorbital region is transversely isotropic and therefore possibly adapted to resist loads in directions parallel to the frontal plane.

Furthermore, Dechow et al. (2010) found significant differences in the material properties of craniofacial bone between dentate and edentulous human crania, suggesting that functional forces are important influences on the material properties in the maxillary, zygomatic and frontal regions. Specifically, the study found that various craniofacial regions in edentulated human crania, when compared with those of dentate crania, had lesser cortical bone thickness and fewer significant directional orientations (anisotropy) in all regions. Edentulous samples had similar or greater values of density in the frontal bone, greater values of density in the zygomatic region, and lower density in the maxillary region. Elastic and shear moduli differences varied by region, alluding to the complexity of bone remodeling by region,

presumably due to changes in loads and patterns of mastication following the loss of teeth and adaptation to denture use (Dechow et al., 2010). Even though the browridge region undergoes markedly less strain than the zygomatic region during molar and incisal mastication, its material properties and overall structure are responsive to changes in masticatory forces. The studies by Dechow et al. (1993; 2010) challenge the assumption that bone remodeling in the supraorbital and zygomatic regions responds equally to peak strains induced by mastication.

The inconsistency between observable strain patterns and the mechanical properties in upper and mid-craniofacial regions could be biochemical. One of the most important contributions of strain gage studies to bone biomechanics is the concept that all vertebrate bones, with only few exceptions, are adapted to withstand a particular range of strain (Rubin and Lanyon, 1982; Frost, 1987; Martin et al., 1998). Frost (1987) proposed that bone mass is determined through a mechanical feedback system which is regulated by hormones and biochemical agents. These hormones and biochemical agents regulate the remodeling response by adjusting the minimum effective strain (MES)[11] of what he calls "the mechanostat". If strain goes below the MES, then bone loss occurs. Frost (1987) suggested that, during normal activity, most vertebrate bone remodels to maintain strain levels between 100 and 1500 microstrain. The typical range of peak strains for vertebrate long bones during vigorous activity is between 2000 and 3000 microstrain (Rubin and Lanyon, 1984; Martin et al., 1998). Strain gage studies suggest that bone in all species remodels to optimize its performance relative to strain.

Turner (1999) elaborated on Frost's (1987) mechanostat theory by proposing the "theory of cellular accommodation." Theoretically, bone cells react strongly to initial changes in mechanical environment, yet the reaction slows down or stops once the cells accommodate to change. The resulting bone mass is then determined by the mechanical or hormonal temporal sequence preceding it. As is demonstrated by Schriefer et al. (2005), in the tibia of rats, there is

[11] The minimum value of strain required to activate a remodeling response.

a greater bone remodeling response to an initially large mechanical load which trails off compared to an initially small load which grows in magnitude. Cortical bone volume fraction of rat tibias that experience an initially large mechanical load that decreases through time will be greater than in those that undergo a smaller, but constant, application of bone loading, which will itself induce more bone formation than an initially small mechanical load that increases over time, assuming that all scenarios maintain the same average amount of loading (Schriefer et al., 2005). Similar experimentation on trabecular bone reveals the same relationship (Kim et al., 2003).

Kupczik et al. (2009) explore the possibility that the supraorbital region is primarily modeled and remodeled in the juvenile primate. They suggest that the comparatively low strains observed in the region in adulthood indicate ontogenetic adaptation. Theoretically, the strains in the supraorbital region of juveniles are higher than those in adults, creating a greater bone remodeling response. Contrary to their hypothesis, Kupczik et al. (2009) find that in juvenile crab-eating macaques, supraorbital strains are not high enough to warrant a bone modeling or remodeling response that results in a robust browridge. While their study cannot support the hypothesis that the supraorbital region is primarily an adaptation to mechanical environment, they do suggest other explanations for browridge development based on Frost's (1987) and Turner's theories (1999). Because MES is site and age dependent, it could be that the MES of the supraorbital region is very low compared to the zygoma. Therefore, the browridge may have a lower strain threshold and demonstrate a greater bone remodeling response than the zygomatic region, which must have a greater strain threshold in order to withstand more frequent loading of a greater magnitude (Turner, 1999; Schriefer et al., 2005; Kupczik et al., 2009). Another possibility could be related to the growth rate of each region. Even though the zygoma is a high strain region, it undergoes very slow growth, while the browridge, which shows very little strain, grows rather rapidly in development. The supraorbital region may adapt so rapidly that high strains are not observable.

2.8 Conclusion

The micro and macrostructural variation of bone tissue influence its mechanical function and collectively the overall behavior of the skeleton. This relationship is affected by innumerable factors, e. g., biomechanical, developmental and biochemical (Currey, 2002).

The relationship of trabecular bone form with whole bone function has been explored by many researchers (Lanyon, 1974; Hayes and Snyder, 1981; Biewener et al., 1996; Cowin, 2001; Pearson and Lieberman, 2004; Pontzer et al., 2006; Ruff et al., 2006). Strain gage experiments in the late 1960s and early 1970s compared trabecular and cortical bone morphology to observable strain patterns induced by real life activities, and provided evidence for the basic theories of Culmann, Von Meyer, and Wolff (Wolff, 1892; Koch, 1917; Lanyon and Smith, 1969; Lanyon, 1973; Lanyon, 1974; Cowin, 2001). Lanyon (1973; 1974) and Hayes and Snyder (1981) determined that trabecular bone anisotropy is significantly correlated with principle tensile and compressive strain orientations. Improved methodologies (MIL, distance transformation, micro-FEA) paired with microcomputed tomography allow for more accurate descriptions of trabecular bone structure and quantifications of mechanical properties.

Studies of the microstructural properties of cortical bone and strain gage studies reveal that material properties and mechanical behavior of bone share an intricate relationship that is site, individual, and species dependent. The variability and complexity of anatomical site and species variation restate the need for similar studies of craniofacial trabecular bone. Furthermore, in primate functional morphology, strain gage experiments have introduced debate into our understanding of the function of upper and mid-craniofacial regions of extinct and extant species. Robust supraorbital regions are hypothesized to derive from the mechanical environment of masticatory loading; however, there is significantly less strain in the supraorbital region compared to the zygomatic region, suggesting that the supraorbital region is overbuilt for mastication (Picq and Hylander, 1989; Hylander et al., 1991).

There could be a biochemical explanation for the inconsistency in supraorbital morphology and the relative strain magnitude measured there. Minimum effective strain is site and age dependent; it could be that the MES of the supraorbital region is lower than the zygomatic region. Also, the rate of growth of each bone could contribute to the initial bone modeling/ remodeling response to strain (Turner, 1999; Schriefer et al., 2005; Kupczik et al., 2009). Because the behavior of these regions is not only affected by the cortical bone bulk, but also by the trabecular structure and organization, it is true that trabecular material and mechanical properties should reveal adaptional relationships to relative strain environments. Analysis of the material properties of trabecular bone in the supraorbital and zygomatic regions could help answer questions about the function of robust supraorbital regions in primates.

Additionally, finite element modeling and analysis is a technique that has been adopted by numerous functional morphologists interested in understanding the relationship between mastication and facial form. Researchers such as Ross et al. (2011) create finite element models from CT scans; these models are used to test hypotheses regarding the relationship of function to craniofacial form by looking at overall strain concentrations and deformation patterns in several primate species. Strait et al. (2005; Ross et al., 2011) found that using correct orthotropic mechanical property data, derived from cortical bone studies, by region, creates more realistic deformation results. Finite element analyses of the primate craniofacial region could benefit greatly from the determination of the mechanical properties of trabecular bone in the craniofacial region of multiple primate species.

CHAPTER 3

MATERIALS AND METHODS

3.1 Sample

The samples used in this study are from a collection of frozen anatomical specimens in the laboratory of Dr. Paul C. Dechow at Texas A&M Health Science Center, Baylor College of Dentistry, in Dallas, Texas. Supraorbital and zygomatic (zygoma and zygomatic arch) regions were dissected and cut from the cadavers of 10 adult humans, 1 sub-adult female chimpanzee, 1 adult female gorilla, and 4 adult baboons using a dremel hand saw (Table 3.1). The samples were stored in a 95% ethanol and isotonic solution. The humans ranged in age from 42 to 88, but the age for one specimen was unknown. The humans came from the willed body program at the University of Texas Southwestern Medical Center, the baboons were obtained from the Southwest National Primate Research Center, the chimp came from Yerkes National Primate Research Center, and the gorilla is a zoo specimen. In the analysis, 2 human supraorbital (from humans 42226 and 25780) and 1 baboon zygoma (from baboon 2) were excluded, due to inadequacies in the sample.

Table 3.1 Specimen Age and Sex;
human specimens are represented by 5 digits and
baboon specimens are represented by the abbreviation BAB.

Crania	Sex	Age
25773	M	77
30001	?	?
24713	M	88
38948	F	36
40111	M	39
40574	M	39
40555	M	53
41969	F	42
42226	M	43
25780	M	73
BAB7	?	adult
BAB2	?	adult
BAB3	?	adult
BAB9	M	adult
Gorilla	F	adult
Chimp	F	subadult

3.2 Methods

3.2.1 MicroCT Scanning and Analysis

MicroCT

Microcomputed tomography is a reliable method for determining density and structure of trabecular bone (Kuhn et al., 1990; Ruegsegger et al., 1996; van Rietbergen et al., 1998a). In order to be scanned, samples must fit into one of five tube sizes, each of which has a specific range of resolutions: standard, medium, and high, as demonstrated in Table 3.2.

Table 3.2 Tube Diameter and Resolution

Tube diameter	Resolution of voxels in micrometers (high, medium, standard):	Ideal for:
12.3 mm	3.5 um, 7um, 14 um	Examination of microstructure
16.4 mm	6 um, 12 um, 24 um	Variations between are based on sample size and analysis goals ↓
20.5 mm	10 um, 20 um, 40um	
30.7 mm	15 um, 30 um, 60 um	
36.9 mm	18.5 um, 37 um, 74 um	Visualization, volume analysis

Once samples are loaded into the microCT, the user must specify scan settings including resolution, E(kVp)[12], I(μA)[13], and integration time[14] to optimize the results of the scanning and analysis. MicroCT scanning works by taking a series of cone beam x-ray projections (Figure 3.1).

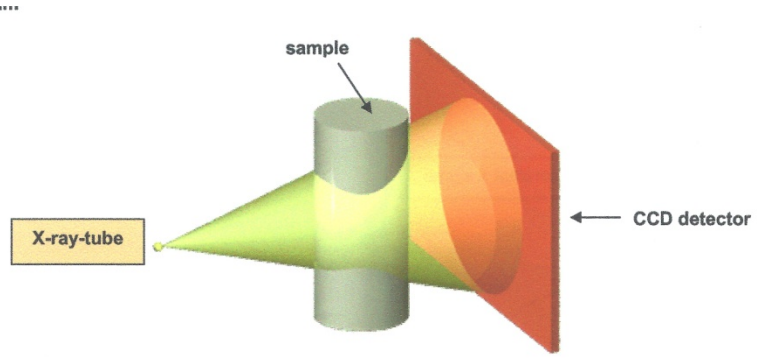

Figure 3.1 X-Ray Beam, Sample Tube, and CCD Detector;
Image from Scanco Medical User Guide

A raw file, or .RSQ, is produced from the projections of each scan and then reconstructed into an .ISQ file, in which the grey scale slices of the specimen can be viewed and contouring of the region of interest can be performed to produce a graphical object within a volume of interest. Analyses binarize the graphical object to create a 3-D reconstruction of the sample and to measure structural properties. An illustration of the process from scanning to analysis (Figure 3.2) and a table describing the types of analysis (Table 3.3) are provided below. Outputs of each analysis are stored on the microCT terminal server and can be imported for statistical analysis.

[12] Energy of the X-ray source; higher energy is used for denser samples, such as those containing metal implants(values include 45, 55, 70).
[13] Beam intensity.
[14] The length of time spent on one projection; ranges from 100 to 800 ms.

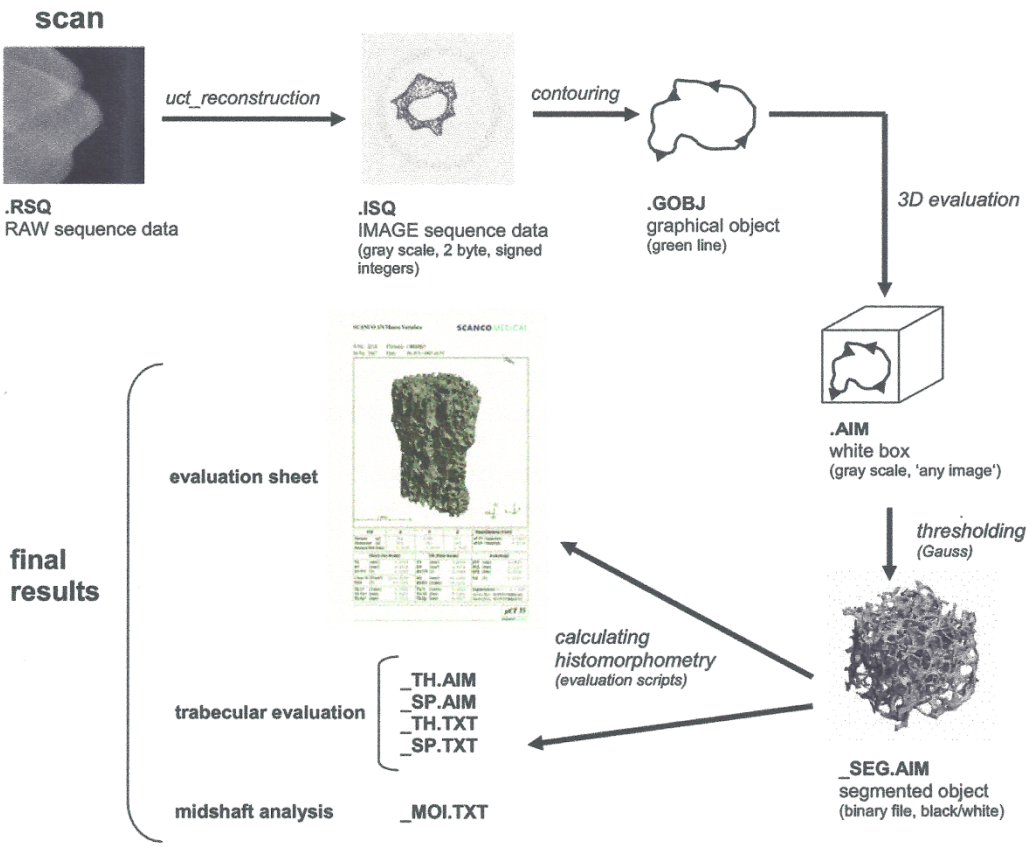

Figure 3.2 Illustration of MicroCT from Start to Finish;
obtained from Scanco Medical User Guide

Table 3.3 MicroCT Analyses

Type of Analysis/Script	Description	Useful for
3-Dimensional Segmentation	Provides a rotational 3D image of sample	Visualization Isolating x,y,z coordinate(s) for further analysis
3-D Segmentation of 2 volumes: pores shown solid within transparent object	Allows user to define thresholds for both bone and negative space, providing a rotational 3-D image of the sample showing solid pores within a transparent solid	Visualization of porous material and orientation of pores, such as the vasculature or Haversion systems within cortical bone
3-D segmentation of 2 volumes with 2 contours	Provides rotational image of sample with solid and transparent areas defined by the user-constructed volume of interest	Visualization of 2 areas defined by Micro-CT user, such as cortical and trabecular bone
Bone Trabecular Morphometry	Provides degree of anisotropy and directional vectors, trabecular number, separation and thickness, structure model index, and connectivity density	Analysis of trabecular structure or other similar structural networks to determine material properties
Bone Volume and Bone Density Evaluation only	Provides material and apparent density, total volume and bone volume, and the ratio of bone volume and total volume	Analysis of solid material, such as cortical bone, to determine its material properties
Finite Element Analysis (FEA)	Designed to simulate mechanical loading on specified region of bone sample	Provides data on the mechanical properties of the sample, such as Poisson's ratio and elastic modulus

Sample Scanning and Analysis

The cut specimens of whole supraorbital and zygomatic bone regions, and whole zygomatic arches, were scanned at medium resolution (37 um), 70 EkVp, 114 µA with an integration time of 400 ms, in 36.9 mm tubes using the Scanco Medical microCT 35 (Scanco Medical, Basserdorf, Switzerland).

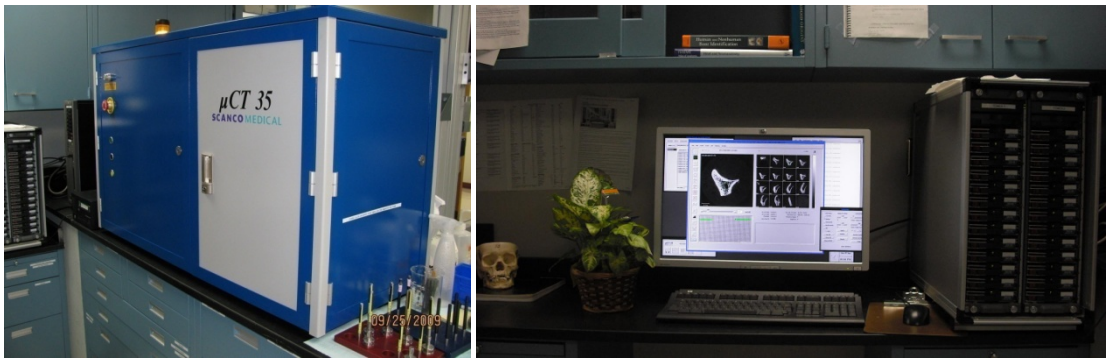

Figure 3.3 Picture of the MicroCT in the Dechow Lab;
(left) Scanco Medical microCT 35; (right) terminal station and hard drive tower

Image Processing Language, provided by the Scanco Medical microCT 35 system, was used to view the reconstructed scans (.ISQs), contour the volumes of interest (VOIs), and apply a threshold level that appropriately binarized the voxels in the volume of interest to run analyses. To maintain consistency and provide comparable results from all analyses of the uCT, the same threshold values were used for all samples. The lower threshold used for all analyses and samples to distinguish bone from space in this experiment was 180 and the upper threshold used was 1000 (upper limit). The threshold was determined visually to be the best representation of bone across samples.

Analyses were selected based on the region contoured and the measurement objective. Each region of bone (supraorbital, zygomatic and zygomatic arch) was divided into sub-regions (discussed in Chapter 4). For each of these sub-regions, an analysis was performed on the whole bony region (cortical plus trabecular), cortical bone only and trabecular only regions (shown in Figure 3.4).

Bone Volume /Total Volume Density Only analysis was used to quantify total volume, bone volume, and bone volume fraction (BVF) of whole and cortical-only VOIs (Figure 3.4A and 3.4B). The percentage of trabecular bone within each sample was hand calculated by subtracting the cortical bone volume of the region from the whole region volume and dividing by the whole region volume. All regions, except for those in the browridge, were contoured

separately. The three browridge regions were combined into one total browridge region, because a larger VOI was sufficient for analyzing trabecular distribution, and cortical and whole BVF. There was not an appropriate way to measure the sinus region in each species due to the large amount of empty space and the posterior cuts.

Bone Morphometric Analysis was used to compute the connectivity density (CD); structure model index (SMI); trabecular number (TN), thickness (TT), and separation (TS); material density (MD); and degree of anisotropy (DA) of trabecular bone VOIs (Figure 3.4C). Abbreviations, methods, descriptions and units are described for each variable in Table 3.4.

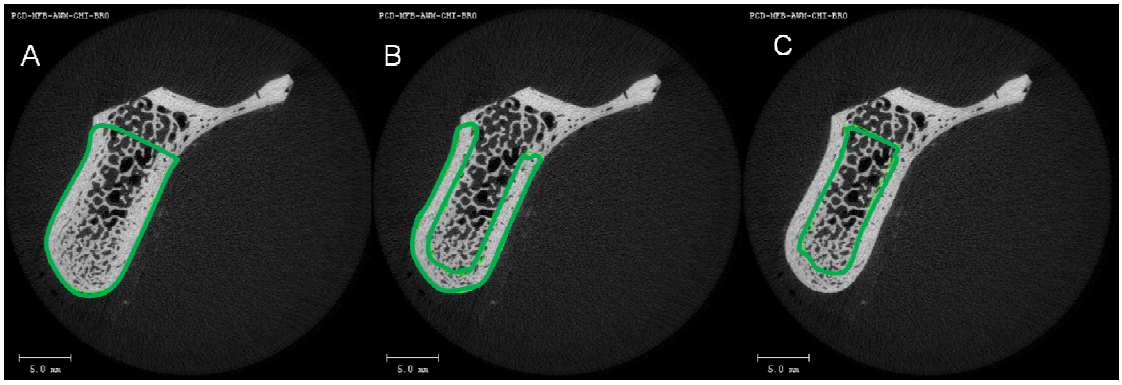

Figure 3.4 Contoured Regions; (A) an image of a slice from the chimp browridge with whole region contoured, (B) same slice with cortical region contoured, (C) same slice with trabecular region contoured

MicroCT Quantitative Methods

Bone volume fraction (BVF), CD, SMI, TN, TT and TS are quantified by the distance transformation method, in which spheres are fitted to the region (trabecular or space) and the mean diameter of the spheres is averaged by volume (Hildebrand and Rüegsegger, 1997). The degree of anisotropy, or DA, is determined by finding the mean intercept length, or the average distance between bone and space interfaces, in multiple planes of three orthogonal directions such as x, y, and z. The average distances in the three orthogonal directions are expressed as vectors H1, H2, and H3 and coordinate points for each vector within a three coordinate system

are provided. The DA is a ratio of the greatest directional value (H2) to the least directional value (H1). Therefore, a DA that is greater than one indicates at least one prominent direction. These values describe the direction in a three coordinate system as well as the magnitude of the direction.

Material density, a measure of the amount of hydroxyapetite mineral per cubic centimeter, is calculated by quantifying the attenuation. Relatively brighter voxels represent higher concentrations of hydroxyapatite and relatively darker voxels represent lower concentrations of hydroxyapatite; a phantom bone specimen containing five densities is used as a standard with which to calibrate the microCT measurements.

Table 3.4 Bone Morphometric Output Variables

Abbreviation	Variable	Method, Description	Unit
BVF	Bone Volume Fraction	Ratio of the number of bone voxels to the total number of voxels in the specified region of interest	fraction
CD	Connectivity Density	Conn-Euler Method (Odgaard and Gundersen, 1993); measures the degree of connectivity between trabeculae	$1/mm^3$
SMI	Structure Model Index	Differential analysis of triangulated surface of trabecular bone; quantifies the structural appearance of trabecular bone, where 0 indicates parallel plates, 3 indicates cylindrical rods, and negative values indicate concave structures, such as air bubbles within the bone	N/A
TN	Trabecular Number	Distance Transformation Method by taking the inverse of TS; mean number of trabeculae	1/mm
TT	Trabecular Thickness	Distance Transformation applied to voxels representing bone; mean thickness of trabeculae	mm
TS	Trabecular Separation	Distance Transformation applied to voxels representing space; mean distance between trabeculae	mm
MD	Material Density	Measure of concentration of hydroxyapatite by calculating average grey level of the bone voxels	mg HA/cm^3
DA	Degree of Anisotropy	Mean Intercept Length; measures average alignment of trabeculae, where DA=length of longest divided by shortest mean intercept length vector; 1=isotropic and >1= anisotropic	N/A

3.3 Anatomical Regions of Interest

3.3.1 Supraorbital Region (SO)

The supraorbital region was divided into three sub-regions. These included the post-orbital region, the browridge, and the frontal sinus. The browridge was further subdivided into lateral, middle and medial regions (Figure 3.5). To obtain these regions, the total length of each browridge was divided by three. The regions were of equal length within each individual and sub-regions were continuous.

Browridge

The browridge region (BR) of the supraorbital analysis was demarcated by the zygomatico-orbtial, or postorbital, suture and the supraorbital notch/foramen. The notch or foramen was chosen because it is clearly marks the medial end of the actual browridge of the supraorbital bone. In specimens without a supraorbital notch or foramen, the ridge portion was medially terminated before the development of the frontal sinus. The frontal sinus was very useful in cases where there was no supraorbital foramen or notch, as the supraorbital foramen or notch and the sinus usually appear around the same area, sometimes overlapping. At the lateral end of the ridge, the suture was used as a terminal point; however, this suture was not always present. In such specimens, the region extended into a comparable area, in which the cerebral surface behind the ridge disappears, so that the ridge begins to break off from the frontal bone. The browridge region, between the zygomatico-orbital suture and the supra-orbital notch, was subdivided into 3 sub-regions of equal length including lateral (LR), middle (MiR), and medial (MeR) regions.

Post-Orbit and Sinus

The area of bone inferior to the zygomatico-orbital suture was included as the post-orbital region (PO) and the area of trabecular bone present behind the frontal sinus cavity in the glabellar region was included as the sinus region (Si).

3.2.2 The Zygoma

The inferior and superior regions of trabecular bone in the zygoma were contoured, as these two regions were the areas in which, across all samples, trabecular bone could be found. The superior region of the zygoma (SZ) began with the presence of trabecular bone around the superior region of the bone, where the specimen had been cut from the postorbital bar and extended down around the lower orbit. The inferior region of the zygoma (IZ) contoured consisted of the main body of the bone, but for the sake of regularity across samples, did not extend to the base of the bone. Instead, trabecular regions of interest in the inferior zygoma consisted of the widest portion of the body of bone. This distinction in sampling region was made because in many samples, trabecular bone is not continuous from superior to inferior in the zygoma, and the inferior region chosen was the most morphologically consistent across species and individuals.

3.3.3 The Zygomatic Arch

The zygomatic arch was divided into three regions of analysis. Regions of analysis in the zygomatic arch (ZA) included the anterior region, or the zygomatic process of the zygomatic bone (ZP); the middle region, or the zygomatic process of the temporal bone (TP); and the posterior region (PZA). For both the temporal and zygomatic processes of the arch, the region of interest extended in so far as there was reasonable room for analysis without major interference from the suture, which for most specimens was quite complex. In two of the human samples, no suture was present separating these bones; therefore the demarcation of the regions involved the use of other morphological traits, such as a bulge and crease in the region that appeared to be where the suture once had been. The TP subregion extended posteriorly until the diameter of the arch began to increase in anticipation for the articular tubercle; for many samples this increase was accompanied by slight triangulation of the diameter. The ZP subregion extended anteriorly up until the cut of the sample, or until a rapid increase in diameter was seen, marking its junction with the zygomatic bone. For the human samples, the posterior

region was demarcated around the articular tubercle of the temporal process of the zygomatic arch. However, in the baboon and ape specimens, the posterior region of analysis was just anterior to the articular tubercle; the morphology of this region is very different among species. For instance, in the baboon specimens, the posterior region of the temporal process is much longer than it is in humans, and in baboons and apes the articular tubercle tends to branch outward into a complex attachment with the temporal bone. In humans, the bone across from the articular process is smooth and discontinuous; it therefore made a logical location for analysis.

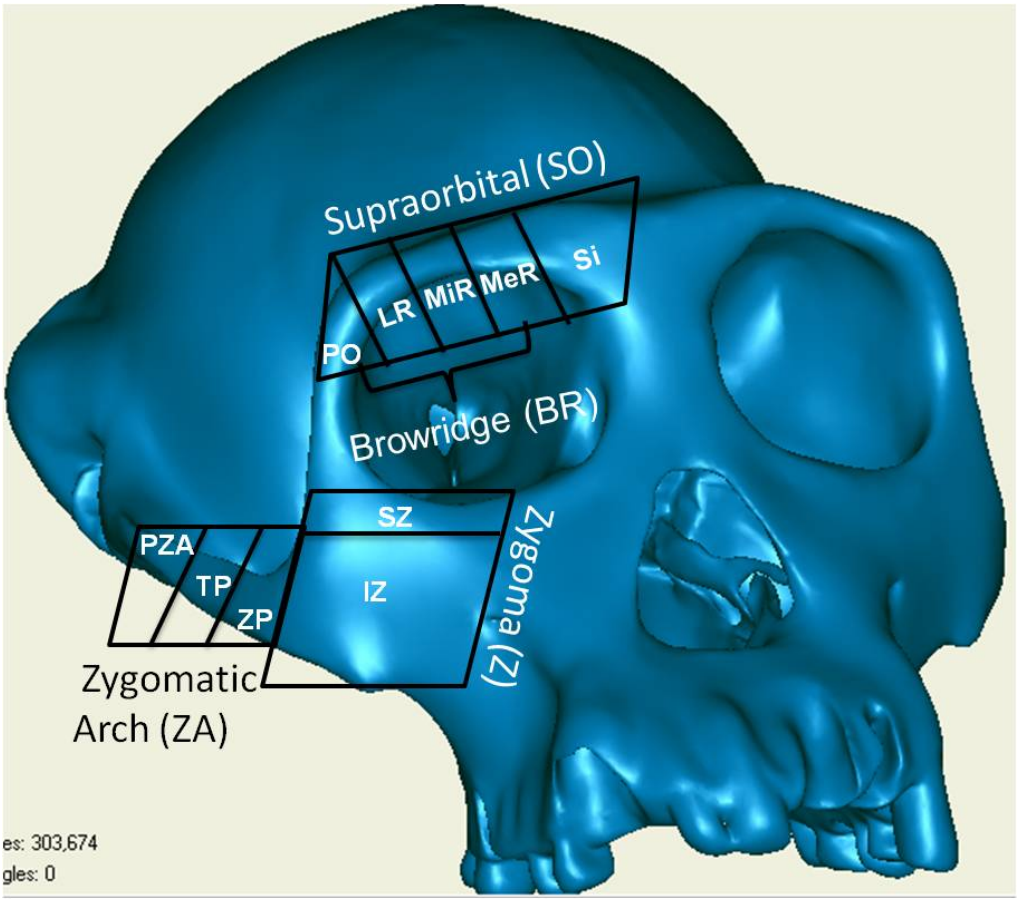

Figure 3.5. Chimpanzee Cranium Showing Regions of Analysis; PO=postorbital, LR=lateral ridge, MiR=middle ridge, MeR=medial ridge, Si=sinus, SZ=superior zygoma, IZ=inferior zygoma, ZP=zygomatic process, TP=temporal process, PZA=posterior zygomatic arch.

3.4 Statistical Analysis

All statistical analyses were performed using SPSS Data Analysis Software.

Univariate Analysis and Significance Testing

The mean and standard deviation for each variable at each location and within each species was calculated and is provided in the Results. Mann Whitney U nonparametric statistical analysis was used to explore differences by region (supraorbital vs. zygoma vs. zygomatic arch) within species and between like regions of different species (human vs. baboon vs. chimp vs. gorilla). The sinus region was excluded from the significance testing because its morphology was highly unusual compared to the other four regions of the supraorbital. The objective of the significance testing was to assess regional variations between different locations of the same species and between the same locations of different species.

Principle Components Analysis: Patterning of Trabecular Bone Properties by Species

Principle components analysis is useful in identifying latent variables, or components, that explain correlations among a larger set of variables. In morphological studies it can be applied to data sets as a method to reduce the number of variables and identify patterns of variation between species. A single PCA was applied to all (n=107) trabecular bone morphometric data to determine the principle components, variable loadings and the percent of variation explained by each component. Primary components, which have an eigenvalue greater than one, were rotated via varimax rotation. Each specimen was assigned a factor loading, or correlation to each principle component; these loadings were plotted on a three dimensional graph and color coded by species. The appropriateness of the PCA model was judged by SPSS output scores: the Kaiser-Meyer-Olkin (KMO) measure of sampling adequacy and the percentage of correlation matrix residuals greater than 0.05. The KMO measure of sampling adequacy is a measure of multicollinearity among samples; the higher the KMO measure of sampling adequacy, the better suited it is for factor analysis. KMO values above 0.6 are recommended. The correlation residuals are the absolute values of the difference between

the original correlation matrix and the rotated correlation matrix and therefore indicate the appropriateness of rotated components.

CHAPTER 4

RESULTS

4.1 Univariate Analysis and Significance Testing

4.1.1 Bone Volume/Total Volume Density Analysis

Human

Table 4.1 lists means and standard deviations for *Bone Volume/ Total Volume Density Only Analysis* for all regions and species (see also Figure 1). Average BVF of whole postorbital and browridge portions of the human specimens is 0.84 (range= 0.72-0.84) and 0.76 (range= 0.68-.0.87), respectively. There is less variation in the bone volume fraction of the cortical bone in both regions; postorbital cortical BVF ranges from 0.94-0.99, and browridge cortical bone volume fraction ranges from 0.92 to 0.98. The browridge portions are on average less dense than the postorbital portions; likewise, on average, there is a greater percentage of trabecular bone in the human browridge than in the human postorbital region.

Table 4.1 Means and Standard Deviations from Whole Bone Analysis

Species	Region	BVF Whole	BVF Cort	% Trab[15]
Human	PO	0.84(0.06)	0.96(0.02)	24 (6)
n=8	BR	0.76 (0.07)	0.95(0.02)	37 (11)
n=10	SZ	0.90 (0.07)	0.96(0.06)	16 (10)
	IZ	0.74 (0.11)	0.94(0.03)	34 (13)
	PZA	0.92 (0.06)	0.99(0.00)	12 (9)
	TP	0.97 (0.04)	0.99(0.01)	3 (7)
	ZP	0.87 (0.14)	0.98(0.01)	15 (16)
Baboon	PO	0.83 (0.06)	0.94 (0.05)	38 (9)
n=4	BR	0.83 (0.06)	0.96 (0.01)	43 13)
n=3	SZ	0.83 (0.08)	0.96 (0.01)	30 (11)
	IZ	0.93 (0.11)	0.99 (0.01)	11 (18)
	PZA	0.87 (0.10)	0.98 (0.02)	29 (10)
	TP	0.92 (0.12)	0.97 (0.03)	17 (13)
	ZP	0.92 (0.09)	0.98 (0.01)	13 (11)
Chimp	PO	0.85	0.90	17
n=1	BR	0.82	0.92	33
	SZ	0.91	0.95	11
	IZ	0.70	0.85	37
	PZA	0.53	0.78	42
	TP	0.61	0.74	32
	ZP	0.70	0.82	36
Gorilla	PO	0.98	0.98	0
n=1	BR	0.98	0.98	0
	SZ	0.97	0.99	12
	IZ	0.94	0.96	6
	PZA	0.88	0.97	12
	TP	0.98	0.99	0
	ZP	0.96	0.97	5

The mean whole BVF of the human SZ region is 0.9 (range= 0.77 to 0.97). IZ regions are markedly less dense with a mean of 0.74 (range= 0.51 to 0.88). The BVF of cortical bone only in both regions are more comparable: the SZ region has a mean BVF of 0.96 (range= 0.8 to 0.99) and the IZ region BVF measures 0.94 (range= 0.86 to 0.98). There is a lot of variation in the fraction of trabecular bone in each region, and a large difference between means. The SZ region has an average of 16% (range= 3 to 34%) and the IZ region has an average of 34% (range= 12 to 58%) trabecular bone.

[15] Percent trabecular bone was calculated by subtracting the volume of the cortical region from the volume of the whole region, and dividing the difference by the volume of the whole region.

Figure 4.2 shows 3D reconstructions from the human ZA whole bone BVF analysis, where bone is transparent (white) and space is red. Of the three locations in the human zygomatic arch, the TP has the highest BVF (0.97; range=0.86-1.0), and the lowest percentage of trabecular bone (3%; range=0-20%). The PZA has a whole region BVF of 0.92 (range=0.84-1.0), and the ZP is the least dense (BVF=0.87; range=0.6-0.99). There is a slightly larger fraction of trabecular bone within the ZP (15%; range=1%-44%) than in the PZA (12%; range=0%-25%) There is little difference in mean BVFs of cortical-only values between regions (0.98-.99).

The human ZA had a significantly greater BVF of whole and cortical regions than both SO and Z regions, and significantly less trabecular bone than both regions.

Table 4.2 Significant Differences between Human Regions Determined by Mann Whitney U Test; *$p \leq 0.05$*

Human	SO vs. Z	SO vs. ZA	Z vs. ZA
BVF Whole	0.293	*0.000**	*0.001**
BVF Cort	0.308	*0.000**	*0.000**
% Trab	0.208	*0.000**	*0.001**

Baboon

Average BVF of the whole postorbital and browridge potions of the baboon specimens are both 0.83, with ranges from 0.77 to 0.9 and 0.75 to 0.89, respectively. There is some variation in cortical BVF in the baboon postorbital region (range= 0.87-0.97; mean=0.94); however, cortical BVF in the baboon browridge is more consistent (range=0.95-0.98; mean=0.96). BVF values for whole and cortical baboon regions are very similar to those for humans. The percentage of trabecular bone is greater in the browridge region (mean=43%) than the postorbital region (mean= 38%); ranges for each location are 0.24-0.52 and 0.3-0.49, respectively.

Baboon SZ regions have on average a whole region BVF of 0.83 (range= 0.74 to 0.89) and IZ region BVF of 0.93 (range= 0.81 to 1.0). Cortical-only BVF of the SZ region is 0.96

(range= 0.96 to 0.97) and cortical-only BVF of the IZ is 0.99 (range= 0.98 to 1.0). The SZ region averages 30% trabecular bone (range=2 to 42%) and the IZ region averages 11% (range=0 to 32%).

The baboon ZP mean whole region BVF (0.92; range=0.8-0.98) is consistent through the arch to the TP (0.92; range=0.74 -0.98), but the PZA has a comparably low mean whole region BVF, but a similar range (0.87; range=0.77 -0.99). Trabecular bone mean percentages are also similar through the anterior arch (13%-17%; ZP range=3%-29% and TP range=9% to 37%), but average higher in the PZA (29%; range=20%-40%). Cortical-only BVF for all regions average between 97% and 98%.

Table 4.3 shows that BVF of cortical bone varied significantly only between the supraorbital and zygomatic arch region (p=0.009). The percentage of trabecular bone within each region varied significantly between the supraorbital region and the zygoma (p=0.039) and between the supraorbital region and the zygomatic arch (p=0.003).

Table 4.3 Significant Differences between Baboon Regions Determined by Mann Whitney U Test; *$p \leq 0.05$*

Baboon	**SO vs. Z**	**SO vs ZA**	**Z vs ZA**
BVF Whole	0.519	0.090	0.963
BVF Cort	0.093	*0.009**	0.573
% Trab	*0.039**	*0.003**	1.00

Chimpanzee

Whole region BVF decreases (from 0.85 to 0.82) and cortical BVF increases (0.90 to 0.92) moving from the chimpanzee postorbital region to the browridge region. There is a moderate increase in the percentage of trabecular bone (from 17% to 33%) from the postorbital region to the browridge.

In the chimp specimen, the SZ is denser than the IZ, with a whole BVF of 0.91 and 0.70, respectively. There is also a decrease in the BVF of the cortical region from superior to

inferior (from 0.95 to 0.85) and an increase in the percentage of trabecular bone in the region (from 11% to 37%).

The whole region BVF in the zygomatic arch decreases from anterior to posterior (ZP BVF=0.70, TP BVF=0.61, PZA BVF=0.53). Cortical bone only BVF follows a slightly different pattern: it is highest in the ZP (0.82), followed by the PZA (0.78), and lowest in the TP (0.74). The percentage of trabecular bone in the chimpanzee zygomatic arch is highest in the PZA (42%), and lowest in the TP (32%).

Gorilla

Whole BVF of the gorilla is large, at 0.98, in the PO and BR region, and although the midsection of the regions are sometimes more porous, there is no easily identifiable trabecular bone present in these regions.

The gorilla zygoma has high BVF values for both whole region and cortical region only in SZ and IZ samples and displays a slight decreasing trend: SZ whole BVF is 0.97 and IZ whole BVF= 0.94; cortical-only analysis obtained 0.99 BVF for the SZ and 0.96 BVF for the IZ. Trabecular bone makes up a small percentage of the SZ volume (12%) and half that (6%) in the IZ.

In the gorilla specimen zygomatic arch region, whole region BVF is high and consistent in the anterior arch (from 0.96-0.98) and lower in the PZA (0.88). Cortical-only BVF is consistent (between 0.97 and 0.99) among the three regions. There is very little, if any discernable trabecular bone along the anterior arch (0%-5%), and only slightly more in the PZA (12%).

Interspecific variation

As can be observed in Figure 4.1, whole BVF is highly variable by species and between locations. The chimp displays a greater range than the other species and the gorilla shows overall higher whole BVF values. The human supraorbital whole BVF is low compared to the same location in the other three species, but only significantly lower compared to the gorilla ($p=0.025$) (Table 4.4). Baboon supraorbital whole BVF is also significantly lower than that for

the gorilla (p=0.037). Whole region BVF is distributed more evenly across the SO region than in the Z and ZA. In the zygoma, whole BVF is higher in the SZ of humans, the chimp and the gorilla, but in baboons, the IZ has higher BVF. Human IZ whole BVF is low and comparable to that of the chimpanzee; the gorilla and baboon samples have higher values, but there were no differences between the entire zygoma that were significant. Significant differences did exist between the zygomatic arch of chimps, such that the ZA of chimps had significantly lower whole BVF relative to humans and baboons (p=0.008 and p=0.009, respectively).

Mean cortical BVF are most similar between humans and baboons, ranging between 0.94 and 0.99. Chimp cortical BVF has a much wider range (0.74 to 0.95) and displays lower values overall, especially in the temporal process of the zygomatic arch (0.74) (Figure 4.1 and Table 4.4). Chimp ZA cortical BVF was significantly lower than that in humans (p=0.005). In contrast to the chimp, gorilla cortical BVF is less variable by region and has higher overall values (0.96 to 0.99). Human cortical BVF in the SO was significantly lower than that of the gorilla (p=0.049). Human ZA cortical BVF also differed significantly from the gorilla (p=0.049). Baboon ZA and Z cortical BVF was significantly higher than that in the chimp (p=0.009 and p=0.046, respectively). Baboon SO region cortical BVF was significantly less compared to the gorilla (p=0.036).

Table 4.4 Significant Differences between Like Regions of Different Species Determined by Mann Whitney U Test; *p≤0.05;WH= whole

	Human vs. Baboon			**Human vs. Chimp**			**Human vs. Gorilla**		
	SO	**Z**	**ZA**	**SO**	**Z**	**ZA**	**SO**	**Z**	**ZA**
BVF WH	0.298	0.248	0.455	0.779	0.819	0.008*	*0.025**	0.110	0.991
BVF Cort	0.976	0.260	0.082	*0.025**	0.110	*0.005**	*0.049**	0.648	*0.049**
%Trab	*0.050**	0.542	*0.014**	0.482	0.954	*0.010**	*0.025**	0.153	0.706

	Baboon vs. Chimp			**Baboon vs. Gorilla**		
	SO	**Z**	**ZA**	**SO**	**Z**	**ZA**
BVF WH	0.602	0.505	*0.009**	*0.037**	0.505	0.942
BVF Cort	0.117	*0.046**	*0.009**	*0.036**	0.739	0.469
%Trab	0.192	0.737	0.060	*0.036**	0.502	0.083

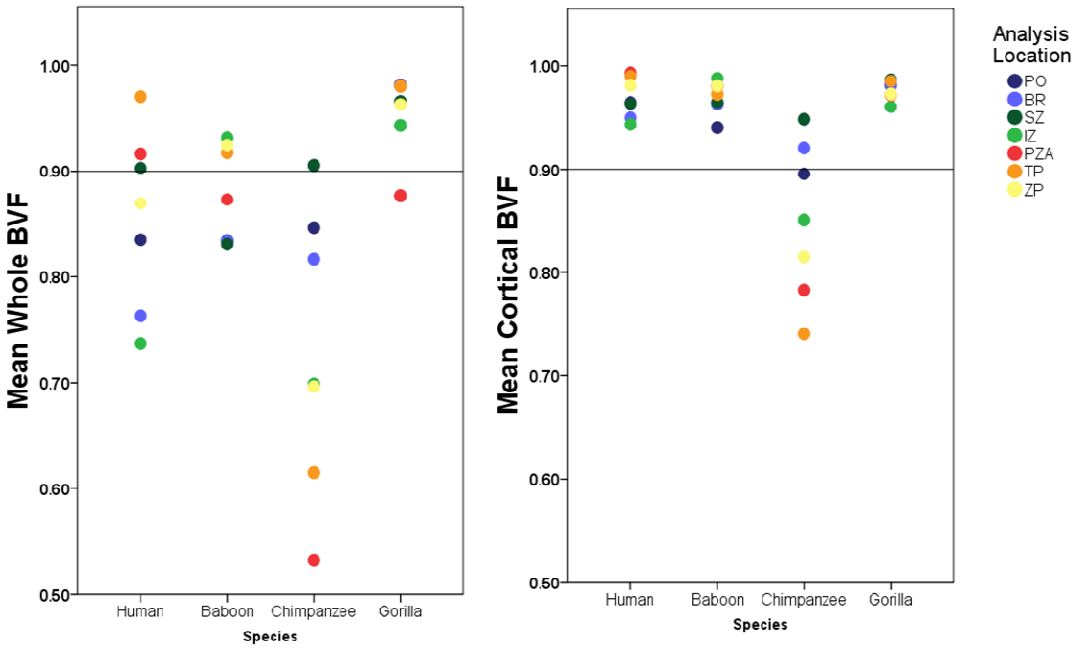

Figure 4.1 Mean BVF of Whole and Cortical Regions by Species and Location

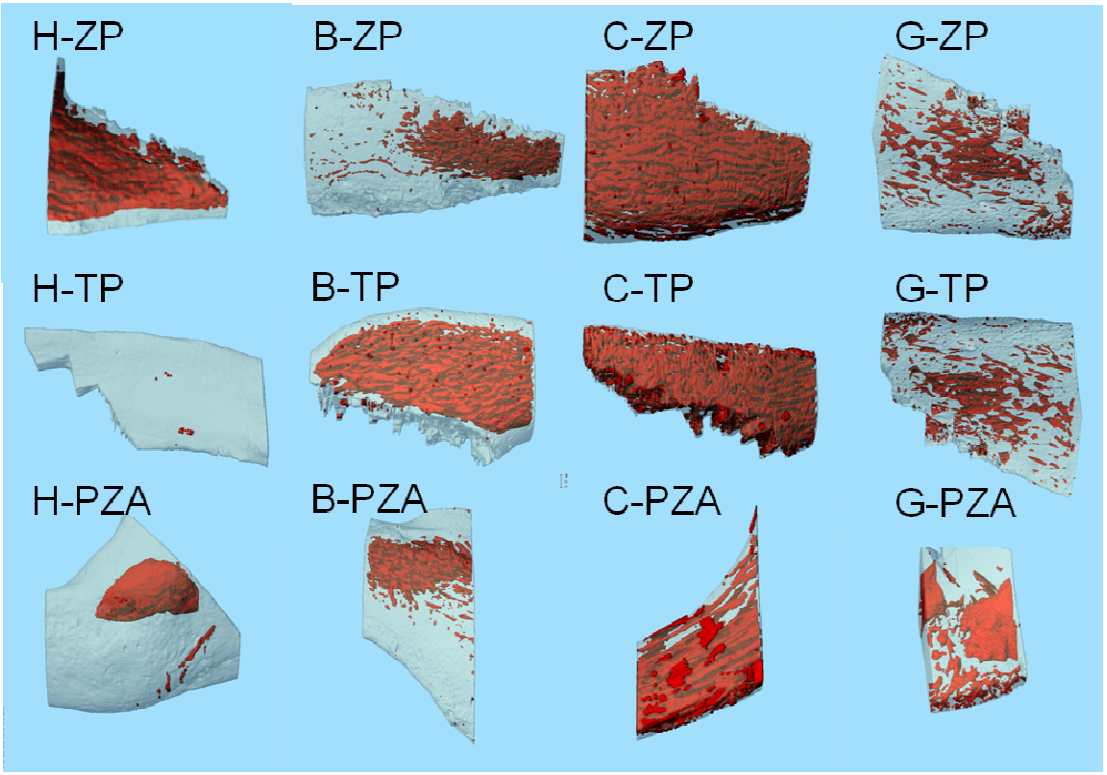

Figure 4.2 3D Reconstructions of Whole BVF Analysis in the Zygomatic Arch Regions of All Four Species Showing Bone as Transparent (white) and Space within the Bone as Red; H=human, C=chimp, B=baboon, and G=gorilla; Left is anterior and top is superior

In the supraorbital region, human, baboon, and chimp samples show an increase in trabecular percentage from the postorbital region to the browridge region (Figure 4.3 and Table 4.1). Both humans and chimp show an increase in trabecular bone percentage from the superior to inferior zygoma, a decrease from the ZP (anterior) to the TP (middle), and an increase from the TP to the PZA. By contrast, among baboons, there is a decrease in trabecular bone percentage from the SZ to IZ regions and an increase in trabecular percentage from the ZP (anterior) to the PZA (posterior). The pattern of trabecular bone percentage in the gorilla zygoma is like that of baboons; it decreases from SZ to IZ. Overall, there is markedly less trabecular bone in the gorilla regions, and in many locations no clear regions of trabecular bone. The fraction of trabecular bone differed significantly between human and baboon SO ($p=0.050$),

human and baboon ZA regions (p=0.014), human and chimp ZA regions (p=0.010), and human and gorilla supraorbital regions (p=0.025) (Table 4.4). Baboon SO regions contained significantly more trabecular bone relative to the gorilla (p=0.036).

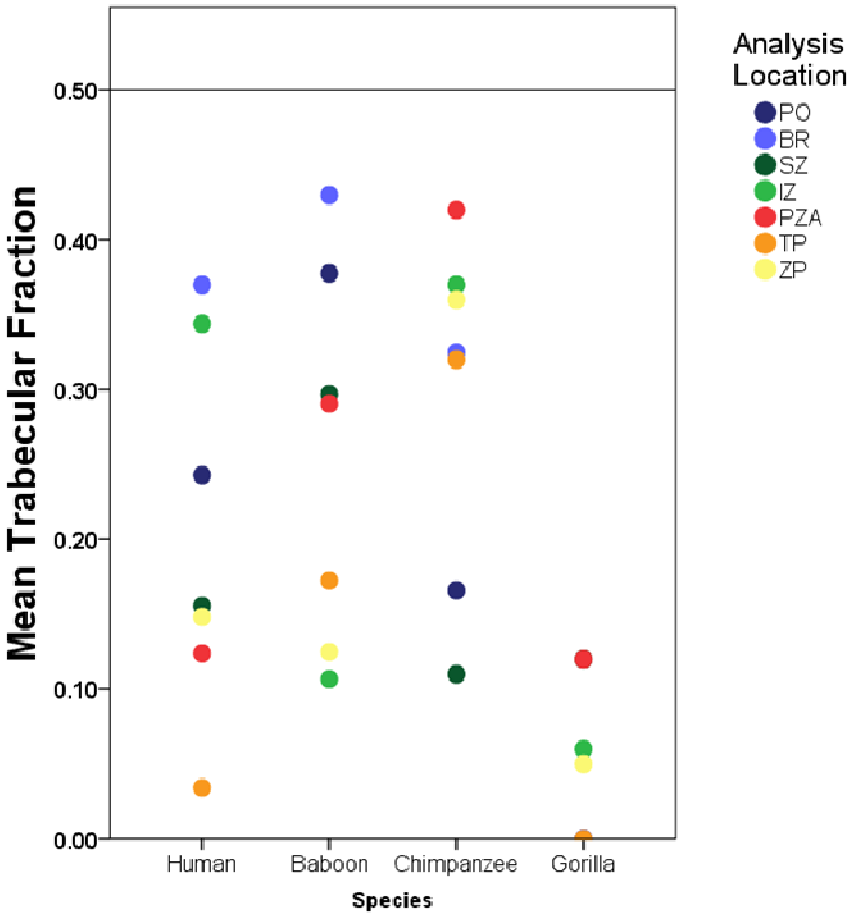

Figure 4.3 Mean Percentage of Trabecular Bone by Species and Location; Expressed as a fraction

4.1.2 Trabecular Bone Morphometric Analysis

Regional Variations in Human and Baboon Samples

As shown in Table 4.5, human samples varied significantly in trabecular number, thickness and separation between the zygoma and zygomatic arch (p=0.001, p=0.006, p=0.015, respectively).

Trabecular number was on average higher in the zygomatic arch, but trabecular thickness and separation was on average higher in the zygoma. Trabecular number was also found to be significantly higher in the zygomatic arch compared to the supraorbital region (p=0.006). SMI, TT and TS also differed significantly between the SO and ZA (p=0.002, p=0.028, and p=0.038, respectively). Material density was significantly higher in the zygoma compared to the supraorbital region (p=0.037). Degree of anisotropy was found to be significantly higher in the zygoma and zygomatic arch compared to the supraorbital region (p=0.000) (see Figure 4.5 for images of trabecular bone from SO and Z regions).

Table 4.5 Significant Differences between Human Regions Determined by Mann Whitney U Test; *$p \leq 0.05$*

Human	SO vs. Z	SO vs ZA	Z vs ZA
BVFTrab	0.820	0.886	0.876
CD	0.080	0.339	0.060
SMI	0.286	*0.002**	0.130
TT	0.336	*0.028**	*0.006**
TN	0.208	*0.006**	*0.001**
TS	0.588	*0.038**	*0.015**
MD	*0.037**	0.051	0.979
DA	*0.000**	*0.000**	0.896

Among baboon regions (Table 4.6), the degree of anisotropy was found to be significantly higher in the zygomatic arch than in the zygoma (p=0.011) and significantly higher in the zygoma compared to the supraorbital region (p=0.002) (see Figures 4.6). Material density was also significantly higher in the zygoma (p=0.012) and the zygomatic arch (p=0.000) compared to the supraorbital region. SMI was significantly lower in the baboon supraorbital region compared to the zygoma (p=0.039; see Figures 4.5 and 4.7). The supraorbital region differed most from other regions.

Table 4.6 Significant Differences between Baboon Regions Determined by Mann Whitney U Test; *$p \leq 0.05$

Baboon	SO vs. Z	SO vs ZA	Z vs ZA
BVFTrab	0.185	0.642	0.190
CD	*0.027**	*0.005**	0.779
SMI	*0.039**	0.114	0.303
TN	0.269	0.330	0.454
TT	0.883	0.063	0.101
TS	0.269	0.642	0.399
MD	*0.012**	*0.000**	0.779
DA	*0.002**	*0.000**	*0.011**

Table 4.7 Means and Standard Deviations of Trabecular Bone Morphometric Analysis

Species	Region	BVF Trab	CD	SMI	Trab #
Human	**PO**	0.50 (0.16)	3.84 (1.26)	0.04 (0.88)	2.10 (0.78)
n=8	**LR**	0.44 (0.10)	2.46 (0.63)	-0.72 (1.02)	1.36 (0.30)
	MiR	0.47 (0.14)	2.36 (1.08)	-1.21 (1.66)	1.45 (0.24)
	MeR	0.49 (0.21)	2.63 (1.45)	-1.85 (2.42)	1.52 (0.55)
	Si	0.53 (0.17)	2.41 (1.20)	-2.84 (3.83)	1.36 (0.78)
n=10	**SZ**	0.48 (0.19)	1.54 (0.49)	-0.31 (2.01)	1.34 (0.34)
	IZ	0.42 (0.15)	3.44 (2.79)	-0.37 (1.44)	1.42 (0.40)
	PZA	0.43 (0.19)	2.46 (1.36)	-0.16 (1.08)	1.69 (0.80)
	TP	0.53 (0.21)	4.06 (2.52)	0.24 (0.73)	2.38 (0.67)
	ZP	0.46 (0.32)	3.27 (1.39)	0.83 (0.77)	2.66 (2.25)
Baboon	**PO**	0.65 (0.12)	6.74 (1.90)	-4.85 (3.31)	2.47 (0.58)
n=4	**LR**	0.73 (0.15)	4.81 (2.02)	-7.08 (3.64)	2.61 (0.61)
	MiR	0.72 (0.11)	3.17 (0.65)	-7.35 (5.00)	2.31 (0.70)
	MeR	0.62 (0.10)	2.96 (0.78)	-4.88 (2.49)	1.81 (0.39)
	Si	0.49 (0.13)	3.02 (1.46)	-2.87 (2.22)	1.53 (0.40)
n=3	**SZ**	0.60 (0.10)	3.00 (1.82)	-3.03 (2.40)	1.96 (0.47)
	IZ	0.52 (0.36)	2.15 (0.62)	-1.93 (3.29)	1.88 (1.38)
n=4	**PZA**	0.69 (0.20)	2.59 (0.94)	-5.47 (5.80)	2.12 (0.64)
	TP	0.78 (0.23)	2.25 (0.76)	-5.78 (6.19)	2.28 (0.65)
	ZP	0.65 (0.17)	2.83 (2.61)	-2.82 (1.15)	1.87 (0.54)
Chimp	**PO**	0.71	4.83	-5.26	2.18
n=1	**LR**	0.74	4.02	-6.19	2.14
	MiR	0.56	3.66	-2.70	1.57
	MeR	0.46	3.56	-1.38	1.40
	Si	0.46	4.92	-1.02	0.00
	SZ	0.66	2.31	-3.55	1.74
	IZ	0.30	2.63	0.45	1.08
	PZA	0.35	2.47	0.48	1.26
	TP	0.40	7.55	0.32	2.07
	ZP	0.56	4.01	-1.61	1.99
Gorilla	**PO**	0.98	0.04	-41.10	1.48
n=1	**LR**	0.95	0.32	-13.94	1.56
	MiR	0.92	0.53	-5.19	1.60
	MeR	0.65	2.49	-2.13	1.51
	Si	0.57	3.05	-1.82	1.82
	SZ	0.87	1.88	-10.03	1.96
	IZ	0.80	2.43	-4.41	1.99
	PZA	0.20	0.12	1.19	0.48
	TP	0.82	2.68	-2.76	2.36
	ZP	0.74	2.85	-1.31	2.39

Table 4.8 Means and Standard Deviations of Trabecular Bone Morphometric Analysis

Species	Region	Trab Thick	Trab Sep	MD	DA
Human	**PO**	0.33 (0.06)	0.54 (0.23)	802.68 (24.92)	1.49 (0.21)
n=8	**LR**	0.37 (0.08)	0.75 (0.23)	805.89 (33.14)	1.48 (0.34)
	MiR	0.39 (0.13)	0.68 (0.15)	810.88 (42.69)	1.45 (0.25)
	MeR	0.39 (0.12)	0.71 (0.34)	801.30 (46.59)	1.70 (0.59)
	Si	0.38 (0.06)	0.65 (0.24)	796.31 (41.11)	1.64 (0.47)
n=10	**SZ**	0.43 (0.12)	0.76 (0.30)	863.04 (33.85)	2.37 (0.38)
	IZ	0.38 (0.09)	0.75 (0.33)	793.27 (30.62)	2.07 (0.49)
	PZA	0.31 (0.07)	0.64 (0.34)	818.07 (26.46)	2.25 (0.88)
	TP	0.29 (0.11)	0.45 (0.12)	854.41 (65.80)	2.21 (0.39)
	ZP	0.26 (0.09)	0.57 (0.37)	824.32 (49.85)	2.55 (0.98)
Baboon	**PO**	0.29 (0.02)	0.30 (0.11)	732.88 (31.85)	1.46 (0.26)
n=4	**LR**	0.33 (0.05)	0.26 (0.13)	752.59 (54.97)	1.44 (0.19)
	MiR	0.36 (0.03)	0.38 (0.17)	768.03 (53.13)	1.28 (0.13)
	MeR	0.34 (0.01)	0.52 (0.13)	764.14 (31.41)	1.20 (0.09)
	Si	0.31 (0.04)	0.65 (0.21)	751.40 (23.60)	1.35 (0.08)
n=3	**SZ**	0.33 (0.06)	0.48 (0.17)	811.29 (44.82)	1.83 (0.08)
	IZ	0.33 (0.07)	0.64 (0.44)	810.33 (27.67)	1.79 (0.46)
n=4	**PZA**	0.29 (0.02)	0.30 (0.11)	732.88 (31.85)	1.46 (0.26)
	TP	0.47 (0.15)	0.29 (0.21)	803.71 (28.98)	2.71 (0.42)
	ZP	0.42 (0.15)	0.61 (0.27)	826.15 (4.96)	2.33 (0.24)
Chimp	**PO**	0.39	0.34	721.64	1.54
	LR	0.41	0.31	738.40	1.53
	MiR	0.37	0.64	730.69	1.41
	MeR	0.32	0.68	710.84	1.17
n=1	**Si**	0.31	0.60	687.61	1.37
	SZ	0.48	0.59	783.95	1.93
	IZ	0.30	0.94	722.26	1.52
	PZA	0.31	0.79	721.43	2.13
	TP	0.23	0.44	704.16	2.34
	ZP	0.32	0.41	710.54	3.07
Gorilla	**PO**	1.18	0.17	804.11	1.43
	LR	0.94	0.20	832.74	2.06
	MiR	0.94	0.47	809.61	1.47
	MeR	0.52	0.58	808.71	1.22
n=1	**Si**	0.43	0.51	756.94	1.41
	SZ	0.66	0.30	822.66	1.71
	IZ	0.65	0.37	807.44	1.95
	PZA	0.57	2.43	793.40	2.00
	TP	0.52	0.21	769.99	2.14
	ZP	0.40	0.26	803.66	4.37

Interspecific Differences between Like Regions

Figure 4.4 shows a cross section through the SO region of all four species. Human supraorbital regions showed the highest number of significant differences compared to other species, especially baboons (Table 4.9). Significant differences between humans and baboons were observed in all parameters except degree of anisotropy and trabecular thickness. Human SO regions had significantly lower BVF of trabecular bone (p=0.000), CD (p=0.005), and TN (p=0.000) than baboons, but significantly higher SMI (more platelike; p=0.000), TS (p=0.000), and MD (p=0.001; Figure 4.7). Human SO regions had significantly higher MD (p=0.001) and SMI (0.018), and lower CD (0.030) than the chimp, but were more similar to the chimp than to baboons and the gorilla. The human SO region differed significantly from the gorilla in all variables except trabecular number, material density, and degree of anisotropy. Trabecular bone in the gorilla SO region had a much higher BVF (p=0.004) and trabecular thickness (p=0.002) and significantly lower trabecular separation (p=0.027), SMI (extreme negative values indicating dense, but porous bone; p=0.005) and CD (p=0.010).

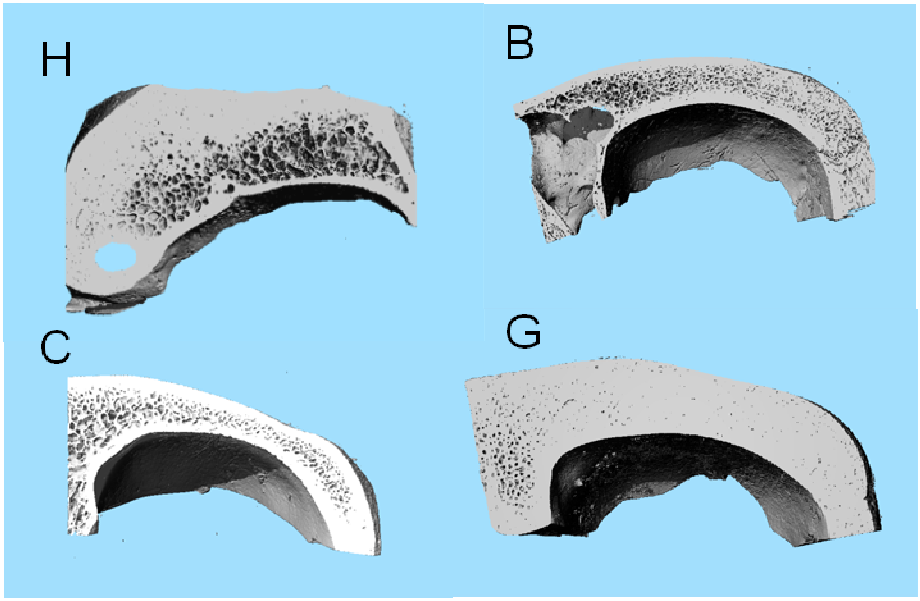

Figure 4.4 Cross Section through the SO of All Species Showing Variation in Trabecular Bone and Frontal Sinus Region; H=human, C=chimp, B=baboon, G=gorilla

In the zygoma, the humans had a significantly higher degree of anisotropy (SZ=2.37, SD=0.38; IZ=2.07, SD=0.49) than the baboon sample (SZ=1.83, SD=0.08; IZ=1.79, SD=0.46), but this was the only location among any of the species that yielded significant differences in DA (p=0.039) (Table 4.8). The human zygoma showed no significant differences in variables compared to the chimp zygoma, but did vary significantly from the gorilla sample in SMI (p=0.030), TN (p=0.030), TT (p=0.022), and TS (p=0.030). The gorilla zygoma had on average fewer, but thicker and less concentrated trabeculae.

Baboons had significantly higher BVF (p=0.008), lower SMI (denser porous bone; p=0.000), and greater TT (p=0.003) than humans in the ZA. Trabecular bone material in the human ZA was on average significantly denser than the chimp ZA (MD p=0.006). Trabeculae were significantly thicker in the gorilla ZA compared to the human ZA (p=0.013).

Table 4.9 Significant differences between Like Regions of Species
Determined by Mann Whitney U Test; *$p \leq 0.05$; Human vs. Baboon, Chimp, and Gorilla

	Human vs. Baboon			**Human vs. Chimp**			**Human vs. Gorilla**		
	SO	**Z**	**ZA**	**SO**	**Z**	**ZA**	**SO**	**Z**	**ZA**
BVF Trab	*0.000**	0.330	*0.008**	0.087	0.732	0.694	*0.004**	*0.030**	0.458
CD	*0.005**	0.503	0.278	*0.030**	0.361	0.275	*0.010**	0.732	0.239
SMI	*0.000**	0.100	*0.000**	*0.018**	0.568	0.631	*0.005**	*0.030**	0.206
TN	0*.000**	0.248	0.653	0.227	0.909	0.760	0.763	*0.030**	0.965
TT	0.336	0.078	*0.003**	0.725	0.909	0.760	*0.002**	0.022*	*0.013**
TS	*0.000**	0.273	0.231	0.227	0.732	0.760	*0.027**	*0.030**	0.760
MD	*0.001**	0.330	0.166	*0.001**	0.087	*0.006**	0.920	0.732	0.106
DA	0.096	*0.039**	0.190	0.821	0.087	0.315	0.763	0.209	0.458

	Baboon vs. Chimp			**Baboon vs. Gorilla**		
	SO	**Z**	**ZA**	**SO**	**Z**	**ZA**
BVF Trab	0.395	0.505	*0.030**	*0.038**	0.182	0.665
CD	0.925	0.739	0.083	*0.003**	0.739	0.773
SMI	0.219	0.505	*0.030**	0.395	0.182	0.083
TN	0.131	0.505	0.386	*0.008**	1.00	1.00
TT	0.089	0.317	0.112	*0.002**	*0.046**	0.386
TS	0.229	0.505	0.470	0.925	0.317	0.885
MD	0.108	0.182	*0.009**	*0.006**	0.505	0.194
DA	0.345	0.739	0.665	0.156	0.739	1.00

There were no significant differences detected between baboon and chimp supraorbital and zygoma regions and baboon and gorilla zygomatic arch regions. The baboon supraorbital sample differed significantly from the gorilla supraorbital in many indices, including BVF of trabecular bone (p=0.038), CD (p=0.003), TN (p=0.008), TT (p=0.002), and MD (p=0.006). The gorilla supraorbital region was both denser materially and by volume, with greater trabecular thickness; the baboon supraorbital sample had greater connectivity density and more trabeculae per mm (see Table 4.7 and 4.9). Trabeculae in the gorilla zygoma were around twice as thick on average as those in the baboon zygoma (p=0.046). Baboon ZA regions differed significantly from chimp ZA regions in BVF of trabecular bone (p=0.030), SMI (p=0.030), and MD (p=0.009). Baboon zygomatic arches contained a greater amount of bone in trabecular regions that was also more materially dense. The chimp SMI in the zygomatic arch region are between 0 and 1, indicating that it maintains a more traditional trabecular structure (0 indicating more plate-like and 3 more rod-like) compared to the baboon sample SMI in this region; the latter were all negative, indicating greater porosity/concavity of structures (see Figure 4.7).

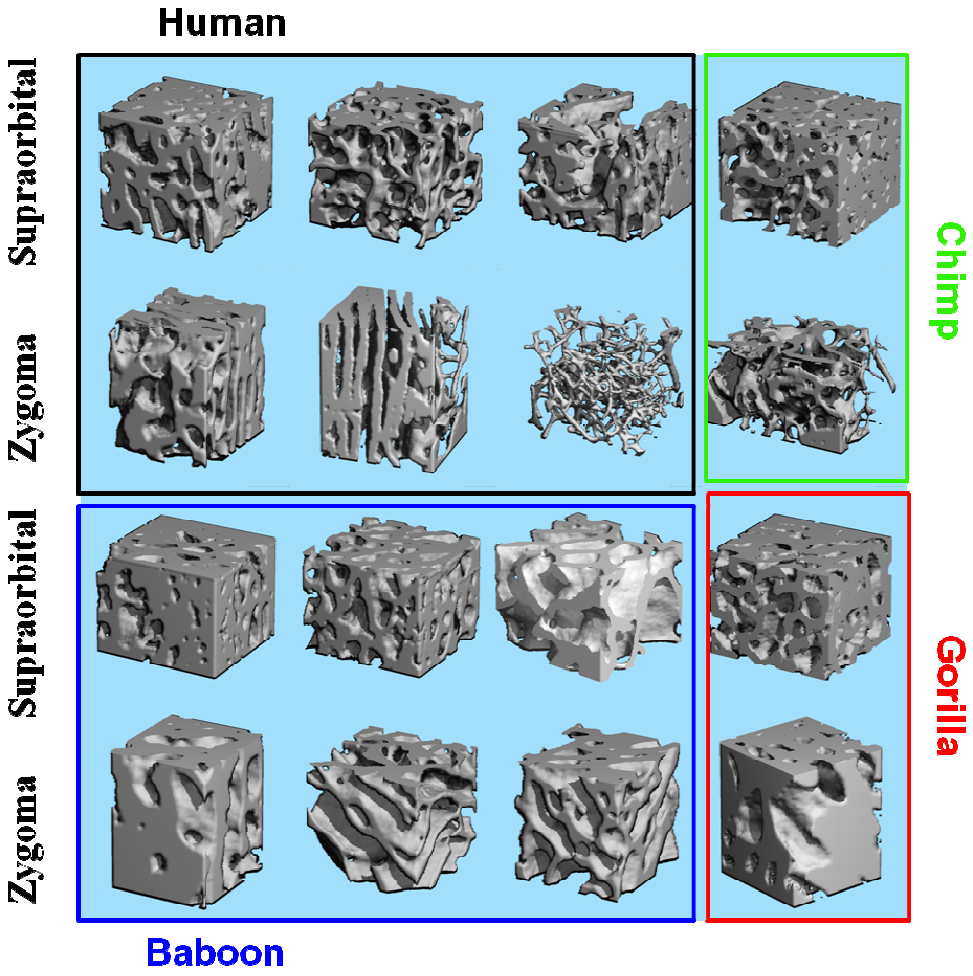

Figure 4.5 Cubic Samples Taken from Supraorbital and Zygomatic Regions to Demonstrate Variation in Trabecular Bone Type.

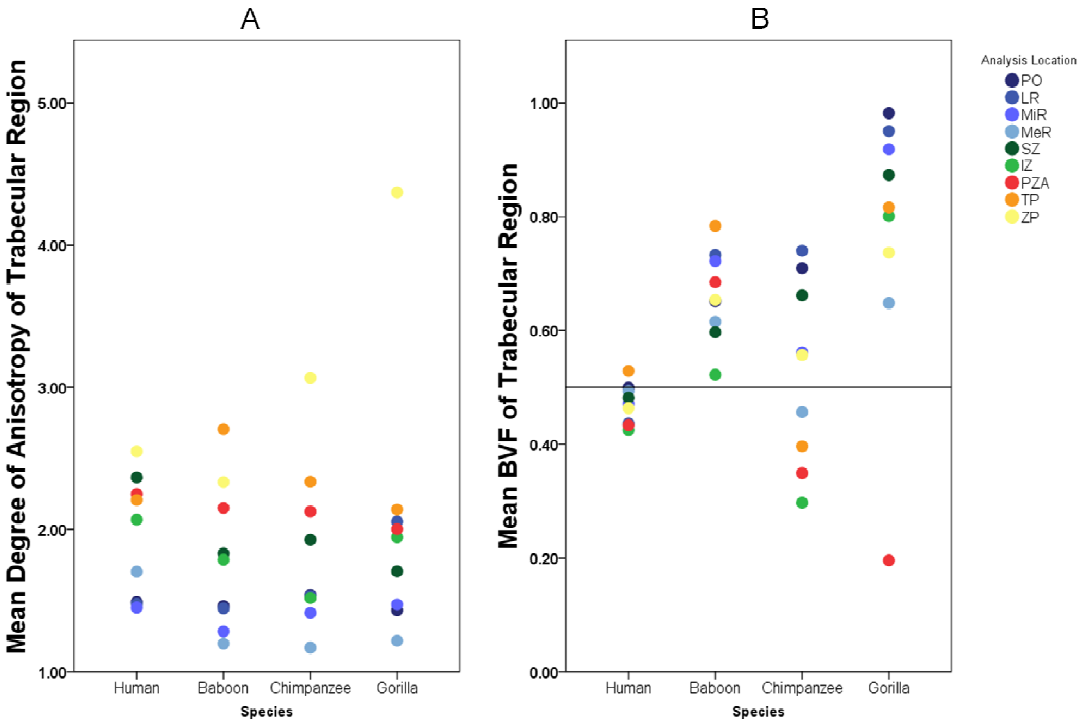

Figure 4.6 (A) The Distribution of Mean DA Across Species and Location; Mann Whitney U tests found only one significant difference in DA between species (human zygoma vs. baboon zygoma; shown in green), but did reveal significant differences between different locations within human and baboon samples. (B) The Distribution of Mean Trabecular BVF Across Species and Location

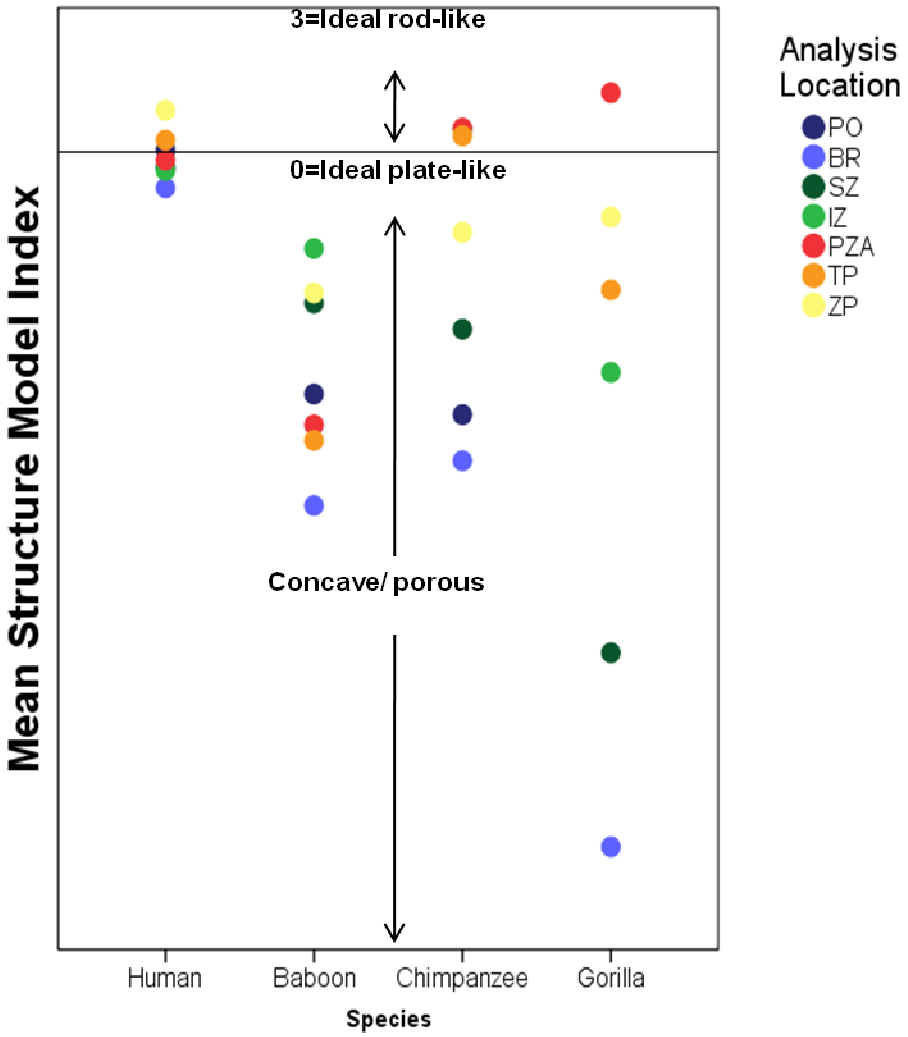

Figure 4.7 The Distribution of SMI across location by species; the concentration of locations around negative SMI values emphasizes the overall differences in trabecular form in facial regions, as 0-3 is the standard range for trabecular bone type post-cranially(Scanco Medical microCT 35 User Manual); Gorilla PO SMI (-41.1) is not shown.

4.3 Principle Components Analysis: Patterning of Trabecular Bone Properties by Species

While in theory it would be interesting to test for patterns and associations between whole and cortical-only measurements and trabecular measurements, whole and cortical-only measurements were ultimately excluded from the principle components analysis. Whole and

cortical-only bone measurements were deemed unsuitable for PCAs with trabecular bone measurements; correlations were above .3, but were low relative to correlations between trabecular bone measurements. Also, some regions differed between analyses and were not suitable for comparison; in the *Bone Volume/Total Volume Density Only Analysis*, the entire browridge was considered as one region, but *in Bone Morphometric Analysis* the browridge was divided into three regions.

PCA of all *Bone Morphometric Analysis* variables in all regions revealed three primary components that explained a total of 83.6% of the variation among variables (KMO=0.609; 35% non-redundant correlation residuals greater than 0.05). Component one accounts for 39 % of the variation and is loaded primarily by TN, TS and CD. Component two accounts for 25.4 % of the variation and is primarily loaded by TT, SMI, and Trabecular BVF. Trabecular BVF was also explained by Component one (see Table 4.10). Component three accounts for 19.2 % of the variation and is loaded by anisotropy and material density. Principle components analysis revealed variable patterning by species that differed by region.

Table 4.10 Principle Components, Variable Loadings, and Cumulative % Variance Explained

Varimax Rotated Component Matrix				
	Component			Cumulative %
	1	2	3	
TN	**.911**	.027	.174	39.070
TS	**-.873**	-.299	.014	
CD	**.639**	-.393	-.507	
TT	-.094	**.907**	.228	64.460
SMI	-.275	**-.850**	.225	
Trab BVF	.671	**.673**	.144	
MD	-.098	.118	**.857**	83.620
DA	.376	-.126	**.765**	

4.2.1 Supraorbital Region

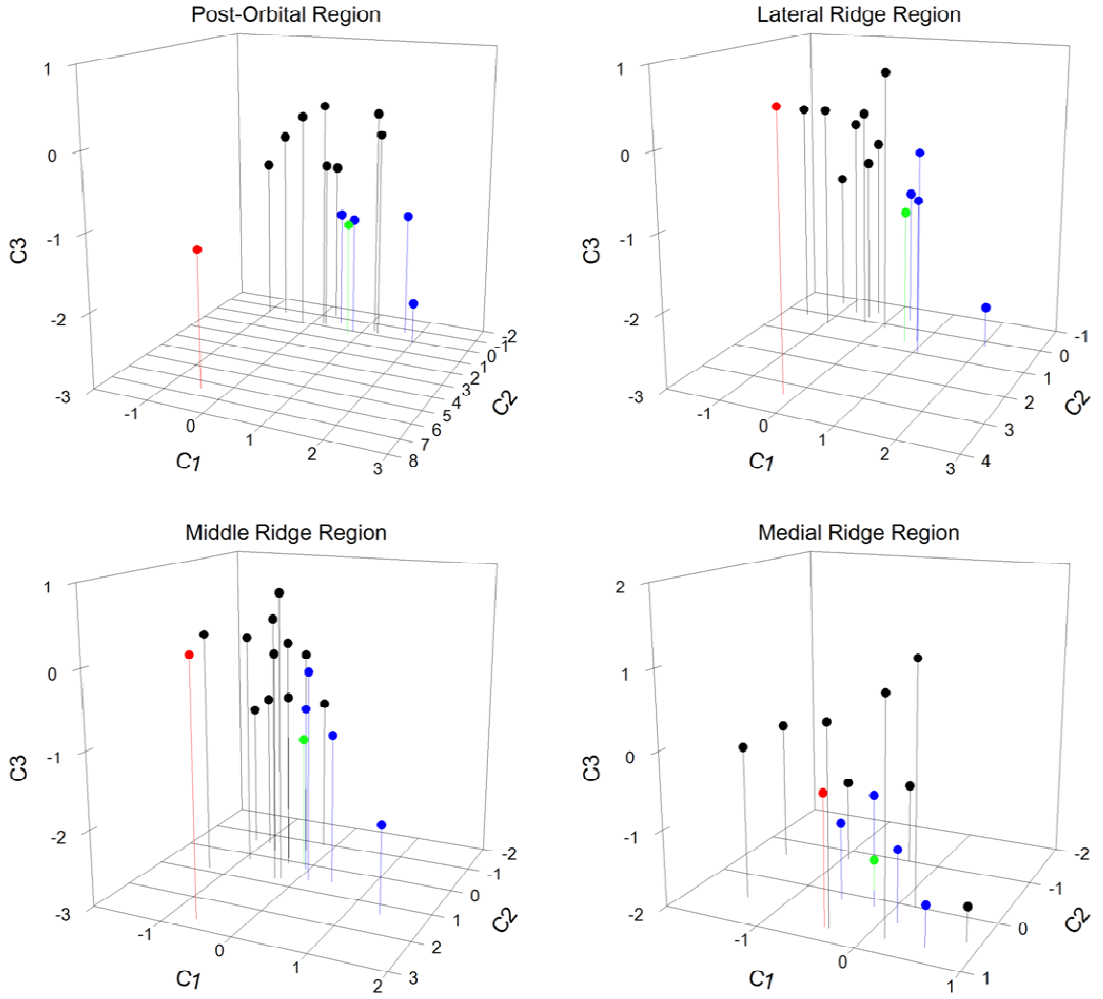

Figure 4.8 PCA Loadings of Supraorbital Regions by Species; component one describes TN, TS, and CD, component 2 describes TT, SMI, and BVFtrab, and component 3 describes MD and DA. black=human, blue=baboon, green=chimp, red=gorilla

In the postorbital region (Figure 4.8), humans and baboons are separated along component one (TN, TS, and CD) and component three (DA and MD), but not on component two (TT, SMI, and BVFtrab). The chimp falls within the baboon cluster within this region. The gorilla is highly separated by component two, but falls within the baboon and chimp cluster on component three and is closer to the human cluster along component one. A similar pattern

exists in the lateral ridge, except that the gorilla falls within the range of the human cluster on component three. The middle ridge follows a similar pattern to both the postorbital region and lateral ridge, but three of the four baboons form a tighter cluster near humans along component three. A drastic change occurs in the medial ridge, where both baboons and humans show large overlap and some variation across all components.

4.2.2 Zygoma

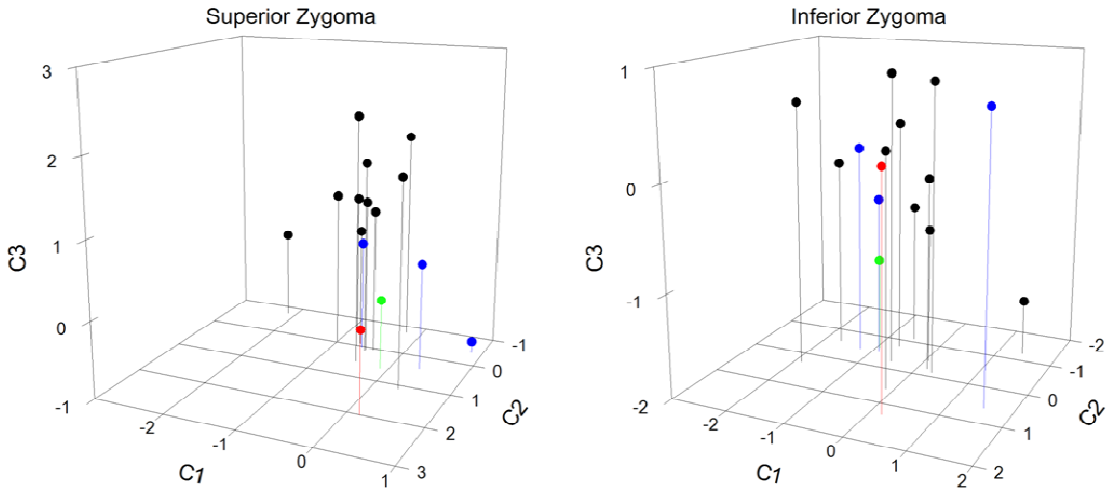

Figure 4.9 PCA Loadings of Zygoma Regions by Species; component one describes TN, TS, and CD, component 2 describes TT, SMI, and BVFtrab, and component 3 describes MD and DA. black=human, blue=baboon, green=chimp, red=gorilla

In the superior zygoma (Figure 4.9), humans and baboons are separated along component one and component three. As in most locations in the browridge, the chimp falls within the baboon cluster, and the gorilla is separated from humans, baboons, and the chimp along component two. The gorilla falls closer to baboons and the chimp along component one for the superior zygoma. Species distribution along components differs drastically in the inferior

region of the zygoma, where there is no differentiation of species by component, except for possibly the gorilla from the other three species along component two.

4.2.3 Zygomatic Arch

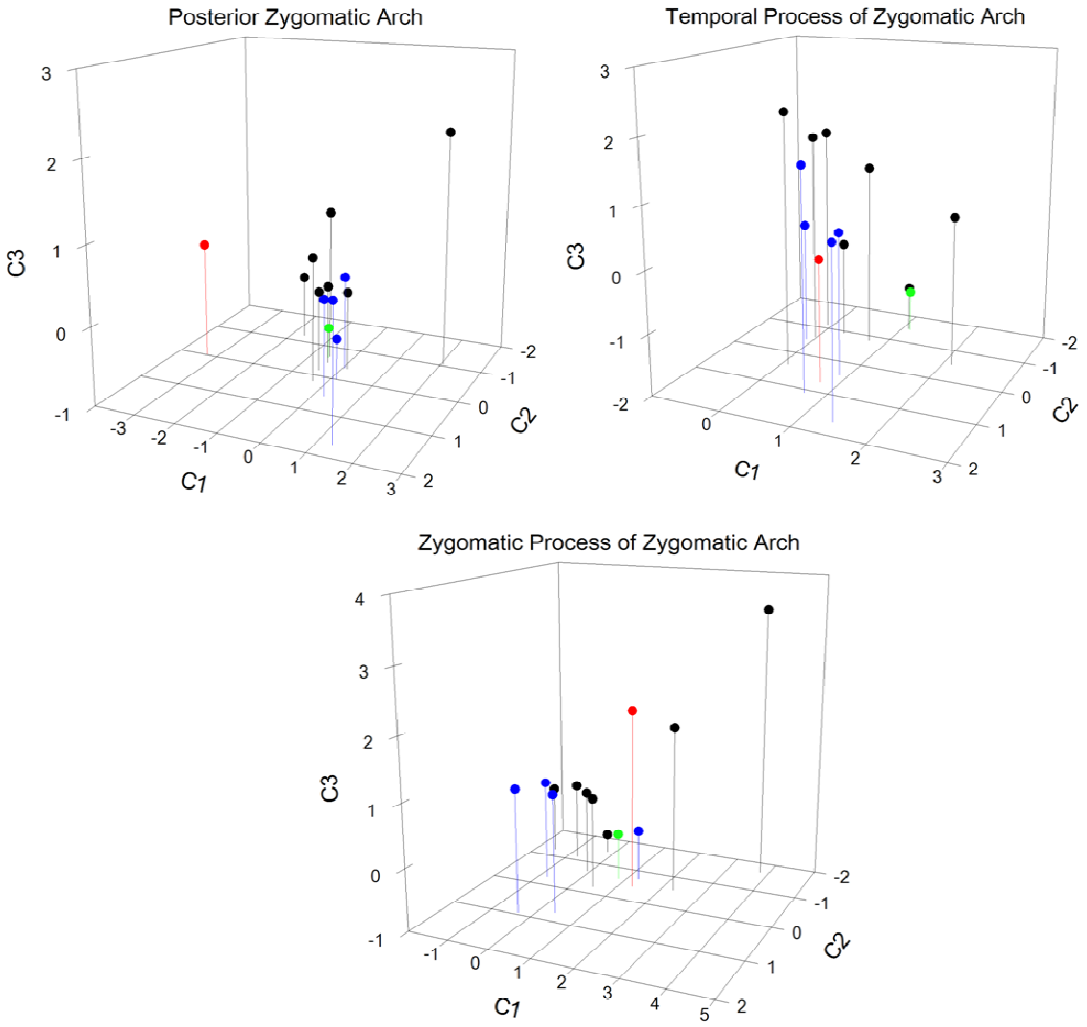

Figure 4.10 PCA Factor Loadings of Zygomatic Arch Regions by Species; component one describes TN, TS, and CD, component 2 describes TT, SMI, and BVFtrab, and component 3 describes MD and DA. black=human, blue=baboon, green=chimp, red=gorilla

In all regions of the zygomatic arch (Figure 4.10), humans and baboons are separated along component two. In the PA the chimp falls within the baboon cluster. In both the TP and ZP, however, the chimp is similar to the low scoring human outlier along component three. The gorilla differs drastically from the other species along component one in the PZA, and from baboons along component three in the ZP. The human outlier in the temporal process of the zygomatic arch was specimen 24713, the 88 year old male.

CHAPTER 5

DISCUSSION AND CONCLUSION

5.1 Discussion

A major problem with this study was sample sizes for chimps (N=1) and gorillas (N=1). However, larger samples of humans and baboons allowed for intraspecific comparisons between regions. All samples showed morphological variation in gross structure and trabecular distribution that sometimes made demarcation of comparable regions difficult, although great care was taken to define reproducible regions based both on gross morphology and trabecular structure. As a result, there is a lot of variation among the volumes analyzed and the number of slices analyzed. Standards and rules were followed to make demarcation of regions less subjective, but not all subjectivity could be avoided.

5.1.1 Strain Gradients in Primate Supraorbital and Zygomatic Regions

The tremendous amount of gross morphological variation in primate craniofacial regions has caused many to hypothesize that such variations are adaptations to feeding strategies. Strain gage analysis has been used to interpret the functional and evolutionary significance of gross morphological structures in craniofacial regions of extinct and extant primates. Many studies have shown that bone surface strain during mastication in the primate supraorbital region is low relative to strain in the infraorbital (zygomatic) region and zygomatic arch (Picq and Hylander, 1989; Hylander et al., 1991; Hylander and Johnson, 1997; Kupczik et al., 2007; Kupczik et al., 2009; Strait et al., 2009; Ross et al., 2011). More specifically, strain is highest in the postorbital bar, compared to other orbital regions, and strain is highest in the anterior root of the zygomatic arch relative to middle and posterior regions, decreasing posteriorly along the arch (Hylander and Johnson, 1997; Ross et al., 2011). At face value, surface strain gradients found in cortical bone of primate craniofacial regions during mastication refute the hypothesis

that the robust supraorbital region found in some extant and extinct primates results from mastication of hard food objects (Picq and Hylander, 1989; Hylander et al., 1991). However, the complexities of the adaptational response of bone to mechanical stress are not fully understood and it has been shown that there are variations in strain thresholds that signal for adaptation (Turner, 1999; Schriefer et al., 2005). Furthermore, it has been demonstrated in humans that changes in mastication can induce a significant remodeling response from cortical bone in the supraorbital region (Dechow et al., 2010). Trabecular bone structure has been used to interpret the functional adaption and evolutionary significance of postcranial bone morphology in primate species, as it offers insight into the distribution of strain throughout the bone and not just on the surface and adds to our interpretation of whole bone morphology (Ryan and Ketcham, 2002; Ryan and Krovitz, 2006). Until now, craniofacial trabecular bone has not been described, except for in the mandibular condyle (van Ruijven et al., 2007).

5.1.2 Intra and Interspecific Trabecular Differences in Homo, Papio, Pan, and Gorilla

In order to determine the relationship between feeding adaptations and upper and mid-craniofacial morphology in primates, this study used microCT to assess the variation of trabecular structure across zygomatic and supraorbital regions in a sample of 10 humans, 4 baboons, 1 chimp, and 1 gorilla. More specifically, the hypothesis that trabecular bone architecture in low strained supraorbital regions would exhibit significantly lower DA and BVF than those in highly strained zygomatic regions was tested. Degree of anisotropy was found to be significantly lower in SO regions of humans and baboons compared to zygomatic regions; however BVF did not differ significantly between regions in either group (Table 4.5-4.6 and Figure 4.6).

All trabecular regions within the supraorbital region of each species had a degree of anisotropy greater than one, and all but five were greater than 1.4, suggesting that the supraorbital region in all species is significantly affected by mechanical stress during mastication (Table 4.8). However, the results indicate that there is a functional relationship

between anisotropy and region. The human and baboon supraorbital region was significantly less anisotropic than both corresponding zygomatic regions, and baboon zygoma regions were significantly less anisotropic than regions in the baboon zygomatic arch. In all species, the degree of anisotropy was higher in both zygomatic regions than that in the supraorbital region. This finding is coherent with findings from strain gage analysis: zygomatic regions are subject to greater strain during mastication than the supraorbital region (Picq and Hylander, 1989; Hylander et al., 1991; Ross et al., 2011). Also consistent with bone strain data, the chimp and gorilla DA in ZA regions clearly decreases from anterior to posterior. This pattern was not as apparent for humans and baboons: human PZA and TP are almost equivalent, but less than ZP, and baboon TP DA was greater than ZP DA, but higher than that of the PZA. However, the averaging of values across location in the human sample group (n=10) could dilute this pattern in this particular sample of humans; moreover, several of the human ZA samples did not have a quantifiable amount of trabecular bone present in regions. Between species regional comparisons of degree of anisotropy may allude to differences in feeding strategies, however only one significant difference was found in interspecific comparisons. Humans had a significantly higher mean DA across the zygoma compared to baboons. There were no significant differences between the chimp or gorilla when compared to humans and baboons; however, a significant difference may be present between species, but not detectable with a sample size of one. On the other hand, baboon zygoma gross morphology is affected by the protrusion of the muzzle, which may distribute bite force throughout craniofacial regions differently; the overlap of DA in the zygoma of humans, chimps, and gorillas could result from a more general tendency towards orthognathicism, relative to baboons.

Zygoma regions of humans and baboons also have greater material density than respective supraorbital regions (Table 4.5-.6). However, the material density in the superior zygoma is without exception higher than in the inferior zygoma (although there is a very small difference in baboon regions), and in humans, the IZ mean material density falls within the

range of material density found in the supraorbital region. The same is not true for DA, except in the chimp specimen where the IZ DA falls within the range of DA values in the supraorbital (Figure 4.7). Relatively lower DA values observed in the IZ compared to those in the SZ are inconsistent with strain gage studies that report that strain is higher in the anterior root of the zygoma (equivalent to IZ region) (Ross et al., 2011).

Degree of anisotropy and apparent density have been found to explain 70% to 80% of the variation in strength and elastic modulus in human postcranial metaphyseal regions and in bovine trabecular bone (Turner, 1992; Goldstein et al., 1993). Trabecular BVF, which is analogous to apparent density[16], is an important indicator of bone strength, having been shown to explain up to 53% of the variance in strength in human femoral regions and 82% when considered along with DA (Ulrich et al., 1999). The results of this study indicate that there are species-specific but not region-specific significant differences in trabecular BVF (Figure 4.6). While humans have higher DA in the supraorbital region than baboons (although not significantly higher), baboons have significantly higher BVF in this region compared to humans. The same is true for human and baboon ZA regions. The gorilla SO BVF is significantly higher than human and baboon BVF SO regions. Baboon BVF in the ZA region is significantly higher compared to the chimp ZA BVF. Significant species-specific differences in BVF may be indicative of species-specific feeding adaptations, discussed below. Furthermore, because BVF of trabecular bone is reflective of multiple measures of trabecular bone structural indices (TT, TS, TN, CD, and SMI), variations in the degree to which BVF is affected by such indices may be indicative of species-specific trabecular bone adaptational responses (Goldstein et al., 1993). These assumptions are supported by the results of this study, where the differences of BVF in each of these regions seem to be affected by different combinations of significant differences in influential structural indices. For example, the significant difference found between the BVF in

[16] Apparent density averages the bone mineral density with space and BVF is a ratio of the volume of bone to the volume of the whole region. Both describe the amount of bone present in an area, but apparent density is more specific, quantifying the actual amount of mineral within the area.

human and baboon ZA regions is accompanied by significant differences in SMI and TT, but that in baboon and chimp ZA regions is accompanied by a significant difference in SMI only. A clearer pattern emerges with PCA and is expounded upon below.

Significance testing by species and location revealed two primary trends in variables that are highly correlated with measures of strength and elastic modulus in trabecular bone studies (Figure 4.6). Anisotropy showed significant differences by region, differences resembling trends in strain gage analysis. BVF on the other hand only showed significant differences between species. By assessing the results for both DA and BVF of trabecular bone (Tables 4.7 and 4.8), it appears that gorillas have the strongest SO trabeculae, followed by the baboon, because both have significantly higher BVF compared to humans, with no significant differences in DA. The gorilla specimen also has significantly higher cortical BVF in the supraorbital region relative to baboons and humans, but baboon cortical BVF is not significantly different from humans (Table 4.4). There are no statistically significant differences between either trabecular BVF or DA in the SO region between the chimp and humans, but the chimp had significantly lower cortical BVF. Based on trabecular BVF, it would also seem that baboons and gorillas exhibit greater strength in zygomatic arch regions compared to the chimp and humans. Cortical BVF in the ZA follows a similar trend, but only gorilla cortical BVF is significantly higher than humans; it is not significantly higher in baboons. Baboon and human cortical BVF in ZA regions is significantly higher than that for the chimp. It is an interesting fact that only one significant difference in BVF of trabecular bone (between the human and gorilla), and only one significant difference for cortical BVF (between baboons and the chimp) of zygoma regions emerged between species. It may be because this region is highly subjected to strain from the masseter muscle, and this strain is consistent across species, due to little morphological variation in attachment (Ross et al., 2011). Morphological variations in jaw and masseter muscle size may be more distributed across the zygomatic arch. The relative contribution of trabecular and cortical bone strength to the strength of the whole region is likely

largely dependent on the relative volume each occupies within the bone. Therefore, the variation in trabecular distribution (described by percentage of trabecular bone in region; see Figure 4.3) complicates the interpretation of combined effects of trabecular and cortical bone morphology on the overall strength of the bone. Significant differences in trabecular percentage are found between all regions except between the human supraorbital and zygoma and between the baboon zygoma and zygomatic arch (Table 4.2 and 4.3). Significant differences are also found for at least one location between all species (Table 4.4). The supraorbital region of humans has significantly more trabecular bone than that of the gorilla and baboons, and baboons have significantly more trabecular bone than the gorilla, a pattern that is consistent with the patterning in BVF of cortical and trabecular bone above. The percentage of the whole ZA region occupied by trabecular bone is significantly higher in chimps and baboons than it is in humans (see Figure 4.2).

These observations are assumptions that can only be validated with actual measures of strength and elastic modulus, but are useful in formulating hypotheses regarding bone adaptational strategies in primate craniofacial regions and how different components (trabecular and cortical) of bone work together. These results suggest that the craniofacial response to masticatory stress is not necessarily equally distributed between cortical and trabecular bone, and that in some species, such as the baboon, trabecular BVF may be crucial to understanding species-specific differences when likeness of cortical regions between baboons and chimps suggest that there are no differences.

5.1.3 Species and Region Specific Patterning among Trabecular Bone Variables

There are significant differences in trabecular bone structural indices other than DA, MD, and BVF between regions and species. The significant differences in TT, TS, TN, SMI, and CD do not seem to follow an identifiable pattern, but may offer insight into trabecular bone adaptational strategies, as they all contribute to BVF (Goldstein et al., 1993). For example, some species may increase BVF by adjusting TT, while others do so by increasing TN.

Differences in adaptational strategy may also be present regionally or may even reflect the type of deformation (bending vs. compression).

Principle components analysis aided in identifying underlying patterns, and illustrating to what extent these patterns characterized species and regions. Most of the variation among all specimens was explained by a component that described TN, TS, and CD, followed by a component that explained TT, SMI, and BVF (Table 4.10). It must be noted that BVF was equally loaded on components one and two, suggesting that it is equally correlated to both sets. This makes sense because BVF is determined by a combination of multiple parameters, including all of those described by components one and two, and therefore may be thought of as more of a secondary variable. The remaining variation was characterized by a component that explained degree of anisotropy and material density. These results suggest that there are three primary mechanisms by which trabecular bone adapts to mechanical stress: one that increases trabecular number and connectivity density and decreases trabecular separation (positive correlation with BVF), one that increases trabecular thickness and decreases structure model index (positive correlation with BVF) and one that increases material density and the degree of orientation of trabeculae.

Similar patterning among species is seen from the postorbital to the middle ridge region of the brow and in the superior zygoma (Figure 4.8 and 4.9). In this pattern, humans differ from baboons and chimps along components one and three. In most SO regions and in the superior zygoma of humans and baboons, differences in BVF are likely obtained through variations in CD, TN and TS. In fact, CD, TN and TS variables were highly significantly different between human and baboon SO: baboons have more, but highly separated trabeculae with greater CD relative to humans. In addition, although human and chimp supraorbital regions are characterized by similar values in BVF, they must obtain this similarity through a different combination of trabecular bone variables (CD, TN and TS), utilizing a strategy more similar to baboons. While differences in TN and TS in the SO region between humans and the chimp

were not significant, the chimp also has more, but highly separated trabeculae with greater CD (significant) relative to humans. The same is true for all three species in the superior zygoma, except that there is less trabecular separation for baboons and the chimp relative to humans, and CD is not significantly different for either baboons or the chimp compared to humans.

Although there are no significant differences between DA across locations, except between human and baboon zygomas, PCA shows that the chimp is more similar to baboons in the distribution of MD and DA across SO regions (excluding the medial ridge) and the superior zygoma. Relative to humans, baboons have lower DA and MD values and the chimp has lower MD values. Some differences of MD between species are significant, like that of the supraorbital region of humans compared to baboons and the chimp, and the SO of the gorilla compared to the baboon. The gorilla is more similar to baboons and the chimp in DA and MD distribution in the PO and SZ region, but more similar to humans in the LR and MiR. The variation in factor loadings in the gorilla specimen across regions is peculiar given the consistency of relative factor loadings in the other three species among these regions and raises questions about the meaning of this variation.

The gorilla specimen is separated from the other species along component two (SMI and TT). Variations in trabecular bone adaptational strategy are consistent across the majority of the supraorbital region, until you begin to approach the most medial region of the browridge, in which trabecular bone variation cannot be explained by species or region. It could be that variations in loadings on component one in different regions are explained by the overwhelming disassociation of the gorilla along component two from the other species. Gorilla SO and SZ bone may increase BVF through a different mechanism than humans, chimps and baboons that involves increasing trabecular thickness and decreasing SMI. Patterns of variation of TN, TS, and CD in the SO and SZ region of gorillas may appear random because they are less important, possible secondary effects of changes that occur in TT and SMI.

These differences disappear in the MeR region; all specimens are clustered closer together among all three axes. A clear pattern also disappears in the inferior zygoma region, but there is a wider distribution among variables. Either the PC model is not appropriate to describe species variation in these regions, or species-specific differences are non-existent as a result of their location. The MeR in each species in located lateral to the supraorbital foramen or notch and is probably least affected by masticatory strain; when mastication occurs, the browridge undergoes bending and the MeR, being the furthest away from masticatory muscles may be least affected by morphological changes. Mean DA values, which may reflect consistencies in strain, are not predictable, however. In humans this region has the highest DA, but in the chimp, gorilla and baboons, it has the lowest DA relative to other SO regions. Ross et al. (2011) produce a FE model of a macaque crania as a hypothesis of craniofacial deformation in the skull resulting from mastication. This model predicts deformation in the orbital region that occurs during SO bending. In this deformation regime, the orbit undergoes tension in the latero-superior corner of the orbit and compression in the medio-superior orbit. The same pattern is observed in humans and gorillas (Ross et al., 2011). The transition from tension to compression occurs in the MeR and may explain why trabecular properties in this region are so variable among species and individuals and why obvious patterns do not emerge. The IZ is subjected to both tensile and compressive forces in the macaque model; its central location to strain induced by mastication may also result in highly variable patterns in trabecular bone properties that show a lot of individual and species variation.

A completely different pattern emerged among principle component correlations across zygomatic arch regions (Figure 4.10). Humans and baboons are separated along component two, and only in the posterior zygomatic arch does the gorilla differ drastically from other species (along component one). There is a lot of variation in the TP along component three, but not in the PZA or ZP, except for two human outliers in both regions and the gorilla in the ZP. The chimp appears to fall in overlapping regions between the humans and baboons along

component two. There is less species-specific variation along component three in all regions, and only individual variation in the TP in component 3. Furthermore, human, baboon, and chimp trabecular bone adaptive strategies to different levels of strain or deformation may differ from those of gorillas.

The lack of species related patterning in the MeR and IZ and differences in strategies between SO and ZA regions may also be attributed to differences in deformation regimes between the regions. The zygomatic arch undergoes very high compressive and tensile strain and is twisted and bent downward during mastication by the masseter muscle. The inferior bending produces shear as it pulls the anterior root of the zygoma across the infraorbital region. The tension in the lateral orbital wall is also produced by the inferior movement of the zygomatic arch; the curvature of the orbit causes unbending of the orbital wall, followed by the unbending of the supraorbital region. This deformation pattern may help explain why SZ and SO regions from the PO to the MiR are similar and why they differ from ZA regions. In addition, MeR regions, by nature of their location experience the least amount of bending. Even though the IZ undergoes tension and compression, it doesn't undergo as much deformation as the zygomatic arch and circumorbital regions. This suggests that deformation patterns may be the driving force behind adaptational strategies such that regions the experience bending and twisting may optimize strength by adjusting TT and SMI, and regions that experience bending may optimize strength by adjusting TN and TS. These strategies may differ by species and may either result from genetic, epigenetic or environmental pressures.

5.1.4 Broad Implications: Hypotheses on the Nature of Trabecular bone Adaptation in the Supraorbital Region of Primates

The data from this study suggest that trabecular bone mechanical properties, such as elastic modulus, are important to deformation response when modeling crania to test hypotheses about feeding adaptations and could affect the outcome of FE modeling. The data presented here do not refute the hypothesis that the robust supraorbital region of *Paranthropus bosei* was an adaptation to hard food dieting. While it can say with some certainty that the

remodeling response of trabecular bone in the supraorbital region does reflect the relative magnitude of strain in the region during mastication, it is unclear whether the same magnitude of strain in the zygomatic region might induce the same degree of anisotropy or material density in that region. A better understanding of the adaptational response of trabecular bone in craniofacial regions could be gained by comparing the primary direction of trabecular orientation to the primary direction of strain in the region during mastication. This might shed light on location specific alignment differences and the question of strain thresholding. If relative magnitudes and directions can be compared, one might gain a sense of whether or not strain of a certain magnitude would induce the same response in trabecular orientation in the zygoma as it does in the supraorbital region. It would also provide an assessment of individual variation in strain distribution and determine if there are morphologically distinct regions of trabecular structure beyond what can be visually assessed. It is also crucial to identity the extent to which trabecular BVF and adaptational mechanisms in craniofacial regions are the product of genetics and epigentics. Based on the results of this study, four possible scenarios are provided that might explain the cortical and trabecular morphology of the supraorbital region.

1. Supraorbital region morphology in robust species is over-designed for mastication and trabecular bone orientation (DA) is more representative of bone's adaptation to stress in the supraorbital region. Relative increases in BVF of trabecular bone may be coupled with browridge protrusion and supraorbital robusticity to add strength to the region as an adaptation independent of feeding strategy.
2. Adaptive strain thresholds differ not only by region, but also by bone type, so that relative anisotropy does not always mirror supraorbital robusticity. Different species may also exhibit different trabecular bone adaptive strategies. For example, in chimps and humans, trabeculae may align in response to mechanical stress, whereas in gorillas and baboons trabecular bone may adapt to mechanical stresses by remodeling bone volume. Also, trabecular and cortical bone structure in supraorbital regions could

contribute to an overall more equalized composite effect, similar to that in zygomatic regions. For example, trabecular bone anisotropy in the supraorbital region may be lower overall relative to zygomatic regions, but this difference may be compensated for in robust species by greater cortical development.

3. Degree of anisotropy is a reflection of relative strain magnitudes among various locations throughout the craniofacial region of catarrhines primates and bone volume fraction is genetically or epigenetically determined. High bone volume fractions of trabeculae is found in the supraorbital region of species with robust supraorbital regions as an adaptional response to the regular mastication of hard food objects.
4. Gross supraorbital morphology and trabecular bone volume fraction may reflect genetic adaptation for fallback food strategies and trabecular bone anisotropy may reflect environmental adaption. Variations in gradient thresholds may still exist between species and regions.

Fallback Food Strategies

Along with low observed strains present in the supraorbital region during mastication, tooth microwear analysis of fossil hominids does not support the evolution of robust craniofacial regions as an adaptation to hard food diets (Grine et al., 2006; Ungar et al., 2008). Dental microwear analyzed in both *Australopithecus afarensis* and *Paranthropus boisei* fossils shows no sign of fracture resistant foods consumed within a few days of the animal's death. This has caused some to speculate that robust craniofacial regions in hominids are adaptations to fallback foods, or food types consumed by animals during periods when preferred foods are scarce and that morphological adaptations should be assessed to consider both genetic and epigenetic influences (Grine et al., 2006; Ungar et al., 2008; Constantino and Wright, 2009).

Fallback food strategies have been investigated in *Homo*, *Pan*, *Gorilla*, and *Papio* genera (Altmann, 2009; Yamagiwa and Basabose, 2009). Lambert (2007) stratifies fallback foods into two extremes: high-quality/less abundant and low-quality/more abundant. Selective

adaptations are affected by where a species falls on the continuum between these two extremes. For example, low quality fallback foods such as leaves and bark are harder to process, and therefore affect the morphology of feeding structures, whereas high quality foods, such as fruits and seeds, are easier to process and have a greater effect on behavioral adaptations. Differences in supraorbital region trabecular BVF between species determined in this study are consistent with Lambert's classification and interpretation of fallback food selective pressures. Both chimps and gorillas prefer a ripe fruit diet, but there appear to be major differences between fallback food strategies. Although there is some overlap in preferred fallback foods between sympatric chimp and gorilla groups in Kahuzi-Biega National Park, gorillas consume significantly more vegetative (leaves, bark, and pith) species compared to chimps, who continue to subsist primarily on fruit during periods when preferred fruit species are scarce (Yamagiwa and Basabose, 2009). Baboons in the Amboseli region of east Africa feed on corms[17], which are extremely mechanically demanding, and sedges out of necessity during periods of preferred food scarcity (Altmann, 2009). It may be that because chimps resort to high quality fallback foods, bone volume fraction in the supraorbital region is relatively low (comparable to human samples). Gorillas and baboons on the other hand resort to more low quality fallback foods, which may explain why the bone volume fractions of supraorbital regions in these species are significantly higher than those of human and chimp specimens.

The fallback food strategies of two species of capuchins may shed some light on the morphological adaptations in the earliest *Homo* and contemporaneous robust Australopithecines (Wright et al., 2009). Both *C. paella* and *C. libidinosus* rely on mechanically tough fallback foods; however, while *C. libidinosus* consumes the tougher of the fallback foods, it is more morphologically gracile. *C. libidinosus* also differs from *C. paella* in that it uses tools to access mechanically tough foods, and the authors of this study hypothesize that tool use broke the dependence of morphology on fallback food strategy. Tool use among early species of

[17] A corm is a short, tough underground plant stem of grasses and sedges that is designed to resist overgrazing of animals during drought periods.

Homo may have selected for the more gracile features of early *Homo*, even if they relied on tough foods during periods of preferred food scarcity.

The difference in bone volume fraction between human and baboon supraorbital regions and human and gorilla supraorbital regions is highly significant. Many of the findings of this study are congruent with the hypothesis that bone volume fraction of trabecular bone in primate supraorbital regions, as well as supraorbital gross morphology, may reflect genetic or epigenetic differences that are determined by fallback food strategies.

5.2 Conclusion

The assessment of trabecular bone architecture in select primate craniofacial regions has provided novel insights into trabecular bone adaptation.

1. Degree of anisotropy differed significantly among most regions in humans and baboons. Average supraorbital degree of anisotropy was less than the average degree of anisotropy in zygomatic regions, including zygoma and zygomatic arch, corresponding to relative measures of bone surface strain during mastication in primates. The same pattern was evident in the chimp and gorilla. Material density also differed significantly by region and mirrored differences in relative surface strain. These results suggest that degree of anisotropy and material density in primate craniofacial regions may reflect remodeling of trabecular bone due to strain endured during day to day mastication.
2. Bone volume fraction, which differed significantly only by species, may be more determined by genetic or epigenetic adaptation to mastication, fallback food strategy, or a non-feeding related adaptation.
3. Variations observed in cortical bone volume fraction among regions and species, percentage of trabecular bone within craniofacial regions, and trabecular bone properties emphasize the complexity of the trabecular bone adaptation response in the supraorbital and zygomatic regions of primates. Significant differences in some

strength indicating variables did not predict significant differences in other strength indicating variables in corresponding regions. For example, baboon supraorbital trabecular bone volume fraction was significantly greater than human supraorbital trabecular bone volume fraction, but differences in cortical bone volume fraction in the same regions were not significant. These inconsistencies are further complicated by differences in the percentage of trabecular bone distributed by region and among species.

4. Principle components analysis predicted three primary mechanisms of trabecular bone remodeling used to increase total strength: one that increases connectivity density and trabecular number and decreases trabecular separation (positive correlation with bone volume fraction); one that increases trabecular thickness and decreases structure model index (positive correlation with bone volume fraction); and one that increases degree of anisotropy and material density.
5. Principle components analysis also found that adaptational strategies are location and species dependent. From the postorbital region to the middle of the browridge, and in the superior region of the zygoma, baboons and the chimp differ from humans in their distribution along principle components that describe trabecular number, trabecular separation, connectivity density, material density, and degree of anisotropy. In these regions, the gorilla differs along the principle component that describes trabecular thickness and structure model index. Patterning of variables is not species-specific in the medial browridge or the inferior zygoma. In the zygomatic arch, humans differ from baboons along the component that describes trabecular thickness and structure model index. In the posterior zygomatic arch, the gorilla differs from all species along the component that describes that connectivity density, trabecular number, and trabecular separation. There is a large distribution of both humans and baboons along the component describing degree of anisotropy

and material density in the temporal process. These differences may be explained by deformation patterns in primates during mastication.

The results of this study not only depict the complexity of trabecular bone adaptational responses, they have significant implications for our understanding of the role of trabecular bone in primate craniofacial regions. Characterizing trabecular bone architecture in craniofacial regions is crucial to our understanding of the functional and evolutionary significance of morphological variation found among extinct and extant primates.

APPENDIX A

HUMAN BV/TV DENSITY ONLY ANALYSIS RESULTS

Human Whole Region Analysis							
			BVF Whole Region	BVF Cortical Bone	% Trabecular Bone in Region	Volume of Entire Analyzed Region	Slices
Supraorbital Region	PO	mean	0.84	0.96	0.24	336.05	57.00
		min	0.72	0.94	0.12	213.30	31.00
		max	0.84	0.99	0.31	436.47	69.00
	BR	mean	0.76	0.95	0.37	2956.97	591.75
		min	0.68	0.92	0.20	1729.53	484.00
		max	0.87	0.98	0.55	5546.20	703.00
Zygoma	SZ	mean	0.90	0.96	0.16	757.01	295.50
		min	0.77	0.80	0.03	356.83	174.00
		max	0.97	0.99	0.34	1097.48	399.00
	IZ	mean	0.74	0.94	0.34	1835.08	305.90
		min	0.51	0.86	0.12	878.87	252.00
		max	0.88	0.98	0.58	3070.39	359.00
Zygomatic Arch	PZA	mean	0.92	0.99	0.12	387.17	274.38
		min	0.84	0.99	0.00	155.00	190.00
		max	1.00	1.00	0.25	654.79	353.00
	TP	mean	0.97	0.99	0.03	206.26	375.22
		min	0.86	0.98	0.00	131.46	305.00
		max	1.00	1.00	0.20	260.05	473.00
	ZP	mean	0.87	0.98	0.15	239.97	333.88
		min	0.60	0.96	0.01	116.71	228.00
		max	0.99	0.99	0.44	389.08	427.00

APPENDIX B

BABOON BV/TV DENSITY ONLY ANALYSIS RESULTS

Baboon Whole Region Analysis							
			BVF Whole Region	BVF Cortical Bone	% Trabecular Bone in Region	Volume of Entire Analyzed Region	Slices
Supraorbital Region	PO	mean	0.83	0.94	0.38	494.54	144.00
		min	0.77	0.87	0.30	260.48	119.00
		max	0.90	0.97	0.49	609.70	169.00
	BR	mean	0.83	0.96	0.43	2726.54	606.75
		min	0.75	0.95	0.24	1642.39	467.00
		max	0.89	0.98	0.52	4260.11	709.00
Zygoma	SZ	mean	0.83	0.96	0.30	732.48	245.67
		min	0.74	0.96	0.20	420.97	220.00
		max	0.89	0.97	0.42	1004.06	280.00
	IZ	mean	0.93	0.99	0.11	459.15	176.00
		min	0.81	0.98	0.00	256.76	139.00
		max	1.00	1.00	0.32	670.42	219.00
Zygomatic Arch	PZA	mean	0.87	0.98	0.29	693.94	234.50
		min	0.77	0.96	0.20	251.62	187.00
		max	0.99	0.99	0.40	1237.86	263.00
	TP	mean	0.92	0.97	0.17	660.26	474.75
		min	0.74	0.93	0.09	455.71	465.00
		max	0.98	0.99	0.37	803.03	489.00
	ZP	mean	0.92	0.98	0.13	864.75	626.75
		min	0.80	0.97	0.03	608.02	536.00
		max	0.98	0.99	0.29	1157.30	672.00

.

APPENDIX C

CHIMP AND GORILLA BV/TV DENSITY ONLY ANALYSIS RESULTS

Chimpanzee Whole Region Analysis						
		BVF Whole Region	BVF Cortical Bone	% Trabecular Bone in Region	Volume of Entire Analyzed Region	Slices
Supraorbital Region	PO	0.85	0.90	0.17	1679.63	259.00
	BR	0.82	0.92	0.33	3076.58	759.00
Zygoma	SZ	0.91	0.95	0.11	276.52	80.00
	IZ	0.70	0.85	0.37	1586.33	250.00
Zygomatic Arch	PZA	0.53	0.78	0.42	144.40	173.00
	TP	0.61	0.74	0.32	231.69	438.00
	ZP	0.70	0.82	0.36	520.51	459.00

Gorilla Whole Region Analysis						
		BV/TV of Whole Region	BV/TV of Cortical Bone	% Trabecular Bone in Region	Volume of Entire Analyzed Region	Slices
Supraorbtial Region	PO	0.98	0.98	0.00	2711.69	237.00
	BR	0.98	0.98	0.00	6773.32	921.00
Zygoma	SZ	0.97	0.99	0.12	1942.83	328.00
	IZ	0.94	0.96	0.06	3323.84	468.00
Zygomatic Arch	PZA	0.88	0.97	0.12	624.13	235.00
	TP	0.98	0.99	0.00	525.98	266.00
	ZP	0.96	0.97	0.05	442.31	239.00

REFERENCES

Aiello L, Andrews P. 2000. The australopithecines in review. Human Evolution 15:17-38.

Altmann SA. 2009. Fallback foods, eclectic omnivores, and the packaging problem. American Journal of Physical Anthropology 140:615-629.

Biewener AA, Fazzalari NL, Konieczynski DD, Baudinette RV. 1996. Adaptive changes in trabecular architecture in relation to functional strain patterns and disuse. Bone 19:1-8.

Bourne BC, van der Meulen MC. 2004. Finite element models predict cancellous apparent modulus when tissue modulus is scaled from specimen CT-attenuation. Journal of Biomechanics 37:613-621.

Carter D, Hayes W. 1977a. The compressive behavior of bone as a two-phase porous structure. The Journal of Bone and Joint Surgery 59:954-962.

Carter D, Hayes W. 1977b. The compressive behavior of bone as a two-phase pourous structure. The Journal of Bone and Joint Surgery 59:954-962.

Constantino PJ, Wright BW. 2009. The importance of fallback foods in primate ecology and evolution. American Journal of Physical Anthropology 140:599-602.

Cowin SC. 2001. Bone Mechanics Handbook, 2nd ed. Boca Raton, FL: CRC Press.

Cruz-Orive LM, Karlsson LM, Larsen SE, Wainschtein F. 1992. Characterizing anisotropy: A new concept. Micron and Microscopica Acta 23:75-76.

Currey JD. 2002. Bones: Structure and Function. New Jersey: Princeton University Press.

Dechow CD, Schwartz-Dabney CL, Ashman R. 1992. Elastic properties of the human mandibular corpus. In: Golstein SA, Carlson DS, editors. Bone Biodynamics in Orthodontic and Orthopedic Treatment. Ann Arbor, Michigan. p 299-314.

Dechow PC, Nail GA, Schwartzdabney CL, Ashman RB. 1993. Elastic Properties of Human Supraorbital and Mandibular Bone. American Journal of Physical Anthropology 90:291-306.

Dechow PC, Wang Q, Peterson J. 2010. Edentulation alters material properties of cortical bone in the human craniofacial skeleton: functional implications for craniofacial structure in primate evolution. Anat Rec (Hoboken) 293:618-629.

Endo B. 1966. Experiemental studies on the mechanical significance of the form of the human facial skeleton. Journal of the Faculty of Science, University of Tokyo 3:5-106.

Evans FG. 1973. Mechanical properties of bone. Springfield, Ill.,: Thomas.

Feldkamp LA, Goldstein SA, Parfitt AM, Jesion G, Kleerekoper M. 1989. The direct examination of three-dimensional bone architecture in vitro by computed tomography. Journal of Bone and Mineral Research 4:3-11.

Frost HM. 1987. Bone "mass" and the "mechanostat": a proposal. Anatomical Record 219:1-9.

Goldstein SA. 1987. The mechanical properties of trabecular bone: Dependence on anatomic location and function. Journal of Biomechanics 20:1055-1061.

Goldstein SA, Goulet R, McCubbrey D. 1993. Measurement and significance of three-dimensional architecture to the mechanical integrity of trabecular bone. Calcif Tissue Int 53 Suppl 1:S127-132; discussion S132-123.

Goulet RW, Goldstein SA, Ciarelli MJ, Kuhn JL, Brown JH, Feldkamp LA. 1994. The relationship between the structural and orthogonal compressive properties of trabecular bone. Journal of Biomechanics 27:375-389.

Grine FE, Ungar PS, Teaford MF, El-Zaatari S. 2006. Molar microwear in Praeanthropus afarensis: Evidence for dietary stasis through time and under diverse paleoecological conditions. Journal of Human Evolution 51:297-319.

Guo XE. 2001. Mechanical properties of cortical bone and cancellous bone tissue. In: Cowin SC, editor. Bone Biomechanics Handbook, 2nd ed. Boca Raton: CRC Press.

Harrigan TP, Jasty M, Mann RW, Harris WH. 1988. Limitations of the continuum assumption in cancellous bone. Journal of Biomechanics 21:269-275.

Harrigan TP, Mann RW. 1984. Characterization of microstructural anisotropy in orthotropic materials. Journal of Material Science 19:761-767.

Hayes WC, Snyder BD. 1981. Toward a quantitative formulation of Wolff's law in trabecular bone. American Society of Mehcanical Engineering Symp 45:43-68.

Hildebrand T, Rüegsegger P. 1997. A new method for the model-independent assessment of thickness in three-dimensional images. Journal of Microscopy 185:67-75.

Humphry. 1858. A Treatise of the Human Skeleton. Cambridge.

Hylander WL, Johnson KR. 1997. *In vivo* bone strain patterns in the zygomatic arch of macaques and the significance of these patterns for functional interpretations of craniofacial form. American Journal of Physical Anthropology 102:203-232.

Hylander WL, Picq PG. 1989. A review of Endo's stress-analysis of the primate skull. American Journal of Physical Anthropology 78:243-244.

Hylander WL, Picq PG, Johnson AD. 1987. A preliminary stress-analysis of the circumorbital region in *Macaca fascicularis*. American Journal of Physical Anthropology 72:214-214.

Hylander WL, Picq PG, Johnson KR. 1991. Masticatory-stress hypotheses and the supraorbital region of primates. American Journal of Physical Anthropology 86:1-36.

Keaveny TM, Hayes WC. 1993. A 20-Year Perspective on the Mechanical-Properties of Trabecular Bone. Journal of Biomechanical Engineering-Transactions of the Asme 115:534-542.

Ketcham R. 2005. Three-dimensional grain fabric measurements using high-resolution X-ray computed tomography. Journal of Structural Geology 27:1217-1228.

Kim CH, Takai E, Zhou H, von Stechow D, Muller R, Dempster DW, Guo XE. 2003. Trabecular bone response to mechanical and parathyroid hormone stimulation: the role of mechanical microenvironment. Journal of Bone and Mineral Research 18:2116-2125.

Klein RG. 2009. The Human Career : Human Biological and Cultural Origins, 3rd ed. Chicago: The University of Chicago Press.

Koch JC. 1917. The laws of bone architecture. American Journal of Anatomy 21:177-298.

Kuhn JL, Goldstein SA, Feldkamp LA, Goulet RW, Jesion G. 1990. Evaluation of a microcomputed tomography system to study trabecular bone structure. Journal of Orthopaedic Research 8:833-842.

Kupczik K, Dobson CA, Crompton RH, Phillips R, Oxnard CE, Fagan MJ, O'Higgins P. 2009. Masticatory Loading and Bone Adaptation in the Supraorbital Torus of Developing Macaques. American Journal of Physical Anthropology 139:193-203.

Kupczik K, Dobson CA, Fagan MJ, Crompton RH, Oxnard CE, O'Higgins P. 2007. Assessing mechanical function of the zygomatic region in macaques: validation and sensitivity testing of finite element models. Journal of Anatomy 210:41-53.

Laib A, Barou O, Vico L, Lafage-Proust MH, Alexander CE, Rugsegger P. 2000. 3D micro-computed tomography of trabecular and cortical bone architecture with application to a rat model of immobilisation osteoporosis. Medical and Biological Engineering and Computing 38:326-332.

Lambert JE. 2007. Seasonality, fallback strategies, and natural selection: a chimpanzee and Cercopithecoid model for interpreting the evolution of the hominin diet. In: Ungar PS, editor. Evolution of the Human Diet: The Known, the Unknown, and the Unknowable. Oxford: Oxford University Press. p 324-343.

Lanyon LE. 1973. Analysis of surface bone strain in the calcaneus of sheep during normal locomotion. Strain analysis of the calcaneus. Journal of Biomechanics 6:41-49.

Lanyon LE. 1974. Experimental support for trajectorial theory of bone-structure. Journal of Bone and Joint Surgery-British Volume B 56:160-166.

Lanyon LE, Rubin CT. 1985. The Effect on Bone Remodeling of Static and Graded Dynamic Loads. Journal of Bone and Joint Surgery-British Volume 67:318-318.

Lanyon LE, Smith RN. 1969. Measurements of bone strain in the walking animal. Res Vet Sci 10:93-94.

Lieberman DE. 1998. Sphenoid shortening and the evolution of modern human cranial shape. Nature 393:158-162.

Martin RB, Burr DB, Sharkey NA. 1998. Skeletal Tissue Mechanics. New York: Springer.

Morgan EF, Bayraktar HH, Keaveny TM. 2003. Trabecular bone modulus-density relationships depend on anatomic site. Journal of Biomechanics 36:897-904.

Nomoto S, Matsunaga S, Ide Y, Abe S, Takahashi T, Saito F, Sato T. 2006. Stress distribution in maxillary alveolar ridge according to finite element analysis using micro-CT. Bull Tokyo Dent Coll 47:149-156.

Odgaard A. 1997. Three-dimensional methods for quantification of cancellous bone architecture. Bone 20:315-328.

Odgaard A, Gundersen HJG. 1993. Quantification of connectivity in cancellous bone, with special emphasis on 3-D reconstructions. Bone 14:173-182.

Pearson OM, Lieberman DE. 2004. The aging of Wolff's "law": Ontogeny and responses to mechanical loading on cortical bone. American Journal of Physical Anthropology:63-99.

Peterson J, Dechow PC. 1998. Using multilevel statistics to assess variation in cranial material properties. Journal of Dental Research 77:760-760.

Peterson J, Dechow PC. 2002. Material properties of the inner and outer cortical tables of the human parietal bone. Anatomical Record 268:7-15.

Peterson J, Dechow PC. 2003a. Material properties of the human cranial vault and zygoma. Anatomical Record Part A-Discoveries in Molecular Cellular and Evolutionary Biology 274A:785-797.

Peterson J, Dechow PC. 2003b. Material properties of the human cranial vault and zygoma. Anat Rec A Discov Mol Cell Evol Biol 274:785-797.

Peterson J, Wang Q, Dechow PC. 2006. Material properties of the dentate maxilla. Anatomical Record A -Discoveries in Molecular Cellular and Evolutionary Biology 288:962-972.

Picq PG, Hylander WL. 1989. Endo stress-analysis of the primate skull and the functional significance of the supraorbital region. American Journal of Physical Anthropology 79:393-398.

Pontzer H, Lieberman DE, Momin E, Devlin MJ, Polk JD, Hallgrimsson B, Cooper DM. 2006. Trabecular bone in the bird knee responds with high sensitivity to changes in load orientation. Journal of Experimental Biology 209:57-65.

Rafferty KL. 1998. Structural design of the femoral neck in primates Journal of Human Evolution 34:361-383.

Rak Y. 1983. The Australopithecine Face. New York: Academic Press.

Rak Y. 1985. Australopithecine taxonomy and phylogeny in light of facial morphology. American Journal of Physical Anthropology 66:281-287.

Rice JC, Cowin SC, Bowman JA. 1988. On the dependence of the elasticity and strength of cancellous bone on apparent density. Journal of Biomechanics 21:155-168.

Richmond BG, Wright BW, Grosse I, Dechow PC, Ross CF, Spencer MA, Strait DS. 2005. Finite element analysis in functional morphology. The Anatomical Record Part A: Discoveries in Molecular, Cellular, and Evolutionary Biology 283A:259-274.

Ross CF. 2001. In vivo function of the craniofacial haft: The interorbital "pillar". American Journal of Physical Anthropology 116:108-139.

Ross CF, Berthaume MA, Dechow PC, Iriarte-Diaz J, Porro LB, Richmond BG, Spencer M, Strait D. 2011. In vivo bone strain and finite-element modeling of the craniofacial haft in catarrhine primates. Journal of Anatomy 218:112-141.

Ross CF, Strait DS, Dechow CD, Richmond BG, Spencer MA, Iriarte-Diaz J. in press. In vivo bone strain and finite-element modeling of the craniofacial haft in catarrhine primates. Journal of Anatomy.

Rubin CT, Lanyon LE. 1982. Limb mechanics as a function of speed and gait - a study of functional strains in the radius and tibia of horse and dog. Journal of Experimental Biology 101:187-211.

Rubin CT, Lanyon LE. 1984. Regulation of bone-formation by applied dynamic loads. Journal of Bone and Joint Surgery-American Volume 66A:397-402.

Ruegsegger P. 2001. Imaging of bone structure. In: Cowin SC, editor. Bone Mechanics Handbook. Boca Raton: CRC Press.

Ruegsegger P, Koller B, Muller R. 1996. A microtomographic system for the nondestructive evaluation of bone architecture. Calcif Tissue Int 58:24-29.

Ruff C, Holt B, Trinkaus E. 2006. Who's afraid of the big bad wolff? "Wolff is law" and bone functional adaptation. American Journal of Physical Anthropology 129:484-498.

Russell MD. 1983. Browridge Development as a Function of Bending Stress in the Supraorbital Region. American Journal of Physical Anthropology 60:248-248.

Russell MD. 1985. The Supraorbital Torus - a Most Remarkable Peculiarity. Current Anthropology 26:337-360.

Ryan TM, Ketcham RA. 2002. The three-dimensional structure of trabecular bone in the femoral head of strepsirrhine primates. Journal of Human Evolution 43:1-26.

Ryan TM, Krovitz GE. 2006. Trabecular bone ontogeny in the human proximal femur. Journal of Human Evolution 51:591-602.

Schriefer JL, Warden SJ, Saxon LK, Robling AG, Turner CH. 2005. Cellular accommodation and the response of bone to mechanical loading. Journal of Biomechanics 38:1838-1845.

Schwartz-Dabney CL, Dechow PC. 2003. Variations in cortical material properties throughout the human dentate mandible. American Journal of Physical Anthropology 120:252-277.

Singh I. 1978. Architecture of cancellous bone. Journal of Anatomy 127:305-310.

Strait DS, Grosse IR, Dechow PC, Smith AL, Wang Q, Weber GW, Neubauer S, Slice DE, Chalk J, Richmond BG, Lucas PW, Spencer MA, Schrein C, Wright BW, Byron C, Ross CF. 2010. The structural rigidity of the cranium of Australopithecus africanus: implications for diet, dietary adaptations, and the allometry of feeding biomechanics. Anat Rec (Hoboken) 293:583-593.

Strait DS, Richmond BG, Spencer MA, Ross CF, Dechow PC, Wood BA. 2007. Masticatory biomechanics and its relevance to early hominid phylogeny: An examination of palatal thickness using finite-element analysis. Journal of Human Evolution 52:585-599.

Strait DS, Wang Q, Dechow PC, Ross CF, Richmond BG, Spencer MA, Patel BA. 2005. Modeling elastic properties in finite-element analysis: how much precision is needed to produce an accurate model? Anat Rec A Discov Mol Cell Evol Biol 283:275-287.

Strait DS, Weber GW, Neubauer S, Chalk J, Richmond BG, Lucas PW, Spencer MA, Schrein C, Dechow PC, Ross CF, Grosse IR, Wright BW, Constantino P, Wood BA, Lawn B, Hylander WL, Wang Q, Byron C, Slice DE, Smith AL. 2009. The feeding biomechanics and dietary ecology of *Australopithecus africanus*. Proc Natl Acad Sci U S A 106:2124-2129.

Susman RL. 1991. Who made the Oldowan tools? Fossil evidence for tool behavior in Plio-Pleistocene hominids. Journal of Anthropological Research 47:129-151.

Tappen NC. 1973. Structure of bone in skulls of Neanderthal fossils. American Journal of Physical Anthropology 38:93-97.

Teaford MF, Ungar PS. 2000. Diet and the evolution of the earliest human ancestors. Proc Natl Acad Sci U S A 97:13506-13511.

Turner CH. 1989. Yield behavior of bovine cancellous bone. J Biomech Eng 111:256-260.

Turner CH. 1992. On Wolff's law of trabecular architecture. Journal of Biomechanics 25:1-9.

Turner CH. 1999. Torward a mathematical description of bone biology: The principle of cellular accomodation. Calcified Tissue International 65:466-471.

Turner CH, Cowin SC, Rho JY, Ashman RB, Rice JC. 1990. The fabric dependence of the orthotropic elastic constants of cancellous bone. J Biomech 23:549-561.

Ulrich D, Van Rietbergen B, Laib A, Ruegsegger P. 1999. The ability of three-dimensional structural indices to reflect mechanical aspects of trabecular bone. Bone 25:55-60.

Ungar PS, Grine FE, Teaford MF. 2008. Dental microwear and diet of the Plio-Pleistocene hominin *Paranthropus boisei*. PLoS ONE 3:e2044.

van Rietbergen B, Majumdar S, Pistoia W, Newitt DC, Kothari M, Laib A, Rüegsegger P. 1998a. Assessment of cancellous bone mechanical properties from micro-FE models based on micro-CT, pQCT and MR images. Technology and Health Care 6:413-420.

Van Rietbergen B, Muller R, Ulrich D, Ruegsegger P, Huiskes R. 1999. Tissue stresses and strain in trabeculae of a canine proximal femur can be quantified from computer reconstructions. Journal of Biomechanics 32:165-173.

Van Rietbergen B, Odgaard A, Kabel J, Huiskes R. 1998b. Relationships between bone morphology and bone elastic properties can be accurately quantified using high-resolution computer reconstructions. Journal of Orthopaedic Research 16:23-28.

Van Rietbergen B, Weinans H, Huiskes R, Odgaard A. 1995. A new method to determine trabecular bone elastic properties and loading using micro-mechanical finite-elements methods. J. Biomechanics 28:69-81.

van Ruijven LJ, Mulder L, van Eijden TMGJ. 2007. Variations in mineralization affect the stress and strain distributions in cortical and trabecular bone. Journal of Biomechanics 40:1211-1218.

Wang Q, Dechow PC. 2006. Elastic properties of external cortical bone in the craniofacial skeleton of the rhesus monkey. American Journal of Physical Anthropology 131:402-415.

Wang Q, Dechow PC, Richmond BG, Ross CF, Spencer MA, Strait DS, Wright BW. 2006a. Fusion of craniofacial sutures in monkey skulls with special reference to the Finite Element Analysis. American Journal of Physical Anthropology:184-185.

Wang Q, Strait DS, Dechow PC. 2006b. A comparison of cortical elastic properties in the craniofacial skeletons of three primate species and its relevance to the study of human evolution. Journal of Human Evolution 51:375-382.

Ward FO. 1838. Outlines of Human Osteology. London.

Whitehouse WJ. 1974. Quantitative Morphology of Anisotropic Trabecular Bone. Journal of Microscopy-Oxford 101:153-168.

Whitehouse WJ, Dyson ED. 1974a. Scanning Electron-Microscope Studies of Trabecular Bone in Proximal End of Human Femur. Journal of Anatomy 118:417-444.

Whitehouse WJ, Dyson ED. 1974b. Scanning electron microscope studies of trabecular bone in proximal end of human femur. Journal of Anatomy 118:417-444.

Whitehouse WJ, Dyson ED, Jackson CK. 1971. Scanning Electron Microscope in Studies of Trabecular Bone from a Human Vertebral Body. Journal of Anatomy 108:481-487.

Wolff J. 1892. Das Gesetz der Transformation der Knochen. In: The Law of Bone Remodeling. Berlin: Springer.

Wood B, Collard M. 1999. The human genus. Science 284:65-71.

Wright BW, Wright KA, Chalk J, Verderane MP, Fragaszy D, Visalberghi E, Izar P, Ottoni EB, Constantino P, Vinyard C. 2009. Fallback foraging as a way of life: using dietary toughness to compare the fallback signal among capuchins and implications for interpreting morphological variation. American Journal of Physical Anthropology 140:687-699.

Wyman J. 1857. On the cancellated structure of the bones of the human body. Boston Journal of Natural History 6.

Yamagiwa J, Basabose AK. 2009. Fallback foods and dietary partitioning among Pan and Gorilla. American Journal of Physical Anthropology 140:739-750.

BIOGRAPHICAL INFORMATION

Leslie C. Pryor Smith began studying anthropology at The University of Georgia in Athens, Georgia, where she obtained a Bachelor of Arts. Her interest in hominid evolution led her to pursue graduate study at the University of Texas at Arlington. She is currently working toward a PhD in biomedical sciences through the Texas A&M Health Science Center, Baylor College of Dentistry, located in Dallas, Texas. She is interested in bone biomechanics as it relates to vertebrate evolution, as well as the nature of the cellular response within bone to mechanical loading and molecular and cellular processes that are involved in bone remodeling. After completing her PhD, Leslie hopes to continue her career in research and teaching.